

UNIVERZA V LJUBLJANI
FAKULTETA ZA FARMACIJO

MATEJA LUMPERT

DIPLOMSKA NALOGA

Univerzitetni študij farmacije

Ljubljana, 2012

UNIVERSITY OF LJUBLJANA
FACULTY OF PHARMACY

MATEJA LUMPERT

**ANALYSIS OF SOLUBLE GUANYLYL CYCLASE
ACTIVATION USING A FLUORESCENT PROBE**

**ANALIZA AKTIVACIJE TOPNE GVANILAT-
CIKLAZE S FLUORESCENČNO SONDO**

Ljubljana, 2012

The research work was carried out at the Institute of Pharmacology, Toxicology and Clinical Pharmacy of Technical University of Braunschweig under the supervision of my co-mentor Prof. Dr. Sönke Behrends and home mentorship of Assist. Prof. Dr. Tomaž Bratkovič. The sequential analysis was performed by GATC Biotech, Köln, Germany.

Acknowledgements

First of all, I would like to express my gratitude to my co-mentor Prof. Dr. Sönke Behrends for giving me the opportunity to work in his research group. I am also thankful to Mareike Busker for valuable advices, critical reading and support during my research. I want to thank to all members of the Institute of Pharmacology, Toxicology and Clinical Pharmacy for their welcoming attitude and helpfulness.

Rada bi se zahvalila svojemu mentorju doc. dr. Tomažu Bratkoviču za pomoč in vse nasvete pri pisanju diplomske naloge. Zahvaljujem se izr. prof. dr. Matjažu Jerasu za temeljit pregled diplomskega naloge. Iskrena hvala tudi moji družini za vso ljubezen, podporo in finančno pomoč, ki mi je omogočila dokončanje študija. Hvala tudi tebi Blaž za vse optimistične spodbude in podporo. Hvala vsem ostalim, ki ste mi vsa ta leta stali ob strani.

STATEMENT

I declare that I have carried out my diploma work independently under the mentorship of Assist. Prof. Dr. Tomaž Bratkovič and co-mentorship of Prof. Dr. Sönke Behrends.

Ljubljana, 2012

Graduation commission president: Prof. Dr. Danijel Kikelj

Graduation commission member: Assoc. Prof. Dr. Matjaž Jeras

Table of contents

| | |
|--|-------------|
| LIST OF ABBREVIATIONS | VI |
| POVZETEK | VIII |
| ABSTRACT | X |
| 1. INTRODUCTION | 1 |
| 1.1. THE NITRIC OXIDE/CYCLIC GMP-SIGNALING PATHWAY | 1 |
| 1.2. SOLUBLE GUANYLYL CYCLASE ISOFORMS | 2 |
| 1.3. SOLUBLE GUANYLYL CYCLASE DOMAIN STRUCTURE..... | 3 |
| 1.4. NITRIC OXIDE | 5 |
| 1.4.1. Nitric oxide donors | 6 |
| 1.4.2. Biological processes controlled by nitric oxide..... | 6 |
| 1.5. CONFORMATIONAL CHANGES UPON SOLUBLE GUANYLYL CYCLASE ACTIVATION... | 7 |
| 1.6. FLUORESCENCE RESONANCE ENERGY TRANSFER..... | 8 |
| 1.6.1. The efficiency of energy transfer..... | 10 |
| 1.6.2. The spectral bleed-trough | 11 |
| 1.7. FLUORESCENT NUCLEOTIDES..... | 12 |
| 1.7.1. Properties of fluorescent nucleotides..... | 12 |
| 1.7.2. Applications of fluorescent nucleotides as molecular probes | 13 |
| 1.7.2.1. Mammalian membrane-bound adenylyl cyclase | 13 |
| 1.7.2.2. Adenylyl cyclase toxin of <i>Bordetella pertussis</i> | 15 |
| 1.7.2.3. Adenylyl cyclase toxin of <i>Bacillus anthracis</i> , edema factor..... | 15 |
| 1.8. ABSORPTION AND EMISSION OF TRYPTOPHAN VERSUS TYROSINE | 16 |
| 1.9. LOCATION OF TRYPTOPHANE RESIDUES IN SOLUBLE GUANYLYL CYCLASE | 17 |
| 2. RESEARCH OBJECTIVES | 18 |
| 3. EXPERIMENTAL WORK | 20 |
| 3.1. MATERIALS..... | 20 |
| 3.1.1. Chemicals and substances | 20 |
| 3.1.2. Solutions, buffers and media | 21 |
| 3.1.3. Vector | 22 |
| 3.1.4. Primers..... | 22 |
| 3.1.5. Enzymes and reagent systems | 23 |
| 3.1.6. Antibodies..... | 23 |
| 3.1.7. Cells..... | 23 |
| 3.1.8. Viruses | 23 |
| 3.1.9. Materials and devices | 24 |
| 3.2. METHODS | 25 |
| 3.2.1. Site-directed mutagenesis | 25 |
| 3.2.1.1. Primer design for site-directed mutagenesis..... | 25 |
| 3.2.1.2. Polymerase chain reaction | 25 |
| 3.2.1.3. Transformation of host cells | 26 |
| 3.2.1.4. Minipreparation of plasmid DNA..... | 26 |
| 3.2.1.5. Plasmid DNA sequencing..... | 27 |
| 3.2.1.6. Maxipreparation..... | 27 |
| 3.2.2. Bac-to-Bac Baculovirus Expression System | 29 |
| 3.2.2.1. General description of Bac-to-Bac Baculovirus Expression System | 29 |

| | |
|---|-----------|
| 3.2.2.2. Transformation of DH10 Bac™ Competent Cells with the plasmid and gene transposition | 30 |
| 3.2.2.3. Isolation of recombinant bacmid DNA | 31 |
| 3.2.2.4. Analyzing recombinant bacmid DNA by PCR..... | 31 |
| 3.2.2.5. Agarose gel electrophoresis..... | 32 |
| 3.2.2.6. Sf9 cells | 32 |
| 3.2.2.7. Transfection of Sf9 cells with recombinant bacmid DNA | 33 |
| 3.2.2.8. Isolation and amplification of P1 viral stock..... | 33 |
| 3.2.2.9. Expression of recombinant soluble guanylyl cyclase in the baculovirus/insect cell system | 34 |
| 3.2.3. Preparation of cytosolic fractions of Sf9 cells..... | 34 |
| 3.2.4. Purification of soluble guanylyl cyclase..... | 35 |
| 3.2.4.1. Purification procedure | 35 |
| 3.2.4.2. Protein concentration..... | 35 |
| 3.2.5. SDS-polyacrylamide gel electrophoresis..... | 36 |
| 3.2.5.1. Sample preparation | 36 |
| 3.2.5.2. SDS-polyacrylamide gel electrophoresis procedure..... | 36 |
| 3.2.6. Coomassie blue staining | 37 |
| 3.2.7. Western blot..... | 37 |
| 3.2.8. Guanylyl cyclase activity assay | 38 |
| 3.2.9. UV/Vis spectroscopy | 38 |
| 3.2.10. FRET experiment | 39 |
| 3.2.10.1. Calculation of FRET efficiency..... | 40 |
| 3.2.11. Direct fluorescence experiments | 41 |
| 4. RESULTS | 43 |
| 4.1. SITE-DIRECTED MUTAGENESIS | 43 |
| 4.2. BAC-TO-BAC BACULOVIRUS EXPRESSION SYSTEM | 43 |
| 4.2.1. Generation of baculovirus | 43 |
| 4.2.2. Expression and purification of soluble guanylyl cyclase | 45 |
| 4.3. SDS-POLYACRYLAMIDE GEL ELECTROPHORESIS AND COOMASSIE BLUE STAINING ... | 45 |
| 4.4. WESTERN BLOT ANALYSIS | 47 |
| 4.5. UV/VIS SPECTROSCOPY | 49 |
| 4.6. GUANYLYL CYCLASE ACTIVITY ASSAY | 52 |
| 4.7. FRET ANALYSIS | 54 |
| 4.7.1. Fluorescence emission spectra..... | 54 |
| 4.7.2. FRET efficiency | 58 |
| 4.8. DIRECT FLUORESCENCE EXPERIMENTS..... | 61 |
| 5. DISCUSSION..... | 63 |
| 5.1. GUANYLYL CYCLASE, 2'-MANT-3'-dGTP AND FRET | 63 |
| 5.2. MUTAGENESIS, EXPRESSION AND PURIFICATION | 64 |
| 5.3. SPECTRAL ANALYSIS..... | 65 |
| 5.4. GUANYLYL CYCLASE ACTIVITY ASSAY | 65 |
| 5.5. FRET..... | 66 |
| 5.5.1. Tryptophan 36..... | 67 |
| 5.5.2. Tryptophan 505..... | 67 |
| 5.5.3. Tryptophan 602..... | 68 |
| 5.5.4. Tryptophan 22..... | 68 |
| 5.6. DIRECT FLUORESCENCE EXPERIMENT | 69 |

| | |
|----------------------------|-----------|
| 6. CONCLUSION | 70 |
| 7. REFERENCES | 71 |
| 8. SUPPLEMENTS..... | 74 |
| SUPPLEMENT 1..... | 74 |
| SUPPLEMENT 2..... | 76 |
| SUPPLEMENT 3..... | 78 |

Table of figures

| | |
|--|----|
| Figure 1: The NO/cGMP-signaling pathway..... | 2 |
| Figure 2: Domain architecture of soluble guanylyl cyclase (sGC). | 3 |
| Figure 3: Organization of heterodimeric sGC based on CC orientation.. | 5 |
| Figure 4: Chemical structure of DEA/NO | 6 |
| Figure 5: Proposed model of the heterodimeric sGC enzyme complex based on the results of FRET analysis and fusion of sGC subunits. | 8 |
| Figure 6: Jablonski diagram illustrating electronic transitions..... | 9 |
| Figure 7: Dependence of energy transfer efficiency (E) on D-A separation..... | 10 |
| Figure 8: A FRET pair with sufficient spectral overlap. | 11 |
| Figure 9: Structure of antraniloyl (Ant) and methylantraniloyl (Mant) derivatives of ATP and GTP. | 12 |
| Figure 10: Absorption spectra of antraniloyl (ANT-) and methylantraniloyl (MANT-) derivatives of ATP and GTP. | 12 |
| Figure 11: Fluorescence emission spectra of MANT-GTP in the absence and presence of C1/C2 and MP-FSK.. | 14 |
| Figure 12: Absorption spectra of tyrosin and tryptophan | 16 |
| Figure 13: Absorption and emission spectra of tryptophan and tyrosin..... | 16 |
| Figure 14: Generation of recombinant baculovirus and the expression of a gene of interest using Bac-to-Bac TOPO Expression System..... | 30 |
| Figure 15: Transposed pFastBac sequence (Invitrogen, 2008) | 31 |
| Figure 16: 2'-MANT-3'-dGTP | 39 |
| Figure 17: Scheme for obtaining the data in FRET experiment using sensitized emission method with three channels..... | 40 |
| Figure 18: Scheme for obtaining the data in the direct fluorescence experiment. | 42 |
| Figure 19: 1% agarose gel electrophoresis of PCR products of recombinant bacmid DNA..... | 44 |
| Figure 20: SDS-PAGE of cytosolic fractions and purified sGC | 46 |
| Figure 21: SDS-PAGE of cytosolic fractions and purified sGC | 46 |
| Figure 22: Western blot analysis of cytosolic fractions and purified sGC. | 48 |
| Figure 23: Spectral analysis of α_2S/β_1 | 49 |
| Figure 24: Spectral analysis of α_2SW36A/β_1 and $\alpha_2SW505A/\beta_1$ | 50 |
| Figure 25: Spectral analysis of α_2S/β_1W602A and α_2S/β_1H105A | 51 |
| Figure 26: Guanylyl cyclase activity of purified α_2S/β_1 in comparison with mutant $\alpha_2SW505A/\beta_1$, α_2SW36A/β_1 , α_2S/β_1W602A , and α_2S/β_1H105A | 53 |
| Figure 27: Fluorescence emission spectra of purified α_2S/β_1 | 55 |
| Figure 28: Fluorescence emission spectra of purified α_2SW36A/β_1 and $\alpha_2SW505A/\beta_1$ | 56 |
| Figure 29: Fluorescence emission spectra of purified α_2S/β_1W602A and α_2S/β_1H105A | 57 |
| Figure 30: FRET efficiencies (%) obtained from three independent FRET experiments..... | 59 |
| Figure 31: Increase of FRET efficiency (%) after addition of DEA/NO. | 60 |
| Figure 32: Normalized fluorescence intensity of 2'-MANT-3'-dGTP in presence of sGC and after addition of DEA/NO | 62 |

LIST OF ABBREVIATIONS

| | |
|--------------------|--|
| A | acceptor |
| AC | adenylyl cyclase |
| ANP | atrial natriuretic peptide |
| ANT- | anthraniloyl |
| ASBT | acceptor spectral bleed-through |
| Bluo-gal | 5-bromo-3-indolyl- β -D-galactopyranoside |
| bp | base pair |
| BSA | bovine serum albumin |
| CAT | catalytic domain |
| CaM | calmodulin |
| CC domain | coiled-coil domain |
| cGK | cGMP-dependent protein kinase |
| cGMP | cyclic guanosine monophosphate |
| CyaA | <i>Bordetella pertussis</i> adenylyl cyclase |
| D | donor |
| Da | Dalton |
| DEA/NO | 1,1-diethyl-2-hydroxy-2-nitroso-hydrazine |
| ddH ₂ O | double distilled water |
| DMSO | dimethyl sulfoxide |
| dNTP | deoxyribonucleotide triphosphate |
| DSBT | donor spectral bleed-through |
| dsDNA | double stranded DNA |
| DTT | dithiothreitol |
| E% | efficiency of energy transfer |
| eCFP | enhanced cyan fluorescent protein |
| ECL | enhanced chemiluminescence |
| <i>E. coli</i> | <i>Escherichia coli</i> |
| EDTA | ethylenediaminetetraacetic acid |
| EF | edema factor |
| eNOS | Endothelial NOS |
| eYFP | enhanced yellow fluorescent protein |
| F | fluorescence |
| FP | fluorescent protein |
| FRET | Fluorescence resonance energy transfer |
| GTP | guanosine triphosphate |
| iNOS | inducible NOS |
| HABA | 2-(4'-hydroxy-benzeneazo)benzoic acid |
| HEPES | 4-(2-hydroxyethyl)-1-piperazineethanesulfonic acid |
| H-NOBA | heme-nitric oxide binding associated |
| H-NOX domain | heme nitric oxide/oxygen binding domain |
| H-NOXA | heme-nitric oxide/oxygen binding associated |

| | |
|-----------------|--|
| HRP | horseradish peroxidase |
| IC | internal conversion |
| IPTG | isopropyl β -D-1-thiogalactopyranoside |
| K_i | inhibition constant |
| LB | Luria Bertani |
| mAC | membrane-bound adenylyl cyclase |
| MANT- | methylanthraniloyl |
| 2'-MANT-3'-dGTP | 2'-O-(N-Methyl-anthraniloyl)-3'-deoxy-guanosine-5'-triphosphate |
| nNOS | neuronal NOS |
| NO | nitric oxide |
| NONOate | diazoniumdiolate |
| NOS | nitric oxide synthase |
| NRD | nonradiative decay |
| PAS domain | Per/Arnt/Sim domain |
| PBS | phosphate buffered saline |
| PCR | polymerase chain reaction |
| PDE | phosphodiesterase |
| PSD-95 protein | postsynaptic density-95 protein |
| R_0 | Förster distance |
| r | distance between the donor and the acceptor |
| SDS | sodium dodecyl sulfate |
| Sf | <i>Spodoptera frugiperda</i> |
| sGC | soluble guanylyl cyclase |
| SOC medium | salt-optimized carbon broth |
| SPER/NO | 1-[N-[3-aminopropyl]-N-[4-(3-aminopropylammonio)butyl]-amino]diazene-1,2-diolate |
| TAE buffer | Tris-acetate-EDTA-buffer |
| <i>Taq</i> | <i>Thermus aquaticus</i> |
| TBST | Tris-buffered-saline-Tween |
| TEA/HCl | triethanolamine/ hydrochloric acid |
| TEMED | N,N,N',N'-tetramethylethylenediamine |
| Tris | Tris-(hydroxymethyl)-aminomethane |
| uFRET | uncorrected FRET |
| UV | ultraviolet |

POVZETEK

Topna gvanilat-ciklaza je znotrajcelični receptor za dušikov oksid (NO) in je sestavljena iz podenot α in β . Vsaka podenota je sestavljena iz štirih domen: N-končne domene H-NOX, centralnih PAS- in CC- ter C-končne katalitične domene. Vezava dušikovega oksida na prostetično skupino hema v domeni H-NOX podenote β_1 poveča sintezo cikličnega gvanozin monofosfata iz gvanozin trifosfata. Ciklični gvanozin monofosfat se kot sekundarni obveščevalec veže na fosfodiesteraze, ionske kanale in proteinske kinaze ter regulira fiziološke procese, ki vključujejo vazodilatacijo, nevrottransmisijo in agregacijo trombocitov. Do sedaj še niso znane relativne pozicije domen v topni gvanilat-ciklazi, prav tako tudi ni pojasnjeno, kako vezava dušikovega oksida poveča katalitično aktivnost encima.

(N-metil)antranoil-substituirani nukleotidi (MANT-NTP) so fluorescenčno označeni nukleotidi in kompetitivni inhibitorji topne gvanilat-ciklaze, adenilat-ciklaze vezane na membrano sesalskih celic, adenilat-ciklaznih toksinov iz vrst *Bordetella pertussis* in *Bacillus anthracis*. Služijo nam lahko tudi kot akceptorji prenosa energije z resonanco fluorescence (FRET), ko konformacija encima omogoča zadostno bližino med njimi in vzbujenimi donorji FRET, ki jih predstavljajo triptofanski in tirozinski ostanki encima. MANT-NTP so občutljivi za okolje, saj se njihova fluorescenca v hidrofobnem okolju poveča.

Izooblika topne gvanilat-ciklaze α_2S/β_1 vsebuje štiri triptofanske ostanke v različnih domenah encima, ki bi lahko služili kot donorji FRET, če bi konformacija encima omogočala zadostno bližino med njimi in fluorescenčno sondo 2'-MANT-3'-dGTP v aktivnem mestu. Z mutacijo posameznih triptofanskih ostankov v topni gvanilat-ciklazi smo analizirali, katera domena oz. kateri triptofanski ostanek je blizu aktivnega mesta encima v prisotnosti in odsotnosti dušikovega oksida.

Z usmerjeno mutagenozo smo v podganji α_2 -podenoti topne gvanilat-ciklaze zamenjali triptofana 36 in 505 z alaninom. Divji tip encima iz podganje α_2S - in humane β_1 -podenote (α_2S/β_1) ter mutantne encime α_2SW36A/β_1 , $\alpha_2SW505A/\beta_1$, α_2S/β_1H105A , α_2S/β_1W602A , smo izrazili z bakulovirusnim ekspresijskim sistemom in očistili z afinitetno kromatografijo. Uporabili smo poliakrilamidno gelsko elektroforezo v prisotnosti natrijevega dodecilsulfata in barvanje gela s Coomassie Brilliant Blue za oceno čistote encima. Identiteto posameznih podenot pa smo potrdili s prenosom western. Izmerili smo

aktivnost očiščene topne gvanilat-ciklaze in spektrofotometrično analizirali njeno vsebnost hema. 2'-MANT-3'-dGTP smo uporabili za merjenje neposredne fluorescence in eksperimente FRET. S spektrofluorometrom smo proučili konformacijo aktivnega mesta topne gvanilat-ciklaze v prisotnosti in odsotnosti dušikovega oksida.

Triptofan 36 na začetku domene H-NOX podenote α_2 in triptofan 602 v katalitični domeni podenote β_1 sta verjetno edina triptofana blizu aktivnega mesta encima v bazalnih pogojih. Ker je triptofan 36 na N-koncu podenote α_2 , aktivni center pa je sestavljen iz C-končnih katalitičnih domen obeh podenot, naš rezultat podpira model, v katerem sta domeni PAS in H-NOX zaviti nazaj proti katalitični domeni topne gvanilat-ciklaze (Haase et al., 2010). Položaj triptofana 36 se verjetno v prisotnosti dušikovega oksida ne spremeni bistveno.

Naši rezultati kažejo, da bi se v prisotnosti dušikovega oksida katalitičnemu centru topne gvanilat-ciklaze lahko približala triptofan 505 na koncu domene CC podenote α_2 in/ali triptofan 602 v katalitični domeni podenote β_1 . Ne vemo, katera predpostavka je pravilna oziroma ali sta mogoče pravilni celo obe. Mutacija triptofana 505 v alanin je povzročila neaktivnost encima, čeprav je ta vseboval hem. Mutantnemu encimu α_2S/β_1W602A se je tudi zmanjšala občutljivost za dušikov oksid, kar je morda povezano s precejšno/delno izgubo hema. Tudi triptofan 22 na začetku domene H-NOX podenote β_1 bi se lako približal aktivnemu mestu encima, vendar te hipoteze nismo testirali za encim α_2S/β_1 , saj se je že pri encimu α_1S/β_1 izkazalo, da mutacija tega triptofana v alanin vodi v mutantni encim brez hema. Rezultati merjenja neposredne fluorescence kažejo, da je okolje 2'-MANT-3'-dGTP v katalitičnem centru topne gvanilat-ciklaze α_2S/β_1 bolj hidrofobno kot puferska raztopina (25 mM HEPES/NaOH, 100 mM KCl, 3 mM MgCl₂; pH 7.4) in da se hidrofobnost aktivnega centra ne spremeni dosti v prisotnosti dušikovega oksida.

Da bi zanesljivo dokazali, kateri triptofanski ostanek se približa aktivnemu centru topne gvanilat-ciklaze v prisotnosti dušikovega oksida so potrebne še nadaljne raziskave.

ABSTRACT

Soluble guanylyl cyclase (sGC) is an intracellular receptor for nitric oxide (NO) consisting of α and β subunits. Each subunit consists of four domains: N-terminal H-NOX domain, PAS domain, CC domain and C-terminal catalytic domain. Binding of nitric oxide to the prosthetic heme group in the β_1 subunit increases synthesis rate of cyclic GMP from GTP several 100-folds. Cyclic GMP as a secondary messenger binds to phosphodiesterases, ion channels and protein kinases to regulate several physiological functions including vasodilatation, neurotransmission and inhibition of platelet aggregation. Relative positions of sGC domains in the holoenzyme have not been determined and translation of NO binding into increased catalytic activity has not been explained.

(N-methyl)anthraniloyl-substituted nucleotides (MANT-NTPs) are fluorescently labeled nucleotides and competitive inhibitors of soluble guanylyl cyclase, mammalian membrane-bound adenylyl cyclase, adenylyl cyclase toxin of *Bordetella pertussis* and *Bacillus anthracis*. They were already used as fluorescence resonance energy transfer acceptors when tyrosine or tryptophan residues were excited and a sufficient proximity between these residues and the MANT-group was provided by the conformation of the enzyme. MANT-NTPs are also environmentally sensitive probes and exhibit increased fluorescence upon exposure to a hydrophobic environment.

There are four tryptophan residues in different domains of soluble guanylyl cyclase isoform $\alpha_2S(\text{rat})/\beta_1(\text{human})$ which might serve as FRET donors when the FRET acceptor 2'-MANT-3'-dGTP is in the substrate binding site and the conformation of the enzyme allows adequate proximity between them. By mutating individual tryptophan residues in the soluble guanylyl cyclase we analyzed which domain or which tryptophan is close to the active site of purified soluble guanylyl cyclase isoform $\alpha_2S(\text{rat})/\beta_1(\text{human})$ in the presence or absence of NO.

Site-directed mutagenesis was used to replace tryptophan 36 and 505 with alanine residues in the rat α_2 subunit of soluble guanylyl cyclase. The wild type enzyme $\alpha_2S(\text{rat})/\beta_1(\text{human})$ and mutant α_2SW36A/β_1 , $\alpha_2SW505A/\beta_1$, α_2S/β_1H105A and α_2S/β_1W602A were expressed with baculovirus/Sf9 system and purified with *Strep*-tag affinity chromatography. SDS-polyacrylamide gel electrophoresis and Coomassie blue staining were used to assess the purity of the enzyme while its identity was verified using western blot analysis. Guanylyl cyclase activity of the purified soluble guanylyl cyclase was measured and heme content was analyzed spectrophotometrically. 2'-MANT-3'-dGTP was used in direct fluorescence

experiments and fluorescence resonance energy transfer experiments were performed to analyze the conformation of the active site of purified soluble guanylyl cyclase in the presence or absence of NO.

Tryptophan 36 at the beginning of H-NOX domain of the α_2 subunit and tryptophan 602 in the catalytic domain of β_1 subunit are very likely to be the only tryptophan residues close to the substrate binding site under basal conditions. Because tryptophan 36 is on the N-terminal end of α_2 subunit and the catalytic center is formed by dimerization of C-terminal catalytic domains of both subunits, our results support the model of Haase et al. (2010), which suggests that PAS and H-NOX domains of sGC are folded back towards the catalytic domain. Position of tryptophan 36 very likely does not change evidently in the presence of NO.

Our results suggest that after binding of NO to the prosthetic heme group of $\alpha_2\text{S}/\beta_1$, tryptophan 505 at the end of the CC domain of α_2 subunit and/or tryptophan 602 in catalytic domain of β_1 subunit could move closer to the substrate binding site. We do not know which assumption is accurate, maybe both of them are, because mutation of tryptophan 505 to alanine led to inactive sGC although it contained heme. The mutant enzyme $\alpha_2\text{S}/\beta_1\text{W602A}$ was also inactive but possibly due to partial heme loss. Tryptophan 22 at the beginning of H-NOX domain of β_1 subunit could also move closer to the substrate binding site but this hypothesis was not tested for $\alpha_2\text{S}/\beta_1$ because mutation of tryptophan 22 led to a heme-free mutant isoform $\alpha_1\text{S}/\beta_1$. Results of direct fluorescence experiment suggest that the environment of 2'-MANT-3'-dGTP in the catalytic center of sGC isoform is more hydrophobic than the buffer solution (25 mM HEPES/NaOH, 100 mM KCl, 3 mM MgCl_2 ; pH 7.4) and that the hydrophobicity of the active center changes only marginally under NO-stimulating conditions.

Further experiments are needed to identify the tryptophan residue that moves close to the substrate binding site under NO-stimulating conditions.

1. INTRODUCTION

1.1. THE NITRIC OXIDE/CYCLIC GMP-SIGNALING PATHWAY

Glyceryl trinitrate or nitroglycerin was first synthesized by Ascanio Sobrero in 1847. It is the most powerful explosive chemical discovered in the nineteenth century and the active ingredient in dynamite. Sobrero instantly noticed the strong headache produced by minute quantities of the substance applied to the tongue what motivated the medical interest in the substance. In 1897, William Murrell first reported on its use and efficacy as a remedy for angina pectoris and since then it has remained the treatment of choice for acute angina pectoris (Behrends, 2003).

This compound relieves the pain associated with angina pectoris by relaxing the vascular smooth muscle, leading to vasodilatation. For years, investigations were focused on the mechanism of smooth muscle relaxation by this molecule, and in the 1980s these efforts led to the discovery that nitric oxide (NO) is a physiologically relevant signaling molecule and to the identification of enzymes that biosynthesize NO and cGMP (Derbyshire and Marletta, 2012).

After stimulation by appropriate external signal, an increase in intracellular free Ca^{2+} occurs, which then leads to formation of Ca^{2+} -calmodulin (CaM) complex (Fig. 1). This complex binds to nitric oxide synthase (NOS), thereby activating NOS to synthesize NO (Marletta, 2004). NO then diffuses across a cell membrane and activates soluble guanylyl cyclase (sGC). NO binds to the heme of sGC and increases synthesis rate of cGMP from GTP several 100-folds. cGMP binds to phosphodiesterases (PDEs), cGMP-gated ion channels, and cGMP-dependent protein kinases to regulate several physiological functions including vasodilatation, neurotransmission and inhibition of platelet aggregation (Schmidt et al. 2009).

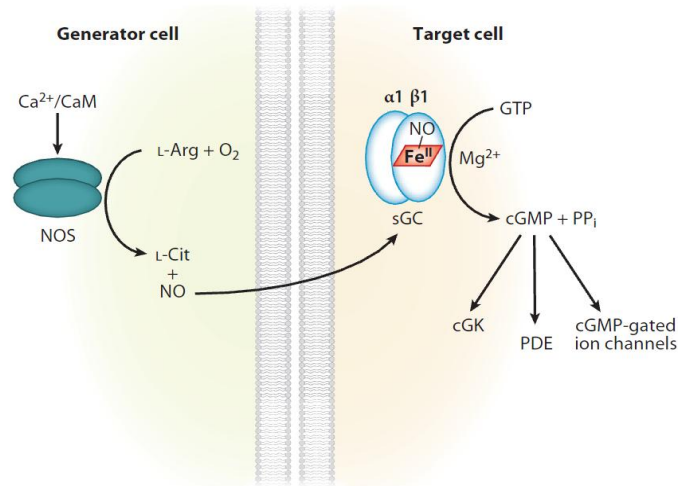


Figure 1: The NO/cGMP-signaling pathway. Abbreviations: CaM, calmodulin; NOS, nitric oxide synthase; L-Arg, L-arginine; L-Cit, L-citrulline; α_1 and β_1 , soluble guanylyl cyclase subunits; sGC, soluble guanylyl cyclase; PP_i, pyrophosphate; cGKs, cGMP-dependent protein kinases; PDEs, phosphodiesterases (Derbyshire and Marletta, 2012).

1.2. SOLUBLE GUANYLYL CYCLASE ISOFORMS

sGC is a heterodimeric protein consisting of two subunits, α and β . Four subunits have been identified, α_1 , α_2 , β_1 and β_2 , however the most commonly studied is the $\alpha_1\beta_1$ isoform (Schmidt et al., 2009). Subunits α_1 and β_1 are expressed in most tissues while the α_2 subunit shows a more restricted expression pattern with high levels in brain, placenta, spleen and uterus (Budworth et al., 1999). Subunits α_1 and α_2 share only 27% identical amino acids in the N-terminal region but they are functionally similar (Russwurm et al., 1998). Subunit β_2 is principally expressed in kidney (Yuen, 1990).

In platelets, $\alpha_1\beta_1$ is the only isoform present and is responsible for NO-induced inhibition of aggregation. In aortic tissue, $\alpha_1\beta_1$ as the major isoform (94%) mediates vasodilation. Minor isoform $\alpha_2\beta_1$, representing only 6% of the total sGC content in aortic tissue can also completely relax α_1 -deficient vessels albeit higher NO concentrations are needed. It is assumed that the majority of sGC is not required for cGMP-forming activity but as a reserve of NO receptor to increase sensitivity toward the labile messenger NO *in vivo* (Mergia et al. 2006).

It has been reported that the $\alpha_2\beta_1$ isoform interacts with synaptic adaptor protein PSD-95 in the rat brain. The interaction is mediated by the α_2 C-terminal peptide. The $\alpha_2\beta_1$ isoform is probably the sensor for the NO formed by the PSD-95-associated neuronal NO synthase (nNOS) (Russwurm, 2001).

1.3. SOLUBLE GUANYLYL CYCLASE DOMAIN STRUCTURE

The rat sGC α_1 and β_1 subunits are 690 and 619 amino acids in length, respectively. These proteins are part of a large family of sGC subunits that are conserved in eukaryotes. Generally, there is the highest sequence variability at the N-terminus of α subunits and the greatest sequence identity at the C-terminus of both, α and β . Each sGC subunit consists of four distinct domains: N-terminal heme nitric oxide/oxygen binding (H-NOX) domain, Per/Arnt/Sim (PAS) domain, coiled-coil domain and C-terminal catalytic domain (Fig. 2) (Derbyshire and Marletta, 2012).

Domain architecture of sGC

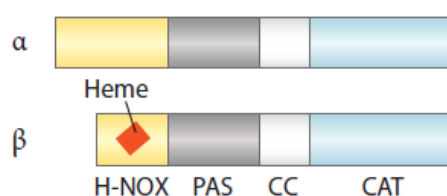


Figure 2: Domain architecture of soluble guanylyl cyclase (sGC). Heme-nitric oxide/oxygen binding domains (H-NOX, yellow), Per/Arnt/Sim domains (PAS, gray), coiled-coil domains (CC, white), and catalytic domains (CAT, blue) are shown. Heme is represented by the red parallelogram (Derbyshire and Marletta, 2012).

The heme-binding domain of sGC is localized at the N-terminus of the β_1 subunit. The presence of the heme prosthetic group is believed to be required for activation of sGC by NO, although there are some reports of non-heme binding site for NO in sGC, which is also involved in the activation process (Cary et al., 2005; Derbyshire and Marletta, 2007). The minimal heme binding domain is comprised of residues 1 to 194 of the β_1 subunit. Genomic analysis placed sGC heme domain within a conserved family of proteins found in prokaryotes and eukaryotes. This family of proteins is termed heme-nitric oxide and oxygen binding (H-NOX) family based on their ligand binding properties - namely, they bind NO and CO, but not O₂ (Schmidt et al., 2009). It is suggested that H-NOX proteins have an evolutionarily conserved function and serve as gas sensors in prokaryotes and eukaryotes (Derbyshire and Marletta, 2012).

Heme is a five-membered nitrogen-containing ring wherein four nitrogen atoms are coordinated with a central ferrous iron. The fifth member of the ring is an imidazole axial ligand coordinated by the histidine 105 of the β_1 subunit (Lucas et al., 2000). When NO

binds, the bond between the histidine 105 and the iron is broken, forming a nitrosyl-heme complex (Krumenaker et al., 2004). Mutation of histidine 105 in the β_1 subunit results in the inability of the sGC heterodimer to bind heme and is therefore unresponsive to NO (Wedel et al., 1994).

The sGC heterodimer contains one heme with a high affinity for NO. Even in aerobic environment, sGC prefers to bind NO rather than oxygen (O_2). Oxidation of the heme group to ferric state results in the loss of enzyme activity and often a complete loss of the heme moiety from the protein (Lucas et al., 2000).

The N-terminus of the α_1 subunit is not involved in heme binding, because the first 259 amino acid residues of the α_1 subunit can be deleted without loss of sensitivity to NO or loss of heme binding of the respective enzyme complex with the β_1 subunit. Further deletion of the first 364 residues leads to an enzyme complex with preserved heme binding but loss of sensitivity to NO. The NO binding to heme induces a typical spectral shift; therefore residues 259 to 364 have an important function for the transduction of the NO activation signal (Koglin and Behrends, 2003).

It has been recently reported that the N-terminus of the α_1 subunit is also dispensable for dimerization of sGC as it influences the subcellular trafficking (Kraehling et al., 2011).

The PAS domain includes residues ~200-350 of the β_1 subunit and 270-400 of the α_1 subunit. It is predicted to adopt a PAS-like fold. Typically PAS domains mediate protein-protein interactions and/or bind small molecules such as heme, flavines and nucleotides (Schmidt et al., 2009). This domain is also termed H-NOXA as it is often associated with the H-NOX domain (Cary et al., 2006).

The coiled-coil domain (CC) comprises residues 348-409 of the β_1 subunit. It appears to be unique to sGC and shares no significant homology with any other protein (Derbyshire and Marletta, 2012). The crystal structure of CC domain of sGC β_1 revealed that each monomer is comprised of a long α -helix, a turn, and a short second α -helix, and that the CC domains form homodimers in an anti-parallel arrangement. Additional analysis (homology modeling) suggests a parallel arrangement in the full length heterodimeric sGC (Fig. 3). Heterodimerization is preferred over homodimerization probably in part due to inter-helix salt-bridge formation (Ma et al., 2010).

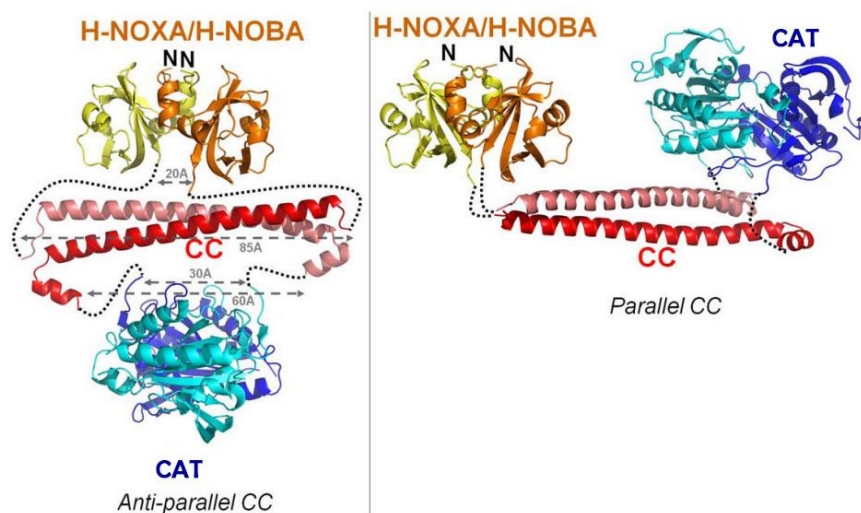


Figure 3: Organization of heterodimeric sGC based on the CC orientation. Possible H-NOXA/CC/CAT organization based on an anti-parallel CC dimer (left) and a parallel CC dimer (right). CAT (blue), H-NOXA/H-NOBA (yellow), and CC (red) domains are depicted. Abbreviations: H-NOXA/H-NOBA, heme-nitric oxide/oxygen binding associated/heme-nitric oxide binding associated; CC, coiled-coil; CAT, catalytic domain (Ma et al., 2010).

The catalytic domains are localized at the C-terminus. The catalytic domain of the α_1 subunit is comprised of residues 467-690 and that of β_1 of 414-619. sGC subunits must heterodimerize for cGMP to be synthesized and the catalytic efficiency is dependent on the heme ligation state of the β_1 H-NOX domain (Schmidt et al., 2009). It has been reported that the catalytic domains (α_{1cat} and β_{1cat}) of sGC are inactive separately, but together the domains exhibit guanylyl cyclase activity (Winger and Marletta, 2005). Architecture of the catalytic domains of sGC is homologous to the catalytic domains of adenylate cyclase, as expected due to their sequence similarity (Winger et al., 2008).

1.4. NITRIC OXIDE

NO is a small, inorganic molecule with 11 valence electrons and, therefore, has one unpaired electron. It is a free radical that has a very short half-life in biological systems (1-3 s) (Schmidt et al., 2009). It is unstable in aqueous aerobic solution. The solution chemistry consumes NO as it diffuses from a generator cell to the target cell, therefore the amount that arrives to the target cell is always low (Marletta, 2004).

1.4.1. Nitric oxide donors

Experimentally, NO donors represent a valuable scientific tool. Currently the only NO donors that release NO in solution without interference from tissue factors are diazeniumdiolates (NONOates). The most commonly used NONOates are DEA/NO and SPER/NO. They are distinguished by their release profiles. The half-lives of DEA/NO and SPER/NO are 2 and 39 minutes at 37 °C, pH 7.4 and 22-25 °C, respectively (Schmidt et al. 2009).

DEA/NO (1,1-diethyl-2-hydroxy-2-nitroso-hydrazine sodium (Fig. 4)) decomposes spontaneously in solution at physiological pH and temperature, to liberate 1.5 moles of NO per mole of the parent compound. NO release process follows the first order kinetics (Cayman chemical, 2012).

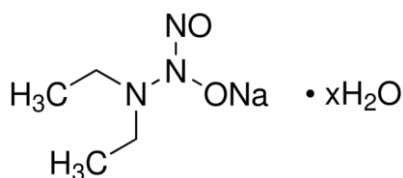


Figure 4: Chemical structure of DEA/NO (1,1-diethyl-2-hydroxy-2-nitroso-hydrazine sodium) (Sigma, 2012).

1.4.2. Biological processes controlled by nitric oxide

NO is synthesized by NOS, which converts L-arginine to citrulline and NO. There are three isoforms of NOS, endothelial, neuronal and inducible (eNOS, nNOS and iNOS). Both eNOS and nNOS are constitutively expressed, while iNOS is induced with appropriate immunostimulatory signals (Schmidt et al. 2009).

NO was first defined as endothelium-derived relaxing factor. In cardiovascular system NO is synthesized in the epithelium of vessels and causes vascular relaxation through interaction with sGC in blood vessel walls (Schmidt et al. 2009).

Neuronal NOS is found post-synaptically in the central nervous system, where it appears to have a neuromodulatory function that is associated with a long-term potentiation and memory. NO is most famous for its ability to relax corpus cavernosum tissue and mediate penile erection (Schmidt et al. 2009).

Induction of iNOS generates relatively high (μM) local concentrations of NO. NO together with superoxide and hypochlorous acid (HOCl) is the central defence against microbial invasion in some leukocytes (e.g. neutrophils). Any cell has the potential to express iNOS. Very severe infections (e.g., toxic shock syndrome) can result in systemic iNOS expression and generation of large quantities of NO (Schmidt et al. 2009).

1.5. CONFORMATIONAL CHANGES UPON SOLUBLE GUANYLYL CYCLASE ACTIVATION

So far the crystal structure of the heterodimeric sGC holoprotein has not been determined and the relative positions of sGC domains are lacking. It is also unknown how NO binding to the N-terminal β_1 H-NOX may influence the conformation of the C-terminal catalytic domain. The classic idea has been that NO binding to β_1 H-NOX induces a conformational shift of the whole enzyme that is transmitted to the C-terminal catalytic domain through the PAS and CC domains. This would be analogous to membrane bound guanylyl cyclase A where binding of atrial natriuretic peptide (ANP) to the extracellular domain is clearly separated from the intracellular catalytic domain by the plasma membrane (Haase et al., 2010).

A more novel concept is that β_1 H-NOX may directly interact with the catalytic region (Haase et al., 2010). Winger and Marletta (2005) have shown that the activity of the heterodimeric complex $\alpha_{1\text{cat}}/\beta_{1\text{cat}}$ is inhibited by the presence of the β_1 H-NOX domain. They suggested a model in which binding of NO to sGC causes relief of an autoinhibitory interaction between the β_1 H-NOX domain and the catalytic domains of sGC.

Haase et al. (2010) used fluorescent fusion proteins of sGC to show close proximity of the N-terminal H-NOX domains and the catalytic region supporting the model of Winger and Marletta. Their results indicate that the domains within sGC are organized in a more compact way allowing for direct interaction of the N-terminal regulatory domains with the C-terminal catalytic region. That means that the PAS and H-NOX domains are folded back towards the catalytic domain and that an elongated organization analogous to the membrane bound guanylyl cyclase, where the regulatory N-terminus is clearly separated from the catalytic domain, is not compatible with their data (Haase et al., 2010).

The NO binding to heme does not change relative positions of the fluorophores fused C-terminally to α and β subunits. Therefore drastic conformational change in the catalytic region after NO binding to heme is very unlikely (Haase et al., 2010).

The organization suggested by Haase et al. (2010) (Fig. 5B) is also in accordance with the organization of heterodimeric sGC based on the parallel CC orientation proposed by Ma et al. (2010) (Fig. 3).

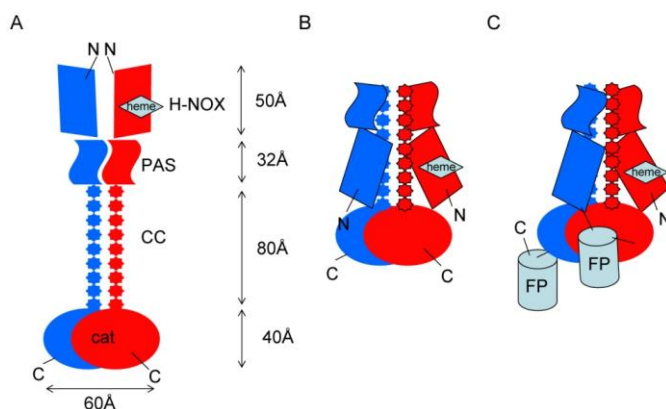


Figure 5: Proposed model of the heterodimeric sGC enzyme complex based on the results of FRET analysis and fusion of sGC subunits (Haase et al., 2010). Elongated model of the sGC (A). Model according to Haase et al. (2010) (B). Model of fluorescent-conjoined sGC (C). The β_1 subunit is shown in red and the α subunit is in blue. Abbreviations: cat, catalytic domain; CC, coiled coil region; PAS, Per-Arnt-Sim fold; HNOX, heme nitric oxide/oxygen binding domain, FP, fluorescent protein.

1.6. FLUORESCENCE RESONANCE ENERGY TRANSFER

Fluorescence resonance energy transfer (FRET) is a physical process by which energy is transferred non-radiatively from an excited molecular chromophore (the donor, D) to another chromophore (the acceptor, A) by means of intermolecular long-range dipole-dipole coupling. The transfer is non-radiative, that is, the donor does not actually emit a photon and the acceptor does not absorb it (Clegg, 1995).

The Jablonski diagram (Fig. 6) illustrates electronic states of a molecule and transitions between them. Irradiation of a chromophore elicits a transition from the S_0 ground state to a higher energy S_1 state to any vibrational level. The internal conversion (IC) represents a rapid internal conversion to the lowest vibrational level in the excited state. From this point the energy is lost relatively slowly by nonradiative decay (NRD, emission of heat) and by emission of a photon (fluorescence, F). FRET provides additional deactivation pathway for an excited donor chromophore if the donor chromophore is in molecular contact with the

acceptor chromophore and providing there is a sufficient spectral overlap (Chhabra and dos Remedios, 2005).

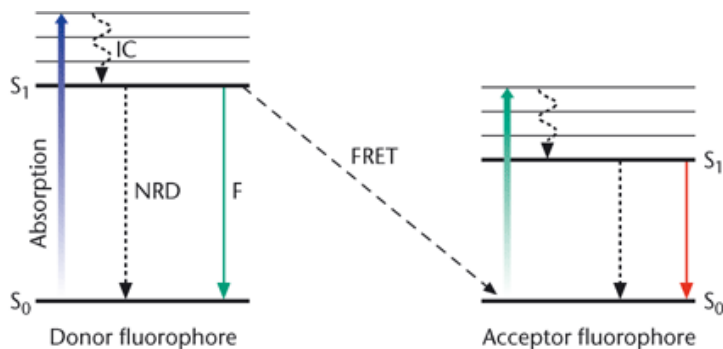


Figure 6: Jablonski diagram illustrating electronic transitions. The thick horizontal lines represent the S_0 and S_1 electronic energy levels, and the thin horizontal lines represent different vibrational levels within the S_1 state. Abbreviations: internal conversion (IC), nonradiative decay (NRD), fluorescence (F), fluorescence resonance energy transfer (FRET) (Chhabra and de Remedios, 2005).

Donor molecule typically emits at shorter wavelengths, which overlap with the absorption spectrum of acceptor. The efficiency of this process is dependent on the extent of spectral overlap of the donor emission spectrum with the acceptor absorption spectrum (Fig. 8), the quantum yield of the donor, the relative orientation of the donor and acceptor transition moments, and the distance between the donor and acceptor molecules (typically 10 to 100 Å) (Periasamy and Day, 2005).

The Förster distance (R_0) is the distance between donor and acceptor at which half of the exciting energy of the donor is transferred to the acceptor, while the other half is dissipated by all other processes, including emission. In other words, for $r = R_0$, 50% of the donor excitation energy is transferred to the acceptor and 50% deactivated in all other processes (radiative and nonradiative) (Periasamy and Day, 2005).

The value of R_0 (in Å) may be calculated from the following equation (Eq. 1):

$$R_0 = [8.79 \times 10^{23} \Phi_D \kappa^2 n^{-4} J(\lambda)]^{1/6} \quad (\text{Equation 1})$$

where

n is refraction index of the medium which is typically assumed to be 1.4 for biomolecules in aqueous solutions but may vary from 1.33 to 1.6 for biological media,

κ^2 is dipole orientation factor equal to $2/3$ for randomly distributed fluorophores and ranges from 0 to 4,

Φ_D is quantum yield of the donor in the absence of acceptor, and

$J(\lambda)$ is spectral overlap integral and λ is wavelength (nm).

1.6.1. The efficiency of energy transfer

The efficiency of energy transfer (E) is a quantitative measure of number of quanta that are transferred from the donor to the acceptor. E is essentially the quantum yield of energy transfer, which is defined by Equation 2 (Clegg, 1995).

$$E = \frac{\text{the number of quanta transferred from } D \text{ to } A}{\text{the number of quanta absorbed by } D} \quad (\text{Equation 2})$$

The efficiency of energy transfer is measured using the relative fluorescence intensity of the donor, in the absence (F_D) and in the presence (F_{DA}) of the acceptor (Equation 3) (Periasamy and Day, 2005).

$$E = \frac{F_D - F_{DA}}{F_D} = 1 - \frac{F_{DA}}{F_D} \quad (\text{Equation 3})$$

The relationship between the efficiency of energy transfer (E) and the distance between the donor and acceptor (r) is given by the Equation 4 (Clegg, 1995):

$$E = \frac{1}{1 + (r/R_0)^6} \quad (\text{Equation 4})$$

Equation 4 shows that efficiency of energy transfer is dependent on the sixth power of the distance (r) between the donor and the acceptor (Clegg, 1995). The energy transfer efficiency is most sensitive to distance changes when the donor-acceptor separation length approaches the Förster distance (R_0) for the two molecules. The efficiency quickly increases to 1.0 as the donor-acceptor distance is below R_0 . For instance, if $r = 0.5R_0$ the energy transfer efficiency is 98.5%, and if $r = 2R_0$ the energy transfer efficiency is only 1.5% (Fig. 7) (Periasamy and Day, 2005).

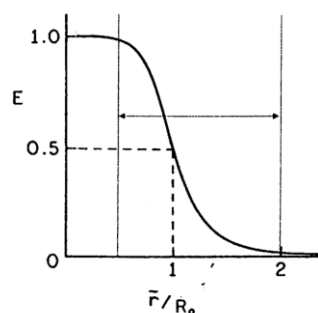


Figure 7: Dependence of energy transfer efficiency (E) on D-A separation. R_0 is the Förster distance (Periasamy and Day, 2005).

1.6.2. The spectral bleed-through

One of important conditions for FRET to occur is the overlap of the emission spectrum of the donor with the absorption spectrum of the acceptor (Fig. 8). The spectral overlap is also the cause of FRET signal contamination, termed spectral bleed-through (SBT). Donor spectral bleed-through (DSBT) refers to the part of the donor emission spectrum that overlaps with acceptor emission, and acceptor spectral bleed-through (ASBT) refers to the part of the acceptor absorption spectrum that is excited by the donor wavelength (Wallrabe and Periasamy, 2005).

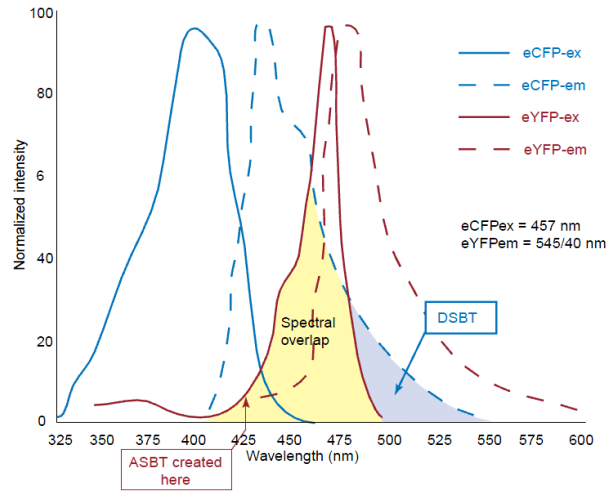


Figure 8: A FRET pair with sufficient spectral overlap. Excitation (solid line) and emission (dashed line) spectra of donor (eCFP) and acceptor (eYFP) are shown. The requirement of FRET for sufficient spectral overlap (yellow) occurs at the expense of spectral bleed-through. Abbreviations: ASBT, acceptor spectral bleed trough; DSBT, donor spectral bleed -rough; eCFP, enhanced cyan fluorescent protein; eYFP, enhanced yellow fluorescent protein (Wallrabe and Periasamy, 2005).

It is important that uncorrected FRET (uFRET) is corrected for donor and acceptor spectral bleed-through. The equation 5 shows the corrected FRET (cFRET) (Wallrabe and Periasamy, 2005).

$$cFRET = uFRET - DSBT - ASBT \quad (\text{Equation 5})$$

The FRET efficiency (E%) can be calculated according to Wallrabe and Periasamy (2005) (Equation 6).

$$E\% = \left(1 - \frac{F_{DA, \text{donnor channel}}}{F_{DA, \text{donnor channel}} - cFRET}\right) \times 100 \quad (\text{Equation 6})$$

where

$F_{DA, \text{donnor channel}}$ is the fluorescence intensity of the donnor channel, when both, the donnor and the acceptor are present in the sample.

1.7.FLUORESCENT NUCLEOTIDES

1.7.1. Properties of fluorescent nucleotides

Anthraniloyl (ANT-) and methylanthraniloyl (MANT-) ATP and GTP (Fig. 9) are ribose-modified fluorescent analogs of adenine and guanine nucleotides, which were first synthesized and spectroscopically analyzed by Toshiaki Hiratsuka in 1983.

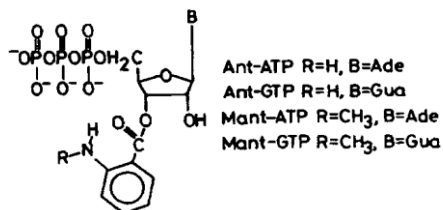


Figure 9: Structure of antraniloyl (Ant) and methylantrniloyl (Mant) derivatives of ATP and GTP (Hiratsuka, 1983).

The spectrum of ANT-ATP (Fig. 10) exhibits two maxima at 252 and 332 nm. A broad band centered at 332 nm is associated with the anthraniloyl group. The spectrum of MANT-ATP is similar to that of ANT-ATP except that an absorption band of the methylanthraniloyl group is centered at approximately 350 nm. The spectrum of the GTP analog is similar to that of the corresponding ATP analog, except that it exhibits a distinct shoulder around 280 nm, which is characteristic of guanine derivatives. Both, ANT-ATP and MANT-ATP fluorescence strongly in the range of 410-445 nm when excited with light in the 330-nm or 350-nm regions (Hiratsuka, 1983).

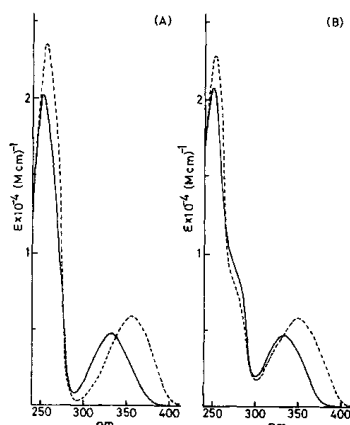


Figure 10: Absorption spectra of antraniloyl (ANT-) and methylantrniloyl (MANT-) derivatives of ATP and GTP. (A), ANT-ATP (—) and MANT-ATP (---) (B), ANT-GTP (—) and MANT-GTP (---). All spectra were measured in 50 mM Tris-HCl (pH 8.0) (Hiratsuka, 1983).

The potential usefulness of these analogs as fluorescent probes of hydrophobic microenvironments is indicated by the fact that the position of emission maxima and quantum yields of analogs vary significantly with solvent polarity. Their quantum yields are relatively low in water but significantly high in organic solvents (Hiratsuka, 1983).

Hiratsuka also reported that anthraniloyl and methylantraniloyl derivatives of nucleosides and nucleotides are stable for long periods of time (8 months in solution at neutral pH at -20 °C without significant degradation). They absorb and emit in the region far from that of proteins and their absorption and fluorescent properties are invariant in the physiological pH region. He concluded that anthraniloyl and methylantraniloyl derivatives of nucleosides and nucleotides are useful as fluorescent substrates for various enzymes and suggested they could be used to investigate structures of nucleoside- and nucleotide-requiring enzymes (Hiratsuka, 1983).

1.7.2. Applications of fluorescent nucleotides as molecular probes

1.7.2.1. Mammalian membrane-bound adenylyl cyclase

2'(3')-O-(N-methylantraniloyl)-substituted GTP analogs are a novel class of potent competitive adenylyl cyclase (AC) inhibitors (Gille and Seifert, 2003). Hydrophobic pocket in the catalytic site of ACs is also conserved in sGC and several MANT-adenine and MANT-guanine nucleotides inhibit sGC with K_i values in the 200-400 nM range. Exchange of $MnCl_2$ for $MgCl_2$ reduces inhibitor potencies at ACs and sGC (Gille et al, 2004).

The crystal structure of the purified catalytic subunits of mammalian membrane-bound adenylyl cyclase (mammalian mAC) in complex with MANT-GTP shows that MANT-GTP resides in a hydrophobic pocket at the interface between catalytic domains (C1 and C2) and prevents mAC from undergoing open to closed domain rearrangement. Mg^{2+} and Mn^{2+} ions serve as co-factors for mAC catalytic activity. MANT-GTP bound into C1·C2 complex coordinates the two metal ions. MANT-GTP· Mg^{2+} complex adopts a slightly more open conformation than the MANT-GTP· Mn^{2+} complex. This structural difference might reflect the higher affinity of C1·C2 complex for MANT-GTP· Mn^{2+} . In addition the inhibitory potency of MANT-GTP is 3-10-fold higher in the presence of Mn^{2+} compared to

Mg^{2+} . It is possible that Mg^{2+} , which possesses a much smaller ionic radius than Mn^{2+} , is more loosely tethered to coordinating groups in the enzyme (Mou et al., 2005).

Enzymatic and crystallographic data were also corroborated by FRET and direct fluorescence experiments. Fluorescence emission from MANT-GTP was measured in the absence and presence of C1·C2 complex and MP-FSK (an AC activator) either by FRET following excitation at 280 nm (Fig. 11A and C) or by direct excitation of MANT fluorescence at 350 nm (Fig. 11B and D). The experiments were conducted in the presence of either Mn^{2+} (Fig. 11A and B) or Mg^{2+} (Fig. 11C and D) (Mou et al., 2005).

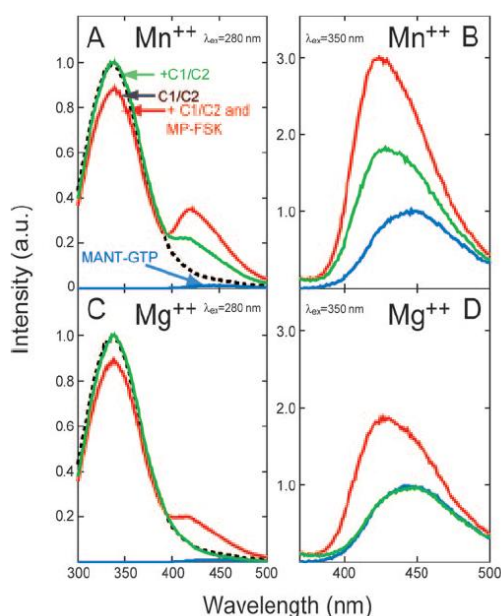


Figure 11: Fluorescence emission spectra of MANT-GTP in the absence and presence of C1·C2 and MP-FSK. Fluorescence emission spectra are shown for MANT-GTP alone (blue line) and C1·C2 only (black dashed line), MANT-GTP in the presence of C1·C2 (green line), and MANT-GTP in the presence of both C1·C2 and MP-FSK (red line). A and C show FRET experiments, B and D direct fluorescence experiments (Mou et al., 2005).

The addition of C1·C2 complex in the presence of Mn^{2+} increased MANT fluorescence upon excitation at 350 nm and shifted the MANT emission maximum from 450 to 420 nm (blue shift, Fig. 11B). The change in fluorescence emission intensity was consistent with the transfer of the MANT group to a hydrophobic environment. The addition of AC activator MP-FSK further increased fluorescence emission of MANT-GTP to about 3-fold above the value of the unbound compound (Mou et al., 2005).

The excitation of the C1·C2 complex in the presence of Mn^{2+} at 280 nm produced a broad emission peak at 350 nm (Fig. 11A) and addition of MANT-GTP caused a shoulder of

FRET-stimulated emission at 420 nm. Upon the addition of MP-FSK, there was a loss in fluorescence intensity at 350 nm with a concomitant increase in emission at 420 nm. Binding of MP-FSK to C1·C2 complex allows efficient FRET between a tryptophan residue in the substrate site, presumably W1020, and the MANT fluorophore (Mou et al., 2005).

In contrast to the results obtained with Mn^{2+} , the addition of C1·C2 complex to MANT-GTP in the presence of Mg^{2+} resulted only in a small fluorescence increase upon excitation at 350 nm (Fig. 11D). The increase in MANT-GTP fluorescence in the presence of both Mg^{2+} and MP-FSK was similar to that observed in the presence of Mn^{2+} alone (Fig. 11B). The blue shift in the fluorescence emission spectrum of MANT was only observed upon the addition of MP-FSK (Fig. 11D). Finally, in the presence of Mg^{2+} , the MP-FSK was much less efficient in promoting FRET than in the presence of Mn^{2+} (Fig. 11C versus A). Collectively, these data are indicative of a much stronger interaction between C1·C2 complex and MP-FSK in the presence of Mn^{2+} than in the presence of Mg^{2+} and confirm the enzymatic and crystallographic findings (Mou et al., 2005).

1.7.2.2. Adenylyl cyclase toxin of *Bordetella pertussis*

MANT nucleotides also inhibit *Bordetella pertussis* adenylyl cyclase (CyaA). When they bind to CyaA, FRET is generated from two tryptophan and multiple tyrosine residues located less than 20 Å from the catalytic site. The excitation of tryptophan and tyrosine residues at 280 nm results in high FRET signals and is more favorable than using tryptophan specific excitation wavelength at 295 nm, which leads to 3- to 4-fold lower FRET signals (Göttle et al., 2007).

1.7.2.3. Adenylyl cyclase toxin of *Bacillus anthracis*, edema factor

Various MANT nucleotides are potent inhibitors of adenylyl cyclase toxin, the edema factor (EF), which is an exotoxin produced by *Bacillus anthracis*. FRET from tryptophan and tyrosine residues located in the vicinity of the catalytic site to MANT-ATP was observed (Taha et al., 2008).

Suryanarayana et al. (2009) examined the effects of defined 2'- and 3'-MANT-isomers of ATP and GTP. In 2'(3')-O-ribosyl-substituted MANT nucleotides, the MANT-group

isomerizes spontaneously between 2'- and 3'-*O*- position of the ribosyl group (Jameson and Eccleston, 1997). Direct MANT fluorescence and FRET is much larger with 2'-MANT-3'-deoxy-GTP and 2'-MANT-3'-deoxy-ATP compared to the corresponding 3'-MANT-2'-deoxy isomers and 2'(3')-racemates. 3'-MANT-2'-deoxy-ATP inhibits EF more potently than 2'-MANT-3'-deoxy-ATP, whereas the opposite is the case for the corresponding GTP analogs. In conclusion, EF interacts differentially with 2'- and 3'-MANT isomers of ATP and GTP, which indicates conformational flexibility of the catalytic site (Suryanarayana et al., 2009).

1.8. ABSORPTION AND EMISSION OF TRYPTOPHAN VERSUS TYROSINE

Absorption of tyrosine is very low at 295 nm and therefore this excitation wavelength is tryptophan specific. At 280 nm tyrosine and tryptophan are excited but the absorption of tryptophan is higher than that of tyrosin (Fig. 12). At 335 nm the emission of tyrosine is very low and only tryptophan emits at this wavelength (Fig. 13).

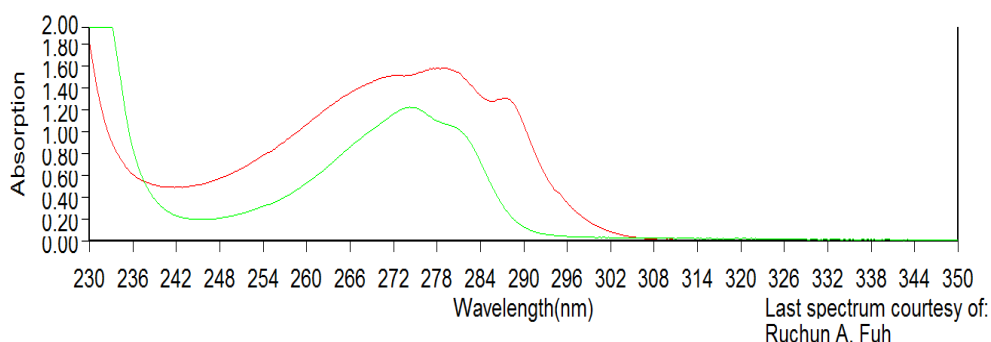


Figure 12: Absorption spectra of tyrosin (green) and tryptophan (red) (Photochemcad 2.1, computer program).

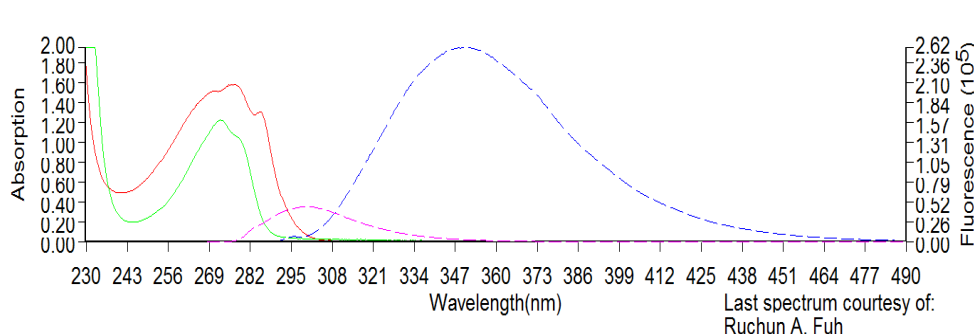


Figure 13: Absorption and emission spectra of tryptophan and tyrosine. Absorption of tryptophan (red), absorption of tyrosin (green), emission of tryptophan (blue), emission of tyrosin (pink) (pH 7) (Photochemcad 2.1, computer program).

1.9. LOCATION OF TRYPTOPHANE RESIDUES IN SOLUBLE GUANYLYL CYCLASE

The human β_1 subunit of sGC has two tryptophan residues. W22 is located in the H-NOX domain and W602 within the substrate binding site. Multiple sequence alignment (Supplement 1) shows that W36 is conserved on N-terminus of human and rat α_2 subunits of sGC but is absent in the α_1 subunit. Tryptophan residue at the end of CC domain is conserved in the human, dog, rat and mouse α_1 and in human and rat α_2 (W467 in human α_1 , W467 in dog α_1 , W466 in rat α_1 , W467 in mouse α_1 , W507 in human α_2 , W505 in rat α_2). The α_1 subunit has a tryptophan residue in the PAS domain which is conserved in humans, dogs, rats, mice (W353 in human α_1 , W352 in rat α_1) but it is absent in the α_2 subunit. The rat, dog and mouse α_1 subunit have an additional tryptophan residue close to the binding site of GTP (W669 in rat α_1) (Supplement 1).

For rat α_1 subunit it was shown that the deletion α_1 460-469 (at the end of the CC domain) (supplement 1, green) and α_1 470-479 (at the beginning of catalytic domain) (supplement 1 grey) resulted in a loss of enzymatic activity for sGC (Rothkegel et al., 2007).

2. RESEARCH OBJECTIVES

sGC is a heterodimeric hemoprotein consisting of α and β subunit. Each subunit consists of an N-terminal H-NOX domain, PAS domain, CC domain and a C-terminal catalytic domain. Binding of NO to the prosthetic heme group in the β_1 subunit increases the synthesis rate of cyclic GMP from GTP several 100-folds. Relative positions of sGC domains in the holoenzyme have not been determined yet and translation of NO binding into increased catalytic activity has not been explained.

(N-methyl)anthraniloyl-substituted nucleotides (MANT-NTPs) are fluorescently labeled nucleotides which were first synthesized by Toshiaki Hiratsuka in 1983. They are competitive inhibitors of mammalian membrane-bound adenylyl cyclase (Gille and Seifert, 2003), soluble guanylyl cyclase (Gille et al, 2004), adenylyl cyclase toxin of *Bordetella pertussis* (Göttle et al., 2007) and adenylyl cyclase toxin of *Bacillus anthracis*, the edema factor (Taha et al., 2008). They served as fluorescence resonance energy transfer acceptors when tyrosine or tryptophan residues were excited and a sufficient proximity between these residues and the MANT-group was provided by the conformation of the enzyme (Mou et al., 2005; Göttle et al., 2007, Taha et al., 2008).

MANT-NTPs are environmentally sensitive probes, which exhibit increased fluorescence upon exposure to hydrophobic environment (Hiratsuka, 1983). They have already been used to analyze the conformation of the catalytic site of adenylyl cyclase toxin of *Bacillus anthracis*, the edema factor (Suryanarayana et al., 2009) and mammalian membrane-bound adenylyl cyclase (Mou et al., 2005).

In our research work we will use 2'-MANT-3'-dGTP to analyze the conformation of the active site of purified soluble guanylyl cyclase isoform α_2/β_1 . The β_1 subunit will be human, while the α_2 subunit will be murine (rat).

To achieve this objective we will use mutagenesis to replace tryptophan 36 and 505 with alanine residues in the rat α_2 subunit of the soluble guanylyl cyclase. We will express the wild type enzyme α_2S/β_1 and mutants α_2SW36A/β_1 , $\alpha_2SW505A/\beta_1$, α_2S/β_1H105A , and α_2S/β_1W602A by using a baculovirus/Sf9 system. We will purify it with *Strep*-tag affinity chromatography. Afterwards SDS-polyacrylamide gel electrophoresis and Coomassie blue staining will be applied to assess the purity of the enzyme while its identity will be verified using western blot analysis.

Guanylyl cyclase activity of the purified soluble guanylyl cyclase will be measured and the heme content in purified sGC will be analyzed spectrophotometrically. 2'-MANT-3'-dGTP will be used in direct fluorescence experiments and in fluorescence resonance energy transfer (FRET) experiments. By using a spectrofluorometer we will analyze the conformation of the active site of the purified sGC in the presence or absence of NO.

3. EXPERIMENTAL WORK

3.1. MATERIALS

3.1.1. Chemicals and substances

| | |
|--|---------------------------------------|
| Acetic acid (glacial) (100%) | Merck (Darmstadt, Germany) |
| Acetic acid (96%) | Merck (Darmstadt, Germany) |
| Agar -agar | Roth (Karlsruhe, Germany) |
| Agarose | Roth (Karlsruhe, Germany) |
| Aluminium sulfate-(14-18)-hydrate | Sigma (Deisenhofen, Germany) |
| Ampicillin | Sigma (Deisenhofen, Germany) |
| Avidin | IBA Biotagnology (Göttingen, Germany) |
| Benzamidine | Fluka (Buchs, CH) |
| Bluo-gal | Invitrogen (Karlsruhe, Germany) |
| Brilliant blue G 250 | Merck (Darmstadt, Germany) |
| Bromophenol blue | Merck (Darmstadt, Germany) |
| Calcium chloride | Roth (Karlsruhe, Germany) |
| Complete Protease Inhibitor Cocktail | Roche (Mannheim, Germany) |
| D-Desthiobiotin | IBA Biotagnology (Göttingen, Germany) |
| DEA/NO | Sigma (Deisenhofen, Germany) |
| dNTP | Ferments (St. Leon-Rot, Germany) |
| DMSO | Roth (Karlsruhe, Germany) |
| DTT | Roth (Karlsruhe, Germany) |
| EDTA | Applichem (Darmstadt, Germany) |
| Ethanol (96%) | Roth (Karlsruhe, Germany) |
| Ethanol (100%) | Roth (Karlsruhe, Germany) |
| Ethidium bromide | Roth (Karlsruhe, Germany) |
| Glucose | Roth (Karlsruhe, Germany) |
| Glycerin | Roth (Karlsruhe, Germany) |
| Glycine | Roth (Karlsruhe, Germany) |
| HABA | Sigma (Deisenhofen, Germany) |
| HCl | Roth (Karlsruhe, Germany) |
| Yeast extract | Roth (Karlsruhe, Germany) |
| IPTG | Sigma (Deisenhofen, Germany) |
| Isopropanol | Roth (Karlsruhe, Germany) |
| Disodium hydrogen phosphate | Roth (Karlsruhe, Germany) |
| Magnesium chloride | Roth (Karlsruhe, Germany) |
| Magnesium sulfate | Roth (Karlsruhe, Germany) |
| Orthophosphoric acid | Sigma (Deisenhofen, Germany) |
| Ponceau S | Sigma (Deisenhofen, Germany) |
| Potassium acetate | Merck (Darmstadt, Germany) |
| Potassium chloride | Roth (Karlsruhe, Germany) |
| Powdered milk | Roth (Karlsruhe, Germany) |
| Sodium chloride | Roth (Karlsruhe, Germany) |
| Sodium hydroxide | Roth (Karlsruhe, Germany) |
| Sodium dodecyl sulfate | Roth (Karlsruhe, Germany) |
| Strep-Tactin [®] Superflow [®] high capacity | IBA Biotagnology (Göttingen, Germany) |

| | |
|--------------|------------------------------|
| TEA/HCl | Sigma (Deisenhofen, Germany) |
| TEMED | Roth (Karlsruhe, Germany) |
| Tetracycline | Sigma (Deisenhofen, Germany) |
| Tris-HCl | Roth (Karlsruhe, Germany) |
| Tris-acetate | Roth (Karlsruhe, Germany) |
| Tryptone | Roth (Karlsruhe, Germany) |
| Tween 20 | Merck (Darmstadt, Germany) |
| Xylencyanol | Roth (Karlsruhe, Germany) |

3.1.2. Solutions, buffers and media

| | |
|--|---|
| Acrylamide/bisacrylamide solution | Rotiphorese [®] Gel 30 Roth (Karlsruhe, Germany) |
| Blocking buffer | 5% powdered milk (w/v) in TBST |
| 0.1% bromophenol blue buffer | 0.1% bromophenol (w/v) in SDS buffer |
| Coomassie staining solution | 0.02% brilliant blue G 250 (w/v); 5% aluminium sulfate-(14-18)-hydrate (w/v); 10% ethanol (96%) (v/v); 2% orthophosphoric acid (w/v) |
| Coomassie destaining solution | 10% ethanol (96%) (v/v); 2% orthophosphoric acid (w/v) |
| 6×DNA loading buffer | 10 mM Tris; 60 mM EDTA; 60% glycerin; 0.03% bromophenol blue; 0.03% xylencyanol; pH 7.6 |
| DNA Standard | GeneRuler™ 1 kb DNA Ladder, 250-10,000 bp; Fermentas (St. Leon Rot, Germany) |
| Fetal bovine serum | PAA (Cölbe, Germany) |
| Gentamicin | 50 mg/ml; Invitrogen (Karlsruhe, Germany) |
| HEPES | Roth (Karlsruhe, Germany) |
| Homogenization buffer | 50 mM TEA/HCl, 1 mM EDTA, 10 mM DTT, pH 7.4 |
| Kanamycin | 50 mg/ml; Sigma (Deisenhofen, Germany) |
| LB agar | LB medium + 1.5% Agar (w/v) |
| LB medium | 1% tryptone (w/v); 0.5% yeast extract (w/v); 1% NaCl (w/v); pH 7.0 |
| 2'-O-(N-Methyl-anthraniloyl)-3'-deoxy-guanosine-5'-triphosphate, triethylammonium salt | Jena Biosciences (Jena, Germany) |
| Molecular weight marker | PageRuler™ Prestained Protein Ladder; Invitrogen (Karlsruhe, Germany) |
| Phosphate buffered saline (PBS) | 1.7 mM potassium dihydrogen phosphate; 150 mM sodium chloride, 5,2 mM disodium hydrogenphosphat; pH 7,4 |
| Penicillin/Streptomycin | 100× ; PAA (Cölbe, Germany) |
| Ponceau S staining solution | 0,5% Ponceau S (w/v); 1% acetic acid (glacial) (v/v) |
| 2× resolving gel buffer | 0.25 M Tris; 0.4% SDS (w/v); pH 8.8 |
| 10% resolving gel (2 gels) | <ul style="list-style-type: none"> • 6 ml H₂O • 3.75 ml 4 × resolving gel buffer • 5 ml 30% acryl-/bisacrylamid solution • 15 µl TEMED • 150 µl 10% ammonium persulfate |
| SDS buffer | 1% SDS, 100 mM DTT, 50 mM Tris, 30% glycerol; |

| | |
|-----------------------------------|--|
| 10× SDS running buffer | pH 7,5 0.25 M Tris; 1.92 M glycine; 1% SDS (w/v); pH 8.3-8,8 |
| Sf-900II SFM-Medium SOC medium | Invitrogen (Karlsruhe, Germany) 1% tryptone (w/v); 0.5% yeast extract (w/v); 1 mM NaCl; 2.5 mM KCl; 10 mM MgCl ₂ ; 10 mM MgSO ₄ ; 20 mM glucose |
| Solution I (Miniprep) | 50 mM glucose, 25 mM Tris pH 8.0, 10 mM EDTA |
| Solution II (Miniprep) | 0.2 m NaOH, 1% SDS (w/v) |
| Solution III (Miniprep) | 3 M potassium acetate, 12 % acetic acid (96%) (v/v) |
| 2 × Stacking gel buffer | 0.25 M Tris; 0.2% SDS (w/v); pH 6,8 |
| 5% Stacking gel (2 gels) | <ul style="list-style-type: none"> • 2.9 ml H₂O • 5 ml 2 × stacking gel buffer • 2 ml 30 % acrylamide/bisacrylamide solution • 6 µl TEMED • 120 µl 10% ammonium persulfate |
| Strep-Washing buffer | 100 mM Tris, 1 M NaCl, 1 mM EDTA, 1 mM benzamidine, 10 mM DTT; pH 8.0 |
| Strep-Elution buffer | 100 mM Tris, 1 M NaCl, 1 mM EDTA, 1 mM benzamidine, 10 mM DTT, 2.5 mM D-desthiobiotin; pH 8.0 |
| Strep-Regeneration buffer | 100 mM Tris, 150 mM NaCl, 1 mM EDTA, 1 mM HABA, pH 8.0. |
| TAE buffer | 40 mM Tris-acetate; 0.1 mM EDTA; pH 8.0 |
| 10× TBST | 1.5 mM NaCl; 100 mM Tris; 1% Tween 20 (v/v) |
| 10× Transfer buffer | 0.25 M Tris, 1.92 M glycin, 0.2% SDS (w/v); pH 8.3 |

3.1.3. Vector

pFASTBAC Invitrogen (Karlsruhe, Germany)

3.1.4. Primers

- Primers for the site-directed mutagenesis

Mutagenic primers listed below were designed for site-directed mutagenesis. Primers were manufactured by Biomers (www.biomers.net).

α_2 SW36A Sense 5'-CTT GTC TAA GCT CTG CGC GAA TGG CAG CCG GAG-3'

α_2 SW36A Antisense 5'-GCT CCG GCT GCC ATT CGC GCA GAG CTT AGA CAA G-3'

α_2 SW505A Sense 5'-ATG TAG CCC AGC AGT TGG CGC AAC GAC AGC AAG TAC-3'

α_2 SW505A Antisense 5'-GTA CTT GCT GTC GTT GCG CCA ACT GCT GGG CTA CAT-3'

- Primers for the sequence analysis

For α_2 SW36A:

pBakPac-FP 5'-TAAAATGATAACCATCTCGC-3'

For α_2 SW505A:

GATC-MBa2W505A-448500 5'-AGGACAAATGATCCATGTC-3'

- Primers for the analysis of recombinant bacmid DNA

pUC/M13 Forward 5'-CCCAGTCACGACGTTGTAAAACG-3'

pUC/M13 Reverse 5'-AGCGGATAACAATTTTCACACAGG-3'

3.1.5. Enzymes and reagent systems

| | |
|--|-----------------------------------|
| Cellfectin [®] | Invitrogen (Karlsruhe, Germany) |
| PureLink [®] HiPure Plasmid Maxi Prep Kit | Invitrogen (Karlsruhe, Germany) |
| Lumi-Light ^{Plus} Western-Blot substrat | Roche (Mannheim, Germany) |
| QuikChange Lightning Site-Directed Mutagenesis Kit | Stratagene (Amsterdam, NL) |
| RNase A | Sigma (Deisenhofen, Germany) |
| Taq DNA Polymerase | Fermentas (St. Leon-Rot, Germany) |

3.1.6. Antibodies

| | |
|--|---------------------------------------|
| Rabbit anti- β_1 sGC Antibody | Sigma (Deisenhofen, Germany) |
| Rabbit anti- α_2 sGC Antibody | Eurogentec (Seraing, Belgium) |
| Goat anti-Rabbit IgG HRP-linked Antibody | Cell Signalling (Schwalbach, Germany) |

3.1.7. Cells

- Max Efficiency[®] DH10 BAC[™] Competent Cells, Invitrogen (Karlsruhe, Germany)

Genotype: F⁻ mcrA Δ (mrr-hsdRMS-mcrBC) ϕ 80lacZ Δ M15 Δ lacX74 recA1 endA1 araD139 Δ (ara, leu)7697 galU galK λ ⁻ rpsL nupG /pMON14272 / pMON7124

- One Shot[®] TOP 10 Competent *E. coli*, Invitrogen (Karlsruhe, Germany)

Genotype: F⁻ mcrA Δ (mrr-hsdRMS-mcrBC) ϕ 80lacZ Δ M15 Δ lacX74 recA1 araD139 Δ (araleu)7697 galU galK rpsL (StrR) endA1 nupG

- Sf9 cells, Invitrogen (Karlsruhe, Germany)

3.1.8. Viruses

Recombinant baculoviruses carrying the expression cassette for α_2 , β_1 , β_1 H105A and β_1 W602A subunits of sGC were previously prepared in viral stocks and stored at 4°C, protected from light (work of Busker M.).

3.1.9. Materials and devices

Analytical balance, PT210, Sartorius (Göttingen, Germany)
Bacteriological incubator (*E.coli*), Kelvitrone®, Heraeus (Hanau, Germany)
Centrifuge Fresco 21, Thermo (Waltham, USA)
Centrifuge Multifuge IS-R, Thermo (Waltham, USA)
Centrifuge Megafuge 1.0R, Heraeus (Hanau, Germany)
Columns for ÄKTA, C 10/10 GE Healthcare (München, Germany)
Digital balance BP210D, Sartorius (Göttingen, Germany)
ECL Chemiluminescence imager, Intas (Göttingen)
Electrophoresis apparatus Mini-PROTEAN Tetra Cell, Biorad (München, Germany)
Fluorescence spectrofluorometer Cary Eclipse, Varian (Palo Alto, USA)
Fast Protein Liquid Chromatography System ÄKTA Purifier™, GE Healthcare (München)
Flow adapter for ÄKTA, AC 10 Healthcare (München, Germany)
Gel documentation systems Gel IX Imager, Intas (Göttingen, Germany)
Incubator for Sf9 cells, Stabilitherm, Thermo (Waltham, USA)
Incubator shaker (Sf9) Excella E24, New Brunswick (Edison, USA)
Incubator shaker (*E.coli*) Innova 4300, New Brunswick (Edison, USA)
Inverted microscope ID 03, Zeiss (Jena, Germany)
Magnetic stirrer KMO2 basic, IKA (Staufen, Germany)
Microbiological safety cabinet Herasafe, Heraeus (Hanau, Germany)
Nitrocellulose Protran, 0.45 µm Roth (Karlsruhe, Germany)
pH Meter 766 Calimatic, Knick (Berlin, Germany)
Pipettes P10, P20, P100, P200, P1000, Gilson (Middleton, USA)
Pipettefiller pipetus-akku®, Hirschmann (Eberstadt, Germany)
Perfusor syringes 20 ml, B.Braun (Melsungen, Germany)
Power supply Power Pac 300, Biorad (München, Germany)
Quartz cuvette with three windows, light path 3 mm × 3 mm, final volume 50 µl, Hellma (Müllheim, Germany)
Refrigerator (-20 °C), Liebherr (Ochsenhausen, Germany)
Refrigerator (4 °C), Liebherr (Ochsenhausen, Germany)
Refrigerator (-80 °C), GFL (Burgwedel, Germany)
Semi dry electroblotter Sedec™ M, Peq Lab (Erlangen, Germany)
Syringe filter 0.45 µm; 0.2 µm, Sarstedt (Nümbrecht, Germany)
Thermocycler Primus advanced, PeqLab (Erlangen, Germany)
Thermomixer compact, Eppendorf (Hamburg, Germany)
Tumbling table WT12, Biometra (Göttingen, Germany)
Ultrasonic homogenizer Sonoplus, Bandelin (Berlin, Germany)
UV-Vis spectrophotometer Cary Scan 50 Varian (Palo Alto, USA)
UV-Vis spectrophotometer Nanophotometer Implen, (München, Germany)
Vortex shaker MS3 basic, IKA (Staufen, Germany)
Water bath Typ 1003, GFL (Burgwedel, Germany)
Water deionization system Ultra Clear, SG (Barsbüttel, Germany)

3.2. METHODS

3.2.1. Site-directed mutagenesis

3.2.1.1. Primer design for site-directed mutagenesis

Mutagenic primers were designed to replace two tryptophan residues with alanine in the rat α_2 subunit of sGC. The rat α_2 subunit was previously inserted into pFastBac plasmid (Invitrogen, Germany) and the *Strep*-tag was fused C-terminally to enable purification with affinity chromatography (work of Busker M.). The size of the α_2S in pFastBac plasmid was 7108 bp. QuikChange Primer Design program (Agilent Technologies) was used to design the mutagenic primers. In mutants, α_2SW36A and $\alpha_2SW505A$, a codon for tryptophan, TGG, was changed into a codon for alanine, GCG.

3.2.1.2. Polymerase chain reaction

Using polymerase chain reaction (PCR) technology, the α_2S /pFastBac plasmid was amplified with designed mutagenic primers and the desired mutation was introduced. The mutagenesis was performed using QuikChange Lightning Site-Directed Mutagenesis Kit (Stratagen, Netherlands) according to the instruction manual (QuikChange Lightning Site-Directed Mutagenesis Kit, catalog # 210518 and #210519). Sample reactions were prepared as indicated below:

- 5 μ l of 10 \times reaction buffer
- 1 μ l of dsDNA template (8.72 μ g/ μ l α_2S /pFastBac)
- 1.2 μ l of sense primer (125 ng)
- 1.2 μ l of antisense primer (125 ng)
- 1 μ l of dNTP mix
- 1.5 μ l of Quick solution reagent
- ddH₂O to a final volume of 50 μ l

A volume of 1 μ l of QuikChange Lightning Enzyme was added to each sample reaction.

PCR was carried out in a thermocycler Primus advanced 96 (PiqLab, Germany). Each reaction was cycled using the following parameters:

- 2 minutes at 95 °C (activation of polymerase)
- 18 cycles
 - 20 seconds at 95 °C (denaturation of DNA)
 - 10 seconds at 60 °C (annealing of mutagenic primers)
 - 3.5 minutes at 68 °C (extension)
- 5 minutes at 60 °C

Dpn I restriction enzyme (2 μ l) was added to digest the methylated nonmutated parental dsDNA. Each reaction mixture was gently mixed, briefly centrifuged and then immediately incubated at 37 °C for 5 minutes.

3.2.1.3. Transformation of host cells

One Shot TOP10 competent *E. coli* cells were transformed with pFastBac plasmids harboring mutated genes for the α_2 subunit of sGC (α_2 SW36A/pFastBac and α_2 SW505A/pFastBac). The transformation was carried out in order to amplify the plasmid DNA and make large quantities of it.

The pre-prepared competent *E. coli* cells were previously perforated with calcium chloride and frozen in a mixture of glycerin and calcium chloride at -80°C. The cells were thawed on ice before transformation. A volume of 2 μ l of plasmid DNA and 98 μ l of *E. coli* Top10 suspension were mixed in a microcentrifuge tube and incubated on ice for 30 minutes. Heat shock was performed by incubation at 42°C for 45 seconds in a Thermomixer compact (Eppendorf). After 45 seconds the microcentrifuge tube was removed from Thermomixer compact (Eppendorf) and placed on ice for 2 minutes. Subsequently, 250 μ l of pre-warmed SOC medium was added and transformation mixture was incubated at 37 °C for 1 hour in Thermomixer under mild shaking. Then 350 μ l of cell suspension was spread on a LB agar plate containing ampicillin (100 μ g/ml). The plate was inverted and incubated at 37 °C overnight.

The next day, 6 prominent colonies of each mutant, α_2 SW36A and α_2 SW505A, were selected for further culturing. 5 ml of LB-medium containing ampicillin (100 μ g/ml) was poured into each 10 ml centrifuge tube. Cells from single colonies were transferred from a plate into the liquid medium with a sterile toothpick. Tubes were incubated at 37 °C overnight in the INNOVA 4300 Incubator Shaker (New Brunswick Scientific, Germany).

3.2.1.4. Minipreparation of plasmid DNA

Minipreparation of plasmid DNA is plasmid isolation from small culture volumes based on alkaline lysis. Overnight culture of *E. coli* Top10, transformed with α_2 SW36A/pFastBac or α_2 SW505A/pFastBac, was poured to fill a 2 ml microcentrifuge tube and centrifuged at 21.000 \times g for 1 minute in Fresco 21 centrifuge (Thermo, USA). Supernatant was discarded and microcentrifuge tubes were placed on ice. The pellet was resuspended in 100

μl of cold solution I containing RNase (1 $\mu\text{g}/\text{ml}$) and lysozym (100 $\mu\text{g}/\text{ml}$), and incubated on ice for 10 minutes. 200 μL of alkaline solution II containing SDS was added to the mixture, briefly mixed with a vortex shaker and incubated on ice for 10 minutes. Lysozyme weakened the cell wall so that the cells were lysed completely with SDS and NaOH. 150 μL of solution III was added, briefly mixed and incubated on ice for 10 minutes. The mixture was centrifuged at $21000 \times g$ for 15 minutes and a clear supernatant was transferred to a new 1.5 ml microcentrifuge tube. A volume of 450 μL of cold isopropanol and 45 μL of cold sodium acetate was added to the supernatant and briefly mixed. The mixture was centrifuged at $21000 \times g$ for 30 minutes to precipitate the plasmid DNA. Supernatant was discarded and 500 μl of cold 70% ethanol was added to the pellet and centrifuged at $21000 \times g$ for 2 minutes to wash the pellet. Supernatant was carefully discarded and the pellet was dried in the Thermomixer at 37 °C for 1 hour. The isolated and dried plasmid DNA was resuspended in 20 μL of ddH₂O and stored at -20 °C. Nanophotometer (Implen, Germany) was used to measure the concentration of the isolated plasmid DNA

3.2.1.5. Plasmid DNA sequencing

In order to verify the accuracy of mutations, 3 samples of isolated plasmid DNA of each mutant, $\alpha_2\text{SW36A}$ and $\alpha_2\text{SW505A}$, were sent to sequence analysis (GATC Biotech, Germany). The sequencing primer was pBakPac-FP for $\alpha_2\text{SW36A}$ and GATC-MBa2W505A-448500 for $\alpha_2\text{SW505A}$.

3.2.1.6. Maxipreparation

Maxipreparation is a method for isolation of plasmid DNA from much larger volumes of bacterial suspension than minipreparation, yielding relatively larger amount of very pure plasmid DNA. PureLink[®] HiPure Plasmid Maxi Prep Kit (Invitrogen) was used for this purpose. The isolation was carried out according to the manufacturer's manual (PureLink[™] HiPure Plasmid DNA Purification Kits for Mini, Midi, and Maxi preparation of Plasmid DNA, Invitrogen, 2010).

One day before maxipreparation 200 ml of liquid LB-medium containing ampicillin (100 $\mu\text{g}/\text{ml}$) was inoculated with the chosen clone from the liquid culture, which has been previously used for minipreparation. For $\alpha_2\text{SW36A}$ the mutant clone 1 was selected and

for α_2 SW505A the clone C. The newly inoculated cultures were incubated at 37 °C overnight in the INNOVA 4300 incubator shaker (New Brunswick Scientific, Germany).

HiPure Maxi Column from PureLink[®] HiPure Plasmid Maxi Prep Kit (Invitrogen) was equilibrated by applying 30 ml of equilibration buffer (EQ1) onto the column. The solution was allowed to drain by gravity flow.

The overnight culture (200 ml) was poured into two 50 ml centrifuge tubes and centrifuged at 15000 × g for 2 minutes in a Megafuge 1.0R centrifuge (Heraeus, Germany). Supernatant was discarded and centrifuge tubes were filled with new liquid culture and centrifuged under the same conditions. 10 ml of Resuspension buffer (R3) from the PureLink[®] HiPure Plasmid Maxi Prep Kit containing RNase A was added to the pellet and resuspended until homogeneity. 10 ml of Lysis buffer (L7) from PureLink[®] HiPure Plasmid Maxi Prep Kit was added and centrifuge tubes were mixed gently by inverting each capped centrifuge tube five times. The lysate was incubated at room temperature for 5 minutes. 10 ml of Precipitation buffer (N3) from PureLink[®] HiPure Plasmid Maxi Prep Kit was added and mixed immediately by inverting the capped centrifuge tube until the mixture was homogeneous. Centrifuge tubes were centrifuged at 15000 × g for 10 minutes at room temperature in the Megafuge 1.0R centrifuge (Heraeus, Germany). Supernatant was removed and loaded onto equilibrated HiPure Maxi Column. The solution was allowed to drain by gravity flow and the flow-through was discarded. The column was washed with 60 ml of Wash buffer (W8). The solution was allowed to drain by gravity flow and flow-through was discarded.

15 ml of Elution buffer from PureLink[®] HiPure Plasmid Maxi Prep Kit was added to the column to elute the DNA. The solution was allowed to drain by gravity flow and the flow-through was collected in a 50 ml elution tube. 10.5 ml of isopropanol was added to the eluate and mixed well. The elution tube was centrifuged at 15000 × g for 30 minutes at 4 °C by using Megafuge 1.0R centrifuge (Heraeus, Germany). Supernatant was discarded and 5 ml of 70% ethanol was added to the pellet and centrifuged at 15.000 × g for 4 minutes at 4 °C in a Megafuge 1.0R centrifuge (Heraeus, Germany). The supernatant was removed. The pellet was air-dried for 10 minutes. The DNA pellet was resuspended in 200 μ l of ddH₂O. The concentration of isolated plasmid DNA was measured with a Nanophotometer (Implen, Germany).

3.2.2. Bac-to-Bac Baculovirus Expression System

3.2.2.1. General description of Bac-to-Bac Baculovirus Expression System

Bac-to-Bac Baculovirus Expression System (Invitrogen) was used to produce recombinant sGC. With this method recombinant baculoviruses were generated and our gene of interest was expressed in insect cells. All the steps were performed according to the user's manual Bac-to-Bac® TOPO® Expression System (Invitrogen, 2008).

In the first step a gene of interest is inserted into pFastBac™ vector. The next step is transformation of *E. coli* host strain, DH10Bac™ with the recombinant pFastBac™ plasmid. The host strain contains a baculovirus shuttle vector (bacmid), bMON14272 (136 kb), with a mini-*att*Tn7 target site and a helper plasmid pMON7124 (13.2 kb), which encodes a transposase. Bacmid contains a segment of DNA encoding the LacZ α peptide into which the attachment site for the bacterial transposon, Tn7 (mini-*att*Tn7) has been inserted. Insertion of the mini-*att*Tn7 attachment site does not disrupt the reading frame of the LacZ α peptide. Recombinant bacmids are generated by transposing a mini-Tn7 element from the pFastBac™ donor plasmid to the mini-*att*Tn7 attachment site on the bacmid. The Tn7 transposition functions are provided by the transposase from the helper plasmid (Bac-to-Bac® TOPO® Expression System: User manual, Invitrogen, 2008).

After transposition the recombinant bacmid is isolated and insect cells are transfected to generate recombinant baculovirus particles. The first and the second viral stocks are amplified to obtain higher viral titers. The third baculoviral stock is used for infection of insect cells to express the recombinant gene (Bac-to-Bac® TOPO® Expression System: User manual, Invitrogen, 2008).

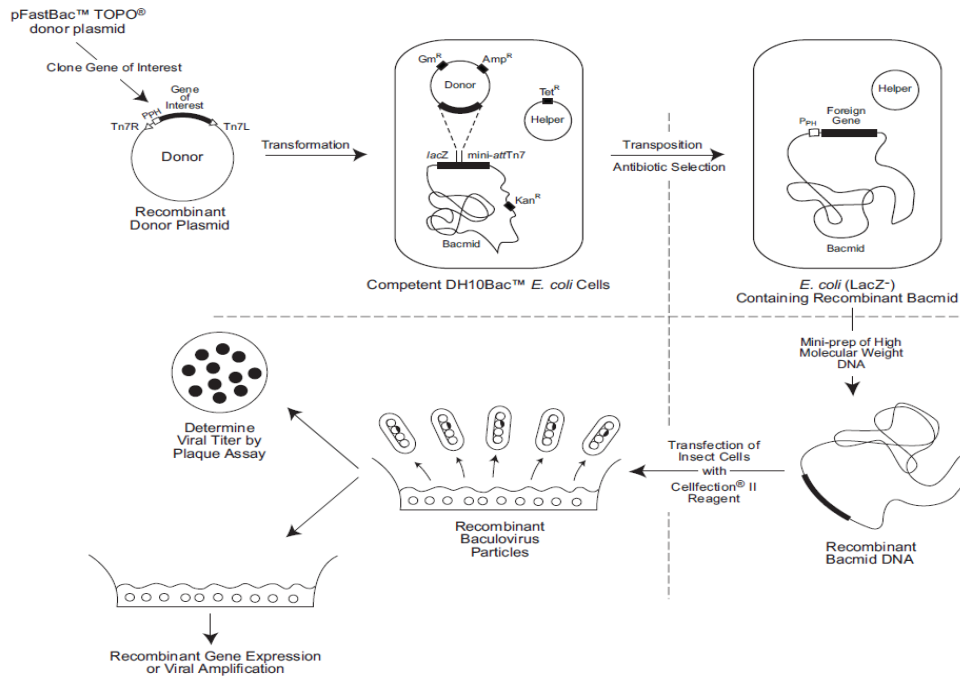


Figure 14: Generation of recombinant baculoviruses and the expression of a gene of interest, using Bac-to-Bac TOPO Expression System (Bac-to-Bac® TOPO® Expression System: User manual, Invitrogen, 2008).

3.2.2.2. Transformation of DH10 Bac™ Competent Cells with the plasmid and gene transposition

Max Efficiency® DH10 Bac™ Competent Cells (Invitrogen) were transformed with pFastBac plasmids containing the mutated α_2 subunit of sGC, α_2 SW36A and α_2 SW505A in order to transpose a gene for α_2 SW36A and α_2 SW505A from the donor pFastBac plasmid to the parent bacmid in DH10Bac™ competent cells and to form an expression bacmid, which was then used to transfect insect cells.

Bacterial cells were transformed essentially as described above (3.2.1.3.), except that they were ultimately spread on LB agar plates containing kanamycin (50 μ g/ml), tetracycline (10 μ g/ml), gentamycin (7 μ g/ml), Blueo-Gal (100 μ g/ml) and IPTG (40 μ g/ml). The plates were inverted and incubated at 37 °C for 72 hours.

After 3 days, 4 prominent white colonies of each mutant, α_2 SW36A and α_2 SW505A, were selected for further culturing. 5 ml of LB-medium containing kanamycin (50 μ g/ml), tetracycline (10 μ g/ml), and gentamicin (7 μ g/ml) was poured into each 10 ml centrifuge tube. Cells from single white colonies were transferred from a plate into the liquid medium with a sterile toothpick. Tubes were incubated at 37 °C overnight in the INNOVA 4300 incubator shaker (New Brunswick Scientific, Germany).

3.2.2.3. Isolation of recombinant bacmid DNA

The procedure for isolation of recombinant bacmid DNA was the same as the miniprep of plasmid DNA (3.2.1.4). Recombinant bacmid DNA was isolated from 4 samples for each mutant, α_2 SW36A and α_2 SW505A. The concentration of isolated bacmid DNA was measured with a Nanophotometer (Implen).

3.2.2.4. Analyzing recombinant bacmid DNA by PCR

The PCR analysis was used to verify the presence of mutated gene for α_2 subunit of sGC, α_2 SW36A and α_2 SW505A, in the recombinant bacmid. pUC/M13 forward and reverse primers which hybridize to the sites flanking the mini-*att*Tn7 site within the *lacZ* α -complementation region were used to facilitate PCR analysis (Fig. 15). If no transposition would occur, the PCR amplification would give a product of 273 bp, which is the distance between the pUC/M13 forward and reverse primer to the insertion site.

The size of transposon construct with α_2 SW36A or α_2 SW505A from Tn7R to Tn7L end is 4417 bp. In case of transposition the amplified size would be 4690 bp which is the sum of the transposon construct (4417 bp) plus the distance from the pUC/M13 forward and reverse primer to the insertion site (273 bp).

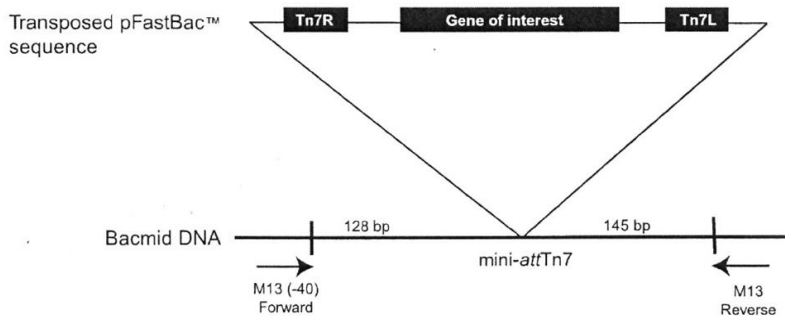


Figure 15: Transposed pFastBac sequence (Invitrogen, 2008).

Sample reactions were prepared as follows:

- 5 μ l of 10 \times reaction buffer
- 1 μ l of recombinant bacmid DNA
- 1.25 μ l of pUC/M13 forward (10 μ M stock)
- 1.25 μ l of pUC/M13 reverse (10 μ M stock)
- 1 μ l of 10 mM dNTP mix
- 3 μ l of 25 mM MgCl₂
- 37 μ l of ddH₂O
- 0.5 μ l of *Taq* polymerase

PCR was carried out in the Primus advanced 96 thermocycler (PeqLab, Germany). The following cycling parameters were used for amplification:

- 3 minutes at 94 °C (initial denaturation)
- 30 cycles
 - 45 seconds at 94 °C (denaturation of DNA)
 - 45 seconds at 55 °C (annealing of primers)
 - 5 minutes at 72 °C (extension)
- 7 minutes at 72 °C (final extension)

30 µl of the the final PCR product was removed and analyzed by agarose gel electrophoresis.

3.2.2.5. Agarose gel electrophoresis

1% (w/v) agarose gel was prepared. Agarose was mixed with TAE buffer (Tris-acetate-EDTA-buffer) and then heated in a microwave oven until it was completely dissolved. After cooling to about 60 °C, ethidium bromide was added to a volume concentration of 0.01%. The solution was poured into a tray and a comb was inserted. Agarose gel was then allowed to solidify at room temperature. The hardened gel in its plastic tray was inserted into an electrophoresis chamber. TAE buffer was added to cover the gel and then the comb was carefully removed. Samples containing the PCR product were mixed with 6 × DNA loading buffer (5:1) and loaded into the sample wells. GeneRuler™ 1 kb DNA Ladder (Fermentas, Germany) was used for sizing the PCR product. The lid and power cables were placed on the apparatus and the electrical current was applied. After adequate migration, the gel was placed in ultraviolet chamber to visualize DNA. Gel IX Imager (Intas, Germany) was used for gel documentation.

3.2.2.6. Sf9 cells

Sf9 insect cell line (Invitrogen) is a clonal isolate derived from ovarian tissue of the fall army worm, *Spodoptera frugiperda*, cell line IPLB-Sf-21-AE, and it is a suitable host for expression of recombinant proteins from baculovirus expression systems (e.g., Invitrogen's Bac-to-Bac® Expression System). The Sf9 cells can be cultured as monolayer cultures in T-flasks, as well as in suspension cultures in shake flasks. In optimal conditions the number of Sf9 cells doubles in 18-24 hours (Invitrogen, 2008).

The culture medium for Sf9 cells was Sf-900 II SFM Medium (Invitrogen) with 10% (v/v) FBS (fetal bovine serum, PAA) and 1% penicillin/streptomycin (PAA).

3.2.2.7. Transfection of Sf9 cells with recombinant bacmid DNA

8×10^5 Sf9 cells were seeded in 2 ml of Sf-900 II SFM medium (Invitrogen) into tissue culture plate wells (35 mm in diameter). The cells were allowed to attach to plastic at room temperature for 15 minutes.

The following solutions were prepared in sterile microcentrifuge tubes:

- solution A: 1 μ g of mini-prep bacmid DNA was diluted with 100 μ l Sf-900 II SFM medium (Invitrogen) without antibiotics,
- solution B: 8 μ l Cellfectin[®] (a cationic lipid formulation, Invitrogen) was diluted to 100 μ l with Sf-900 II SFM without antibiotics.

Solution A was combined with solution B to obtain the DNA-lipid mixture (210 μ l). The mixture was gently mixed, incubated for 15 to 30 min at room temperature and then dripped onto attached Sf9 cells. Sf9 cells were incubated for 3 h at 27 °C in the Stabilitherm incubator (Thermo, USA).

The liquid above the cells was then removed and 2 ml of culture medium for Sf9 cells was added. The well plates were wrapped in parafilm to prevent the loss of fluid and incubated at 27 °C for 5 days in the Stabilitherm incubator (Thermo, USA).

3.2.2.8. Isolation and amplification of P1 viral stock

Sf9 cells were scraped off the bottom of the wells with a spatula and the cell culture was filtered through a 0.2 μ m filter. The P1viral stock was a small-scale stock (2 ml). It was used for virus amplification to generate P2 stock.

100 ml of Sf9 cell suspension with a concentration of 1×10^6 cells/ml were infected with the whole P1viral stock. The infected Sf9 cell suspension was incubated at 27 °C and 140 rpm in the Innova 44 incubator shaker (New Brunswick Scientific, Germany) for 7 days or until at least 60% of infected cells were dead.

The cell suspension was then transferred into sterile 50 ml tubes and centrifuged at 400 rpm for 10 minutes in the Megafuge 1.0R centrifuge (Heraeus, Germany) to remove cells

and large debris. The supernatant was filtered through the 0.22 μm filter to obtain a clear P2 viral stock.

Amplification procedure was scaled-up to 500 ml in order to prepare P3 stock. 500 ml of Sf9-cell suspension in concentration of 1×10^6 cells/ml was prepared. The Sf-9 cells were infected with 5 ml of P2 viral stock and incubated at 27 °C and 140 rpm the Innova 44 incubator shaker (New Brunswick Scientific, Germany) for 5 to 7 days or until at least 60 % of infected cells were dead.

The cell suspension was transferred into sterile 50 ml tubes and centrifuged at 400 rpm for 10 minutes in the Megafuge 1.0R centrifuge (Heraeus, Germany) to remove cells and large debris. The supernatant was filtered through the 0.22 μm filter to obtain a clear P3 viral stock, which was further used for expression of sGC.

3.2.2.9. Expression of recombinant soluble guanylyl cyclase in the baculovirus/insect cell system

The wild type sGC ($\alpha_2\text{S}/\beta_1$) and sGC mutants, $\alpha_2\text{SW36A}/\beta_1$, $\alpha_2\text{SW505A}/\beta_1$, $\alpha_2\text{S}/\beta_1\text{H105A}$ and $\alpha_2\text{S}/\beta_1\text{W602A}$ were expressed with the baculovirus/insect cell system. The Sf9 cells were simultaneously infected with two baculoviruses, one carrying the expression cassette for α_2 and the other for the β_1 subunit of sGC.

500 ml of Sf9 cell suspension in concentration of 2×10^6 cells/ml was prepared in a 5 l shake flask. 25 ml of α_2 and 25 ml of β_1 viral stock (P3) was poured into the suspension culture and incubated at 27 °C and 140 rpm in the Innova 44 incubator shaker (New Brunswick Scientific, Germany) for 72 hours.

3.2.3. Preparation of cytosolic fractions of Sf9 cells

After 72 h, the cell suspension was filled into 50 ml tubes and centrifuged for 5 minutes at 4000 rpm and 4 °C in the Megafuge 1.0R centrifuge (Heraeus, Germany). Supernatant was discarded. All the following steps were performed at 4 °C or on ice. The cell pellet was resuspended in 15 ml ice cold homogenization buffer containing a tablet of Complete protease inhibitor cocktail (Roche, Germany) and 150 μl of avidin (100 mM). Subsequently the cells were homogenized with Sonoplus ultrasonic homogenizer (Bandelin, Germany). They were exposed to the ultrasound for 4 cycles for 16 seconds with 50% of maximal power. Ice-cooling of the sample was used to help dissipate heat

generated by the ultrasound. While the sample was incubated for 30 min at 4 °C, the avidin was allowed to bind to the biotin released from the homogenized cells. The sample was centrifuged at $15000 \times g$ for 2 h at 4 °C in the Multifuge IS-R centrifuge (Thermo, USA). By using a perfusor syringe (Braun, Germany) supernatant was filtered through 0.45 μm filter. Approximately 15 ml of cytosolic fraction was obtained for protein purification.

3.2.4. Purification of soluble guanylyl cyclase

The sGC was purified with affinity chromatography system which is based on the selective binding of *Strep*-tag II fusion proteins to *Strep*-Tactin. The *Strep*-tag® principle and *Strep*-tag® purification cycle is described in Supplement 2.

3.2.4.1. Purification procedure

The α_2 subunit of sGC was C- terminally fused to *Strep*-tag to enable purification with affinity chromatography. *Strep*-tag®-*Strep*-Tactin® system is based on the selective binding of *Strep*-tag II fusion proteins to *Strep*-Tactin, which is immobilized on affinity column. Purification of sGC was performed with ÄKTA Purifier™ (GE Healthcare, Germany), which is a fully automated fast protein liquid chromatography system. Affinity chromatography was done with 4 ml of *Strep*-Tactin Superflow high capacity (IBA, Germany) in a C 10/10 column (GE Healthcare, Germany) with a flow adapter AC 10 (GE Healthcare, Germany).

Before use, the column was equilibrated with 10 column volumes of washing buffer. Supernatant containing cytosolic fraction of Sf9 cells was applied to the *Strep*-Tactin® column with a flow rate of 1 ml/min. Afterwards, the column was washed with 5 column volumes of washing buffer with a flow rate of 1 ml/min. Elution was carried out with 5 column volumes of elution buffer with a flow rate of 1 ml/min and the elution volume was fractioned in 0.5 ml. Peak fractions showing absorption at 280 nm/430 nm were pooled and concentrated. At the end the *Strep*-Tactin® column was regenerated with 15 column volumes of regeneration buffer and 8 column volumes of washing buffer with a flow rate of 1 ml/min.

3.2.4.2. Protein concentration

Peak fractions were concentrated using Amicon centrifugal filter devices with a 30-kDa cut-off (Millipore). At the beginning the peak fractions were collected in a centrifugal

device Amicon Ultra-15 Centrifugal Filter Units with Ultracel®-30K (30 kDa) membrane (Millipore) with a maximal initial volume of 15 ml. The sample was then centrifuged at $4.000 \times g$ and $4\text{ }^{\circ}\text{C}$ in the Megafuge 1.0R centrifuge (Heraeus, Germany) for 12 minutes or until the final concentrate volume reached 500 μl . The concentrated protein was obtained by a second centrifugation step where approximately 500 μl of the supernatant was transferred into a centrifugal filter device Amicon Ultra-0.5 ml Centrifugal Filter with Ultracel®-30K (30 kDa) membrane (Millipore) and centrifuged at 14.000 rpm and $4\text{ }^{\circ}\text{C}$ in a Fresco 21 table centrifuge (Thermo, USA) until the protein concentration reached 5 $\mu\text{g}/\mu\text{l}$. The concentration of sGC was measured with the NanoPhotometer (Implen, Germany). The sGC was stored at $4\text{ }^{\circ}\text{C}$.

3.2.5. SDS-polyacrylamide gel electrophoresis

3.2.5.1. Sample preparation

Samples for SDS-polyacrylamide gel electrophoresis were purified sGC (1 μg) and cytosolic fractions (50 μg). Firstly, 10 μl of a sample was prepared with dilution in PBS to reach the end concentration of 0.1 $\mu\text{g}/\mu\text{l}$ for the purified enzyme and 5 $\mu\text{g}/\mu\text{l}$ for the cytosolic fraction. Secondly, 10 μl of pre-prepared SDS-buffer was added to the sample and heated for 3 minutes at $99\text{ }^{\circ}\text{C}$ in the Thermomixer compact (Eppendorf, Germany). When the sample cooled, 1 μl of 0.1% bromophenol blue buffer was added. Bromophenol blue served as a tracking dye. The prepared samples were stored at $-20\text{ }^{\circ}\text{C}$.

3.2.5.2. SDS-polyacrylamide gel electrophoresis procedure

Discontinuous polyacrylamide gels were prepared from 5% stacking and 10% resolving gel. A glass cassette was made of two glass plates, which were assembled with a casting frame and put on a casting stand. A solution of 10% resolving gel was poured on the bottom of the glass cassette and isopropanol was added to overlay the solution before applying stacking gel in order to produce a smooth separating surface between resolving and stacking gel. The resolving gel was allowed to polymerize for 15 minutes. Isopropanol was rinsed with distilled water and the solution of stacking gel was poured on the top of the resolving gel and a gel comb was inserted. The stacking gel was allowed to polymerize for 15 minutes.

Electrophoresis was carried out in a Mini-PROTEAN Tetra Cell electrophoresis apparatus (Biorad, Germany) with a Power Pac 300 power supply (Biorad, Germany). Once the gel

polymerized, the glass cassette was clamped into a Mini-PROTEAN Tetra Cell Electrophoresis Module (Biorad, Germany) and placed into a cell tank. The inner chamber was filled with SDS running buffer until the buffer level exceeded the level of the wells and the outer chamber was filled up to the mark on the cell tank. After the comb was taken out, the samples and pre-stained protein molecular weight marker PageRuler™ Prestained Protein Ladder (Invitrogen, Germany) were loaded into gel wells. The lid was placed on the top of the cell tank and the power leads were connected to the power supply. Electrophoresis was carried out with a voltage of 100 V. The electrophoresis ran until the blue dye front reached the bottom of the glass cassette.

After the SDS-polyacrylamide gel electrophoresis was complete, the running buffer was discarded and the glass cassette was removed from the Mini-PROTEAN Tetra Cell Electrophoresis Module (Biorad, Germany). The polyacrylamide gel was removed from the glass cassette and used for Coomassie blue staining and western blotting.

3.2.6. Coomassie blue staining

The proteins in polyacrylamide gel were stained with Coomassie blue according to Kang et al. (2002). The polyacrylamide gel was rinsed twice with distilled water for 10 minutes to remove SDS. Then the polyacrylamide gel was overlaid with Coomassie blue staining solution and placed on a WT12 tumbling table (Biometra, Germany) to be stained for 12 h. The SDS gel was destained with a coomassie destaining solution to reduce the background. Finally the stained polyacrylamide gel was scanned for documentation.

3.2.7. Western blot

Western blot was used to detect the α_2 and β_1 subunits of sGC in samples containing cytosolic fractions or the purified enzyme. After the proteins were electrophoretically separated with SDS-polyacrylamide gel electrophoresis, the protein bands were electrophoretically transferred to a Protran nitrocellulose membrane (0.45 μm) (Roth, Germany) with a Sedec™ M semi dry electroblotter (Peq Lab, Germany). Transfer buffer was used in semi dry blotting and the process was performed by applying 350 mA for 2 h. To control the quality of transfer, the nitrocellulose membrane was reversibly stained with Panceau S. The staining lasted 3 minutes and then the nitrocellulose membrane was rinsed with water for 3 minutes.

Unspecific binding sites on nitrocellulose membrane were saturated by immersing the membrane for 1 hour in TBST buffer containing 5% powdered milk. Then the nitrocellulose membrane was incubated for 1 hour in TBST buffer containing antibodies directed against either α_2 or β_1 subunit of sGC. The nitrocellulose membrane was washed three times for 10 minutes with TBST buffer and subsequently incubated for 1 hour with horseradish peroxidase-labeled anti-rabbit IgG antibodies (Cell Signaling, Germany). After washing it three times with TBST buffer the nitrocellulose membrane was processed with Lumi-Light^{PLUS} Western Blotting Substrate (Roche, Germany) according to the recommendations of the manufacturer. The signals were detected by using the ECL Chemiluminescence imager (Intas, Germany).

3.2.8. Guanylyl cyclase activity assay

Guanylyl cyclase activity assay measures the amount of [³²P]cGMP produced from [α -³²P]GTP. The method is based on a protocol described by Schultz and Böhme (1984). The activity was determined for α_2 S/ β_1 , α_2 SW36A/ β_1 , α_2 SW505A/ β_1 , α_2 S/ β_1 H105A, and α_2 S/ β_1 W602A. Samples for the assay were prepared as indicated below but the assay itself was performed by Anja Stieler. Each time 50 ng of purified sGC was assayed.

10 ml of freezing medium was prepared (i.e., 9 ml of TEA-lysis buffer, 1 ml of glycerol and 5 mg of BSA). sGC was added to freezing medium with an end concentration of 2.5 ng/ μ l. The mixture was divided into 0.5 ml microcentrifuge tubes and immediately frozen with liquid nitrogen. The samples were stored at -80°C until use.

3.2.9. UV/Vis spectroscopy

UV/Vis spectroscopy was used to analyze the heme content in purified sGC α_2 S/ β_1 and sGC mutants, α_2 SW36A/ β_1 , α_2 SW505A/ β_1 , α_2 S/ β_1 H105A, and α_2 S/ β_1 W602A. For measurements the Cary Scan 50 UV/Vis spectrophotometer (Varian, USA) was used. Samples contained purified sGC and 2'-MANT-3'-dGTP at final concentration of 3 μ M. The buffer solution was composed of 50 mM TEA/HCl, 10 mM DTT, 5 mM MnCl₂ and 1 mM EDTA (pH 7.4). The final volume of the sample was 50 μ l. The experiments were performed in the presence and absence of NO (100 μ M). The heme analysis of purified enzymes was carried out simultaneously with the FRET experiment and the same samples were used.

3.2.10. FRET experiment

FRET experiment was designed according to the work of Busker et al. (2010). Fluorescence resonance energy transfer (FRET) manifests itself through a decrease in donor fluorescence intensity accompanied by an increase in acceptor fluorescence intensity. The FRET donors were tyrosine and tryptophan residues of sGC and the FRET acceptor was fluorescently labeled nucleotide 2'-MANT-3'-dGTP, which competes with GTP for binding to the substrate binding site of sGC (Fig. 16).

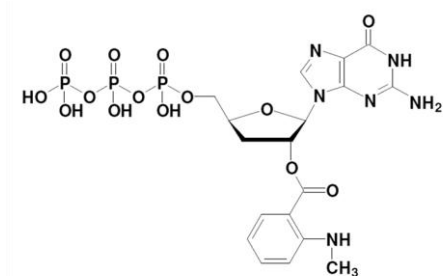


Figure 16: 2'-MANT-3'-dGTP (Jena, Data sheet, <http://www.jenabioscience.com/images/29c8187439/NU-231.pdf> (27.8.2012))

To detect FRET between tyrosine and tryptophan residues of sGC and 2'-MANT-3'-dGTP, the fluorescence emission spectra were obtained using Cary Eclipse fluorescence spectrofluorometer (Varian, USA). Purified sGC was excited at 280 nm and 295 nm (tryptophan specific excitation wavelength) and emission spectra were recorded from 300 nm to 500 nm for purified the enzyme alone (3 μ M) and in the presence of 2'-MANT-3'-dGTP (3 μ M) and DEA/NO (100 μ M).

The FRET efficiency between tryptophan residues of sGC and 2'-MANT-3'-dGTP was measured using sensitized emission method with three channels. The three channels were termed donor, FRET, and acceptor channel. Using the fluorescence spectrofluorometer the purified sGC was excited at 295 nm for tryptophan specific wavelength and the emission was detected at 335 nm (the donor channel). 2'-MANT-3'-dGTP was directly excited at 335 nm and the emission was detected at 430 nm (the acceptor channel). The FRET channel was selected at excitation wavelength of 295 nm and the emission was detected at 430 nm.

| Excitation at 295 nm | | | |
|--------------------------------|--------------------|-------------------|-----------------------|
| | Donor channel (DD) | FRET channel (DA) | Acceptor channel (AA) |
| ex. - em. wavelenght (nm) | '295-335 | '295-430 | '335-430 |
| Sample | | | |
| sGC | | | |
| 2'-MANT-3'-dGTP | | | |
| sGC + 2'-MANT-3'-dGTP | | | |
| sGC + 2'-MANT-3'-dGTP + DEA/NO | | | |

Figure 17: Scheme for obtaining the data in FRET experiment using sensitized emission method with three channels. The data was used to calculate the FRET efficiency.

FRET measurements were carried out in a quartz cuvette with three windows, light path of 3 mm × 3 mm and final volume 50 µl (Hellma, Germany), at 37 °C. Samples for FRET measurements contained purified sGC and 2'-MANT-3'-dGTP at final concentration of 3 µM. The buffer solution was composed of 50 mM TEA/HCl, 10 mM DTT, 5 mM MnCl₂ and 1 mM EDTA (pH 7.4). The final volume of the sample was 50 µl. The experiments were performed in the presence and absence of DEA/NO (100 µM). It was possible to observe the sample before and after addition of 2'-MANT-3'-dGTP and DEA/NO. It was assumed that the concentration of sGC remained constant pre- and post-addition of 2'-MANT-3'-dGTP and DEA/NO.

3.2.10.1. Calculation of FRET efficiency

The donor spectral bleed-trough (DSBT) and the acceptor spectral bleed-trough (ASBT) into the FRET channel were calculated according to Equations 7 and 8, respectively.

$$DSBT = \frac{F_{D, \text{FRET channel}}}{F_{D, \text{donor channel}}} \times F_{DA, \text{donor channel}} \quad (\text{Equation 7})$$

where

$F_{D, \text{FRET channel}}$ is the fluorescence intensity of the FRET channel, when only the donor is present in the sample,

$F_{D, \text{donor channel}}$ is the fluorescence intensity of the donor channel, when only the donor is present in the sample,

$F_{DA, \text{donor channel}}$ is the fluorescence intensity of the donor channel, when both, the donor and the acceptor are present in the sample.

$$ASBT = \frac{F_{A, FRET\ channel}}{F_{A, acceptor\ channel}} \times F_{DA, acceptor\ channel} \quad (\text{Equation 8})$$

where

$F_{A, FRET\ channel}$ is the fluorescence intensity of the FRET channel, when only the acceptor is present in the sample,

$F_{A, acceptor\ channel}$ is the fluorescence intensity of the acceptor channel, when only the acceptor is present in the sample,

$F_{DA, acceptor\ channel}$ is the fluorescence intensity of the acceptor channel, when both, the donor and the acceptor are present in the sample.

FRET ($F_{DA, FRET\ channel}$) was corrected (cFRET) for the donor and the acceptor spectral bleed-through (Equation 9).

$$cFRET = F_{DA, FRET\ channel} - DSBT - ASBT \quad (\text{Equation 9})$$

where

$F_{DA, FRET\ channel}$ is the fluorescence intensity of the FRET channel, when both, the donor and the acceptor are present in the sample.

The FRET efficiency (E%) between tryptophan residues of sGC and 2'-MANT-3'-dGTP before and after addition of DEA/NO was calculated according to Wallrabe and Periasamy (2005) (Equation 6).

To show the increase of FRET efficiency after addition of DEA/NO the difference between the FRET efficiency in basal and under NO-stimulating conditions was calculated according to Equation 10.

$$\Delta E(\%) = E(\%)_{NO} - E(\%)_{BASAL} \quad (\text{Equation 10})$$

3.2.11. Direct fluorescence experiments

With direct fluorescence experiments we wanted to analyze the environment of 2'-MANT-3'-dGTP in sGC. The experiments were designed according to the work of Busker et al. (2010). 2'-MANT-3'-dGTP was directly excited at 350 nm and its emission was measured at 445 nm. Fluorescence was measured for 2'-MANT-3'-dGTP alone and in the presence of sGC and DEA/NO.

The measurements were carried out with the Cary Eclipse fluorescence spectrofluorometer (Varian, USA) at 37 °C, in a quartz cuvette with three windows, a light path of 3 mm × 3 mm and the final volume of 50 µl (Hellma, Germany) was used. Samples contained purified sGC and 2'-MANT-3'-dGTP at final concentration of 3 µM. The buffer solution was composed of 25 mM HEPES/NaOH, 100 mM KCl and 3 mM MgCl₂, (pH 7.4). The experiments were performed in the presence and absence of DEA/NO (100 µM).

| Excitation with 350 nm, emission at 445 nm | |
|--|---------------------|
| Sample | Direct fluorescence |
| sGC | _____ |
| 2'-MANT-3'-dGTP | _____ |
| 2'-MANT-3'-dGTP + sGC | _____ |
| 2'-MANT-3'-dGTP + sGC + DEA/NO | _____ |

Figure 18: Scheme for obtaining the data in the direct fluorescence experiment.

It was possible to observe the sample before and after the addition of sGC and the NO donor (DEA/NO). It was assumed that the concentration of sGC remained constant pre- and post-addition of 2'-MANT-3'-dGTP and DEA/NO.

The 2'-MANT-3'-dGTP is unstable and even if stored and handled appropriately its fluorescence decreases within a longer period of time. Therefore, data obtained in the direct fluorescence experiment are normalized to the fluorescence intensity of 2'-MANT-3'-dGTP for representation.

4. RESULTS

4.1. SITE-DIRECTED MUTAGENESIS

To analyze the activation mechanism of sGC, tryptophans 36 and 505 of its α_2 subunit were replaced with alanine residues. The gene encoding the α_2 subunit was previously inserted into pFastBac plasmid (Invitrogen), and the mutations were introduced using QuikChange Lightning Site-Directed Mutagenesis Kit (Stratagen, Netherlands). One Shot[®] TOP 10 Competent *E. coli* (Invitrogen) were transformed with recombinant plasmid DNA in order to multiply the α_2 SW36A/pFastBac and the α_2 SW505A/pFastBac. The recombinant plasmid DNA was isolated via minipreparation and used for gene sequencing in order to verify the accuracy of missense mutations. Wild type α_2 subunit of sGC was aligned with the mutated versions α_2 SW36A and α_2 SW505A. The multiple sequence alignments are presented in the Supplement 3 and the altered codon is framed with a red line. Tryptophan residues 36 and 505 were successfully replaced with alanine in the α_2 subunit of sGC. Clone 1 of *E. coli* Top10 with the inserted α_2 SW36A/pFastBac and clone C with α_2 SW505A/pFastBac were selected for further study. Large quantities of pure recombinant plasmid DNA from the selected clones were obtained by maxipreparation. PureLink HiPure Plasmid DNA Purification Kit (Invitrogen) was used for isolation.

4.2. BAC-TO-BAC BACULOVIRUS EXPRESSION SYSTEM

4.2.1. Generation of baculovirus

Baculoviruses carrying the expression cassette for α_2 SW36A and α_2 SW505A were generated using Bac-to-Bac Baculovirus Expression System (Invitrogen). *E. coli* DH10 BAC[™] (Invitrogen) was transformed with the plasmid DNA, α_2 SW36A/pFastBac and α_2 SW505A/pFastBac, and the DNA of the α_2 subunit was transposed from the inserted plasmid into the host bacmid.

PCR analysis was performed to verify the presence of transposed α_2 SW36A and α_2 SW505A in the isolated recombinant bacmid DNA. pUC/M13 Forward and Reverse primers which hybridize to sites flanking the mini-attTn7 site were used to facilitate the PCR analysis. 1% agarose gel electrophoresis was used to determine the presence and the size of PCR products.

The PCR product was present in almost all samples except in the sample H (Fig. 19). The size of the product in the agarose electrophoresis gel lies approximately between 4500 and 5000 bp. The calculated size of the amplified product providing that the transposition occurred is 4690 bp and this size is close to the estimated size seen in the agarose electrophoresis gel. We can conclude that DNA for α_2SW36A and $\alpha_2SW505A$ was present in the isolated bacmid DNA.

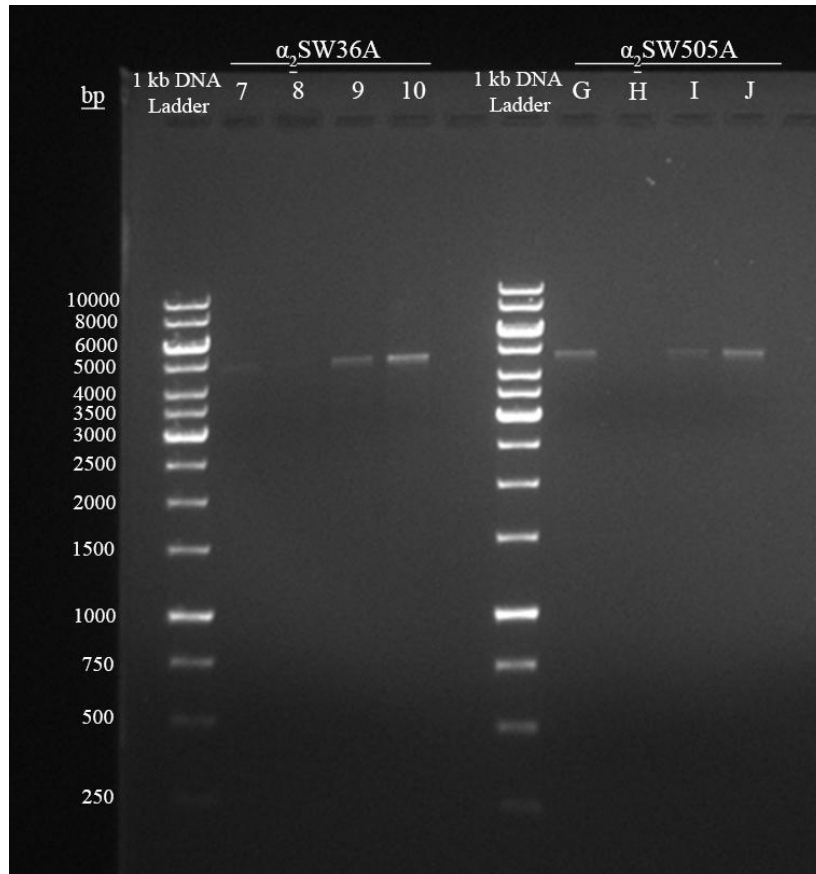


Figure 19: 1% agarose gel electrophoresis of PCR products of recombinant bacmid DNA. Lanes 7, 8, 9, and 10 are PCR amplifications of a part of recombinant bacmid DNA containing α_2SW36A subunit of sGC (4690 bp). Lanes G, H, I, and J are PCR amplifications of a part of recombinant bacmid DNA containing $\alpha_2SW505A$ subunit of sGC (4690 bp). GeneRuler™ 1 kb DNA Ladder (Fermentas) was used as a DNA marker.

Sf9 cells were transfected with the isolated recombinant bacmid DNA carrying the expression cassette for α_2SW36A and $\alpha_2SW505A$. Recombinant baculoviruses budded from the infected cells and virus particles were then harvested. The first and the second viral stock were used for amplification and the third stock was used for the expression of sGC.

4.2.2. Expression and purification of soluble guanylyl cyclase

Three independent experiments were carried out with α_2 S/ β_1 , α_2 SW36A/ β_1 , α_2 SW505A/ β_1 , and α_2 S/ β_1 H105A, and only two with α_2 S/ β_1 W602A. The sGC was obtained for each experiment separately.

The wild type of sGC (α_2 S/ β_1) and sGC mutants, α_2 SW36A/ β_1 , α_2 SW505A/ β_1 , α_2 S/ β_1 H105A, and α_2 S/ β_1 W602A were expressed with the baculovirus/insect cell system. The Sf9 cells were simultaneously infected with two baculoviruses, one carrying the expression cassette for α_2 and the other for β_1 subunit of sGC. Suspension culture (500 ml) of infected Sf9 cells was incubated for 72 h to express the recombinant sGC. Sf9 cells were then homogenized to release the sGC from the cells. Approximately 15 ml of the cytosolic fraction was prepared for subsequent protein purification.

The α_2 subunit of sGC was C-terminally fused to *Strep*-tag II to enable the purification with affinity chromatography. *Strep*-tag II fusion proteins selectively bound to *Strep*-Tactin, which was immobilized on the affinity column. The purification of sGC was performed with a fully automated fast protein liquid chromatography system ÄKTA PurifierTM (GE Healthcare, Germany).

4.3. SDS-POLYACRYLAMIDE GEL ELECTROPHORESIS AND COOMASSIE BLUE STAINING

SDS-polyacrylamide gel electrophoresis was performed for cytosolic fractions and purified enzymes of the wild type sGC isoform α_2 S/ β_1 and mutants, α_2 SW36A/ β_1 , α_2 SW505A/ β_1 , α_2 S/ β_1 H105A, and α_2 S/ β_1 W602A. Samples contained 50 μ g of proteins from cytosolic fractions and 1 μ g of purified sGCs. The proteins were separated according to their size in 10 % polyacrylamide gel and stained with Coomassie blue according to Kang et al. (2002) for visualization.

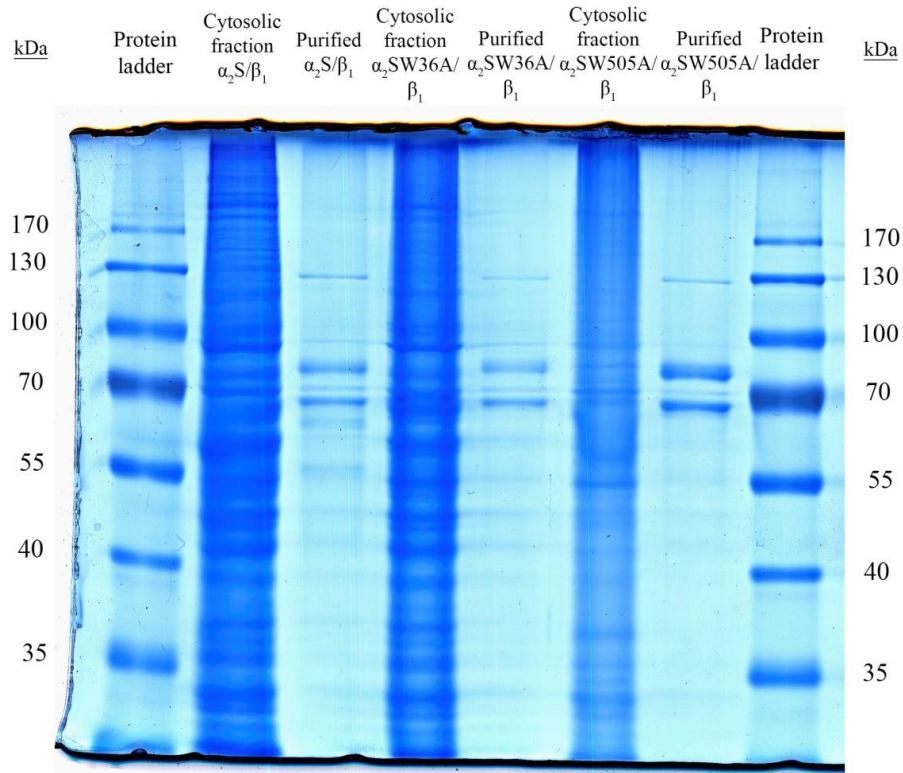


Figure 20: The SDS-PAGE of cytosolic fractions and purified sGC. Proteins were separated in 10 % polyacrylamide gel and stained with Coomassie blue. The first and the last lane containe molecular weight marker/PageRuler™ Prestained Protein Ladder (Invitrogen). The samples are indicated above the gel.

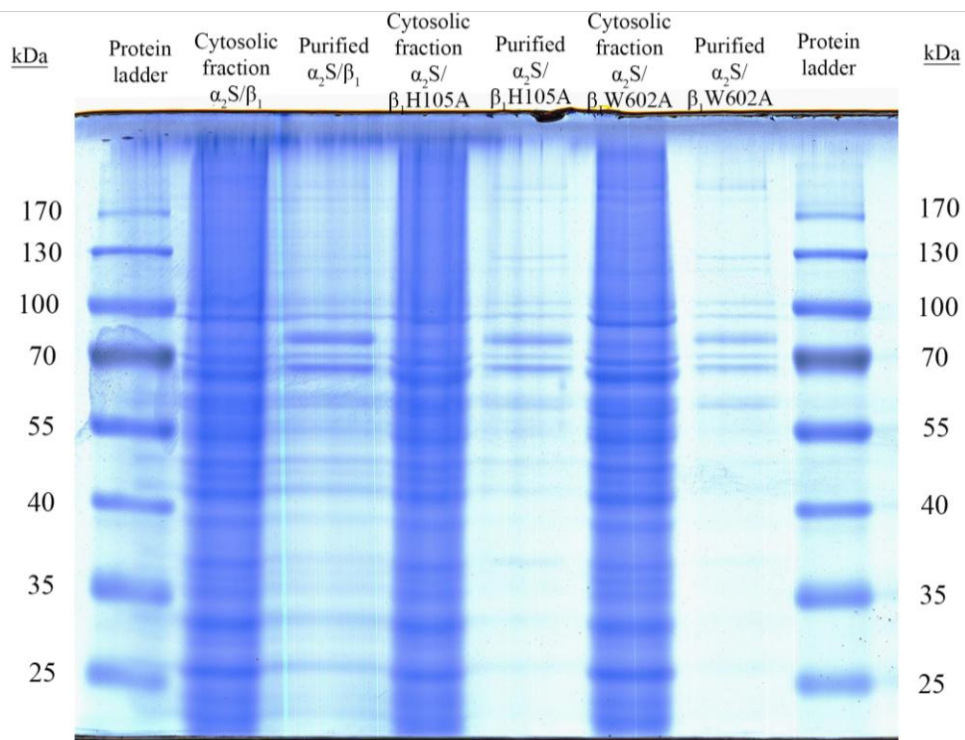


Figure 21: The SDS-PAGE of cytosolic fractions and purified sGC. Proteins were separated in 10 % polyacrylamide gel and stained with Coomassie blue. The first and the last lane containe molecular weight marker/PageRuler™ Prestained Protein Ladder (Invitrogen). The samples are indicated above the gel.

The affinity chromatography purification removed a large amount of unwanted proteins from the cytosolic fractions and the number of bands visualized on polyacrylamide gel was reduced (Figure 20 and 21). Samples of purified enzyme contain two bands, which stand out and probably represent the α_2S (82.7 kDa) and β_1 (70.5 kDa) subunits of sGC. Impurities were present in all samples containing purified sGC but the purity was higher in samples from the first polyacrylamide gel (Fig. 20) than in those from the second one (Fig. 21).

4.4. WESTERN BLOT ANALYSIS

Subsequent western blot analysis against the α_2 and β_1 subunit of sGC was performed to verify the identity of the proteins in samples containing cytosolic fractions and the purified enzyme (Fig. 22).

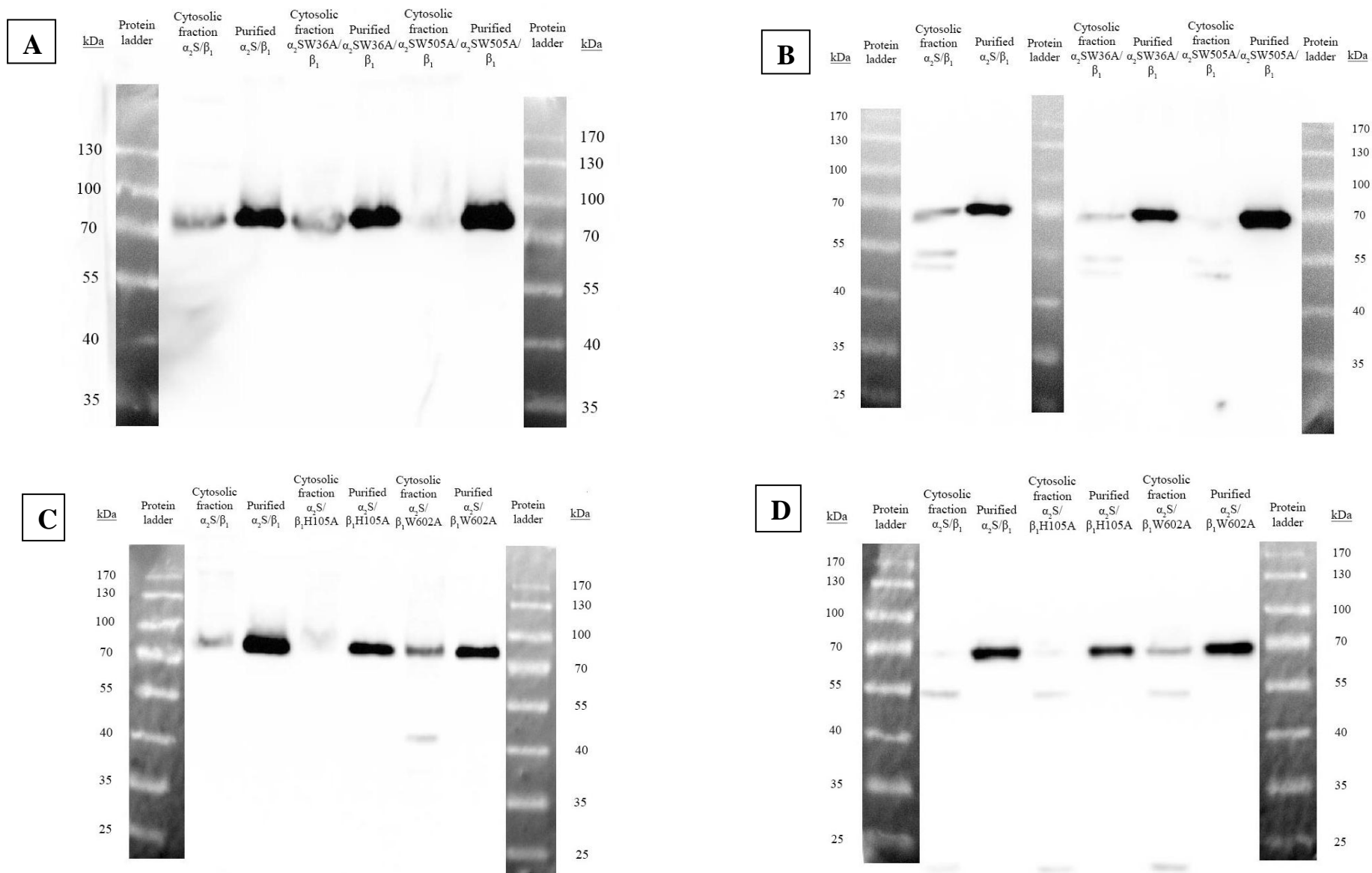


Figure 22: Western blot analysis of cytosolic fractions and purified sGC. Proteins were separated in 10 % polyacrylamide gel and immunoblotted with antibodies against the α_2 (A and C) or β_1 (B and D) subunit of sGC. The first and the last lane contain molecular weight marker. The samples are indicated above the gel.

The α_2 and the β_1 subunit of sGC were identified in all cytosolic fractions and all samples containing purified sGC (Fig. 22). Non-specific bands were present in all cytosolic fractions when antibodies against the β_1 subunit of sGC were used (Fig. 22B and 22D). These bands were absent in samples containing the purified sGC. When antibodies against the α_2 subunit of sGC were used, there was a non-specific band present only in one sample, namely the α_2S/β_1W602A cytosolic fraction (Fig. 22C).

4.5. UV/VIS SPECTROSCOPY

UV/Vis spectroscopy was used to analyze the heme content in purified sGC isoform α_2S/β_1 and in sGC mutants, α_2SW36A/β_1 , $\alpha_2SW505A/\beta_1$, α_2S/β_1H105A , and α_2S/β_1W602A . Heme analysis was carried out simultaneously with the FRET experiment, therefore the same samples were used. The Cary Scan 50 UV/Vis spectrophotometer (Varian, USA) was used to record absorption spectra of purified enzymes (3 μ M) in basal conditions and following the addition of 2'-MANT-3'-dGTP (3 μ M) and DEA/NO (100 μ M) (Fig. 23-25).

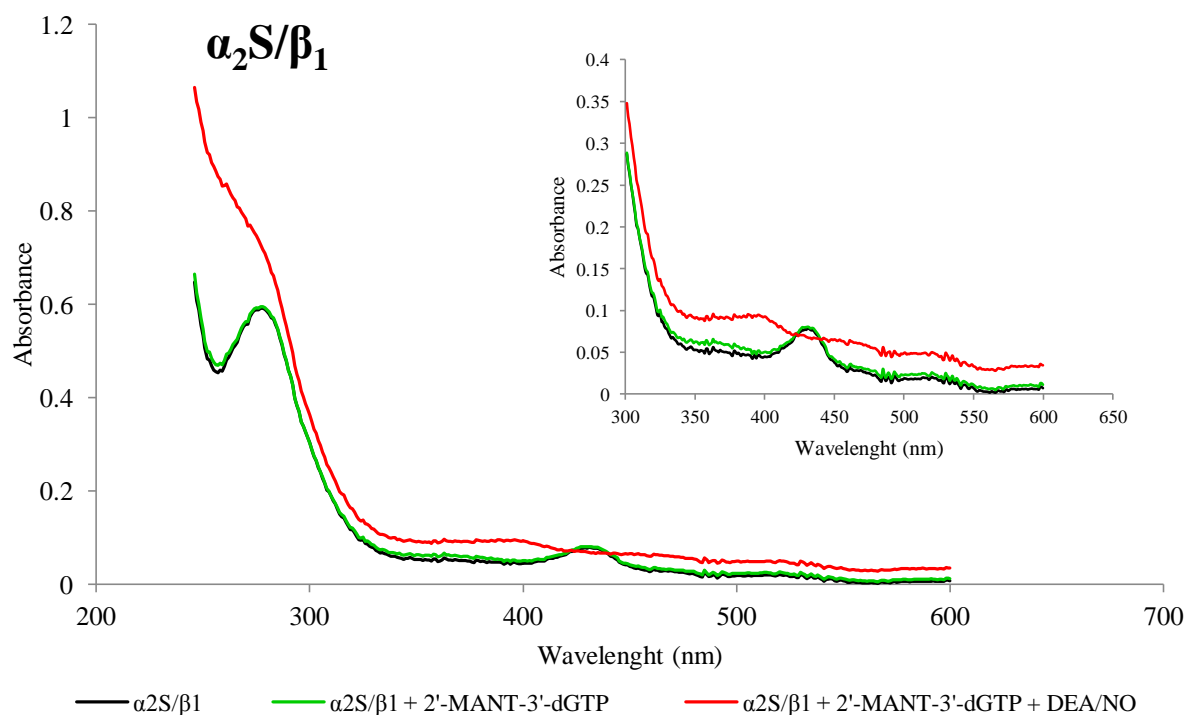


Figure 23: Spectral analysis of α_2S/β_1 . The absorption spectra of α_2S/β_1 under basal conditions (black line), in the presence of 3 μ M 2'-MANT-3'-dGTP (green line) and in the presence of 3 μ M 2'-MANT-3'-dGTP and 3 μ M DEA/NO (red line). The smaller graph shows more details from a section between 300 and 600 nm of the larger graph. The assay buffer consisted of 50 mM TEA/HCl, 10 mM DTT, 5 mM $MnCl_2$ and 1 mM EDTA (pH 7.4).

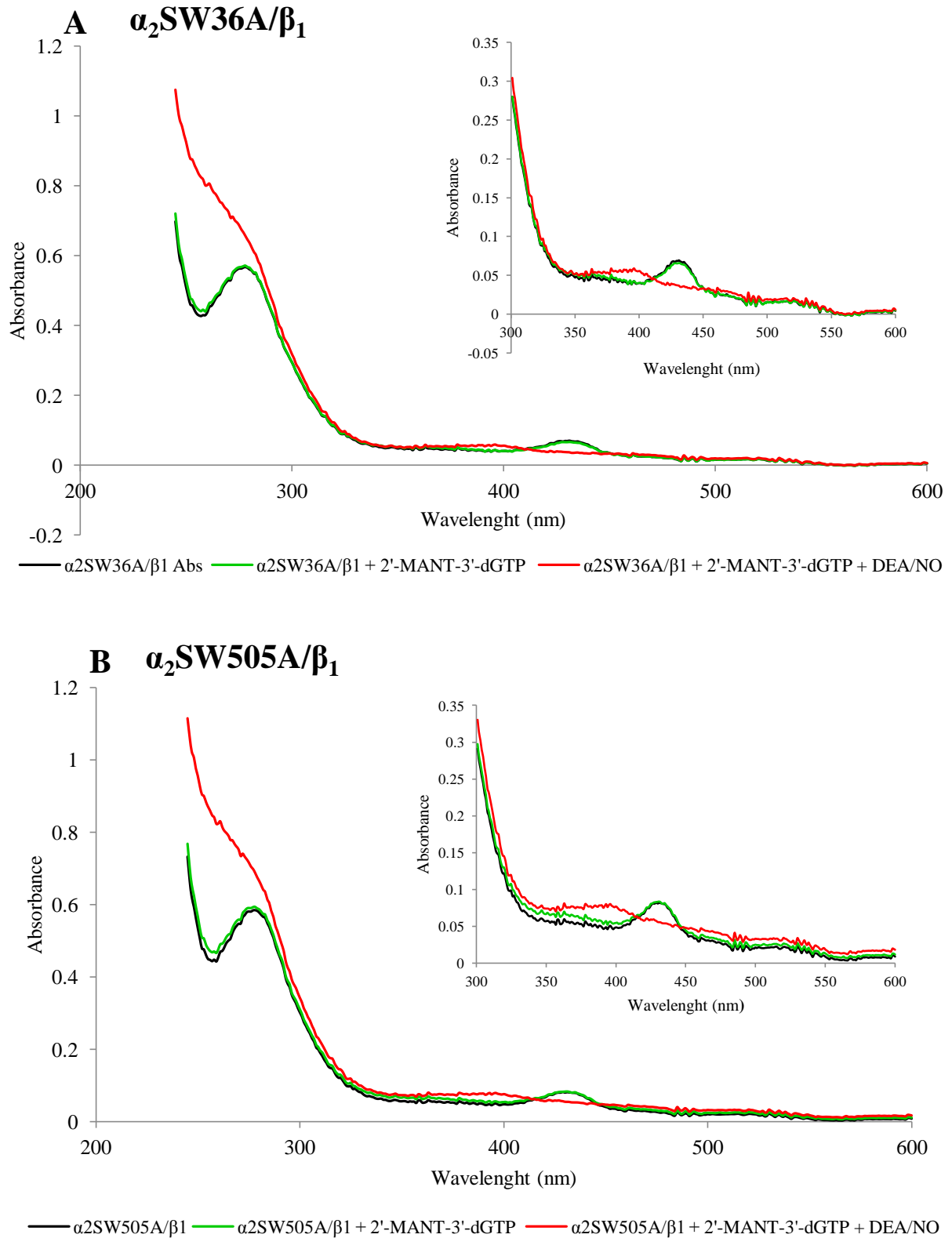


Figure 24: Spectral analysis of $\alpha_2\text{SW36A}/\beta_1$ (A) and $\alpha_2\text{SW505A}/\beta_1$ (B). The absorption spectra of $\alpha_2\text{SW36A}/\beta_1$ / $\alpha_2\text{SW505A}/\beta_1$ under basal conditions (black line), in the presence of 3 μM 2'-MANT-3'-dGTP (green line) and in the presence of 3 μM 2'-MANT-3'-dGTP and 3 μM DEA/NO (green line). The smaller graph shows more details from a section between 300 and 600 nm of the larger graph. The assay buffer consisted of 50 mM TEA/HCl, 10 mM DTT, 5 mM MnCl_2 and 1 mM EDTA (pH 7.4).

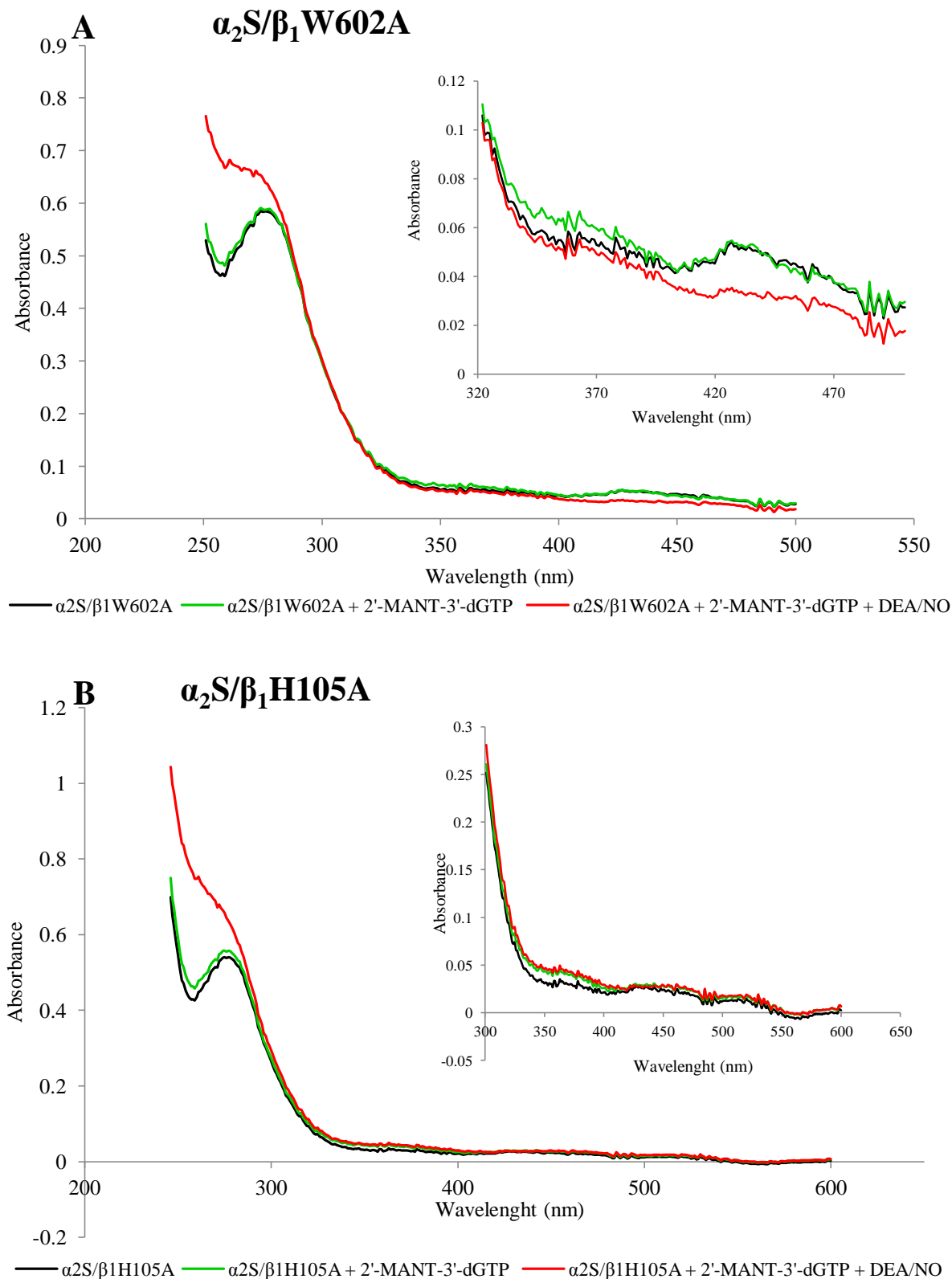


Figure 25: Spectral analysis of α_2S/β_1W602A (A) and α_2S/β_1H105A (B). The absorption spectra of $\alpha_2S/\beta_1W602A/\beta_1/\alpha_2S/\beta_1H105A$ under basal conditions (black line), in the presence of $3\ \mu\text{M}$ 2'-MANT-3'-dGTP (green line) and in the presence of $3\ \mu\text{M}$ 2'-MANT-3'-dGTP and $3\ \mu\text{M}$ DEA/NO (red line). The smaller graph shows more details from a section between 320 and 500 nm/300 and 600 nm of the larger graph, respectively. The assay buffer consisted of 50 mM TEA/HCl, 10 mM DTT, 5 mM MnCl_2 and 1 mM EDTA (pH 7.4).

The spectral analysis of purified enzymes showed that α_2S/β (Fig. 23), α_2SW36A/β_1 (Fig. 24A), and $\alpha_2SW505A/\beta_1$ (Fig. 24B) have absorption maxima at 430 nm. This peak is characteristic of a 5-coordinate ferrous heme group of the prosthetic heme group in sGC (Soret band). The absorption maximum at 430 nm did not change in the presence of 2'-MANT-3'-dGTP (3 μ M) but shifted from 430 to 396 nm after the addition of DEA/NO (3 μ M). This indicates the binding of NO to the prosthetic heme group of sGC and the formation of nitrosyl-heme complex. The characteristic peak at 430 nm was absent in the absorption spectra for α_2S/β_1H105A (Fig. 25B). At 430 nm the absorption of α_2S/β_1W602A (Fig. 25A) was very small and there was only a minor difference in spectra when absorption of α_2S/β_1W602A was compared to α_2S/β_1H105A . All purified enzymes had an absorption peak at 280 nm which is characteristic for proteins. At this wavelength tryptophan and tyrosine residues absorb light (Fig. 12 and 13).

4.6. GUANYLYL CYCLASE ACTIVITY ASSAY

The guanylyl cyclase activity of the purified sGC was measured in order to investigate if mutations of the wild type sGC isoform α_2S/β affected the responsiveness of the enzymes to NO and moreover if the mutations play a role in the enzyme activation mechanism. The altered enzyme activity could in turn influence the results obtained from the FRET analysis. A single guanylyl cyclase activity assay was carried out for each type of enzyme.

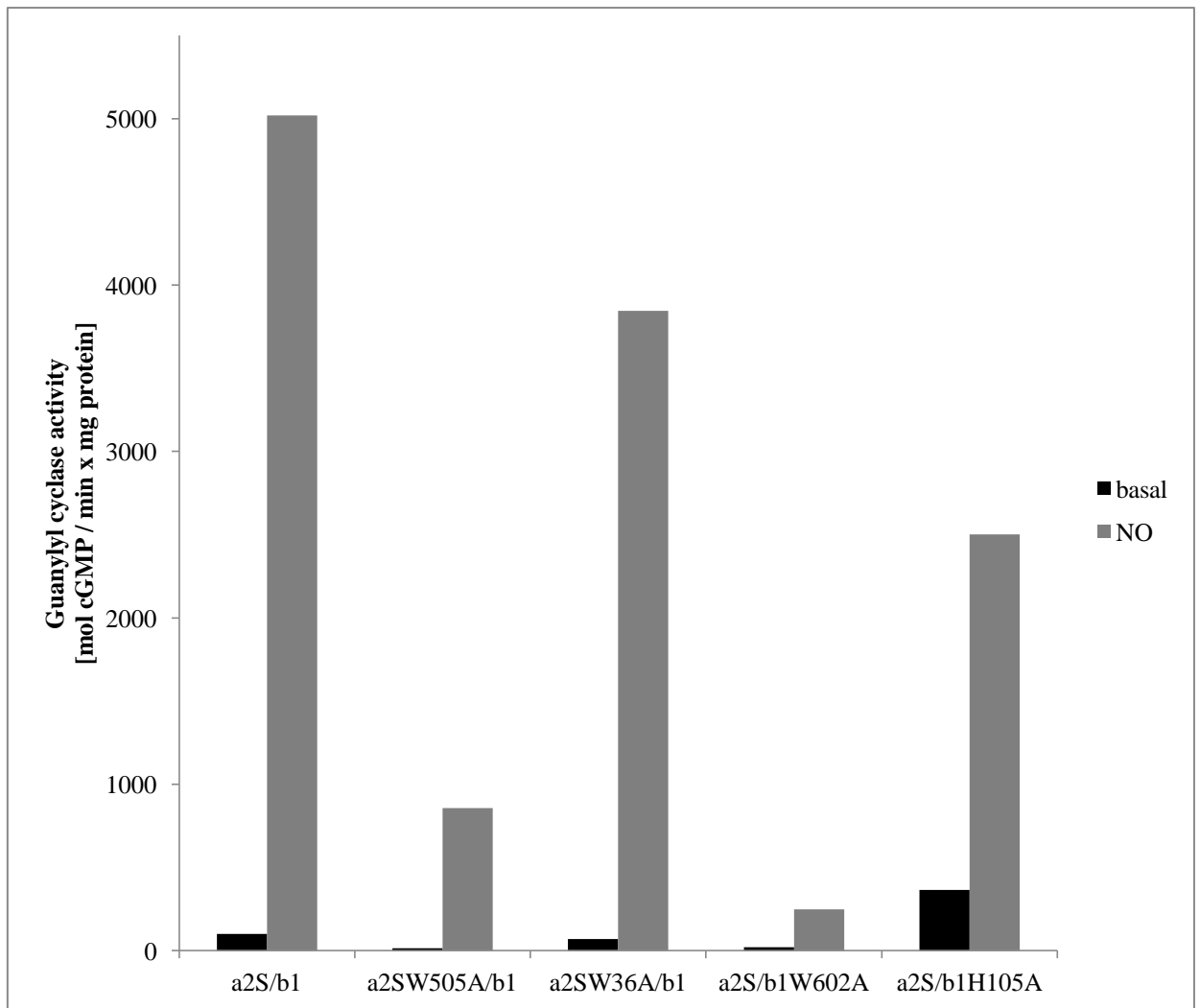


Figure 26: Guanylyl cyclase activity of purified α_2S/β_1 in comparison with mutant $\alpha_2SW505A/\beta_1$, α_2SW36A/β_1 , α_2S/β_1W602A , and α_2S/β_1H105A .

The basal activity of the wild type enzyme α_2S/β_1 is low and remarkably increases under NO-stimulating conditions. The activity of α_2SW36A/β_1 is also notably increased upon NO stimulation; therefore the sensitivity of sGC to NO is maintained despite the mutation of tryptophan 36 to alanine. The mutation of tryptophan 505 however results in loss of a large part of NO sensitivity. The mutant α_2S/β_1W602A almost completely lost its sensitivity to NO. The increase of its activity after the addition of DEA/NO was even smaller than for the mutant $\alpha_2SW505A/\beta_1$. In contrast, partial NO sensitivity of α_2S/β_1H105A was preserved.

4.7. FRET ANALYSIS

There are four tryptophan residues placed in different domains of the sGC isoform α_2S/β_1 . The FRET analysis of sGC tryptophan mutants was performed to show close proximity or long distance between a specific tryptophan residue and a catalytic center of the sGC before and after the addition of the sGC activator (NO). With this method we could therefore indirectly analyze the organization and activation of sGC.

Tryptophan residues alone can be excited with excitation wavelength of 295 nm and they emit fluorescence with an emission maximum at 335 nm. 2'-MANT-3'-dGTP is a competitive inhibitor of sGC and binds to the catalytic center of the enzyme. 2'-MANT-3'-dGTP is also a fluorescent molecular probe and can be excited at 335 nm. If a specific tryptophan residue is or comes in close proximity to 2'-MANT-3'-dGTP, the transfer of energy or FRET will appear between the tryptophan (a FRET donor) and 2'-MANT-3'-dGTP (a FRET acceptor) upon excitation of tryptophan at 295 nm. At 280 nm both, the tryptophan and tyrosine residues are excited with emission maximum at 335 nm. Göttle et al. (2007) reported that excitation at 280 nm results in higher FRET signals than at the excitation wavelength of 295 nm.

4.7.1. Fluorescence emission spectra

Fluorescence emission spectra were recorded to analyze the occurrence of FRET between tryptophan residues and 2'-MANT-3'-dGTP in the presence and absence of DEA/NO (NO-donor). Using a Cary Eclipse fluorescence spectrofluorometer (Varian, USA) the purified sGC was excited at 280 nm and 295 nm (tryptophan specific excitation wavelengths) and the emission spectra were recorded from 300 nm to 500 nm. The emission spectra were obtained for the purified enzyme alone (3 μ M) and in the presence of 2'-MANT-3'-dGTP (3 μ M) and DEA/NO (100 μ M). The figures below show the fluorescence emission spectra for α_2S/β_1 , α_2SW36A/β_1 , $\alpha_2SW505A/\beta_1$, α_2S/β_1H105A , and α_2S/β_1W602A .

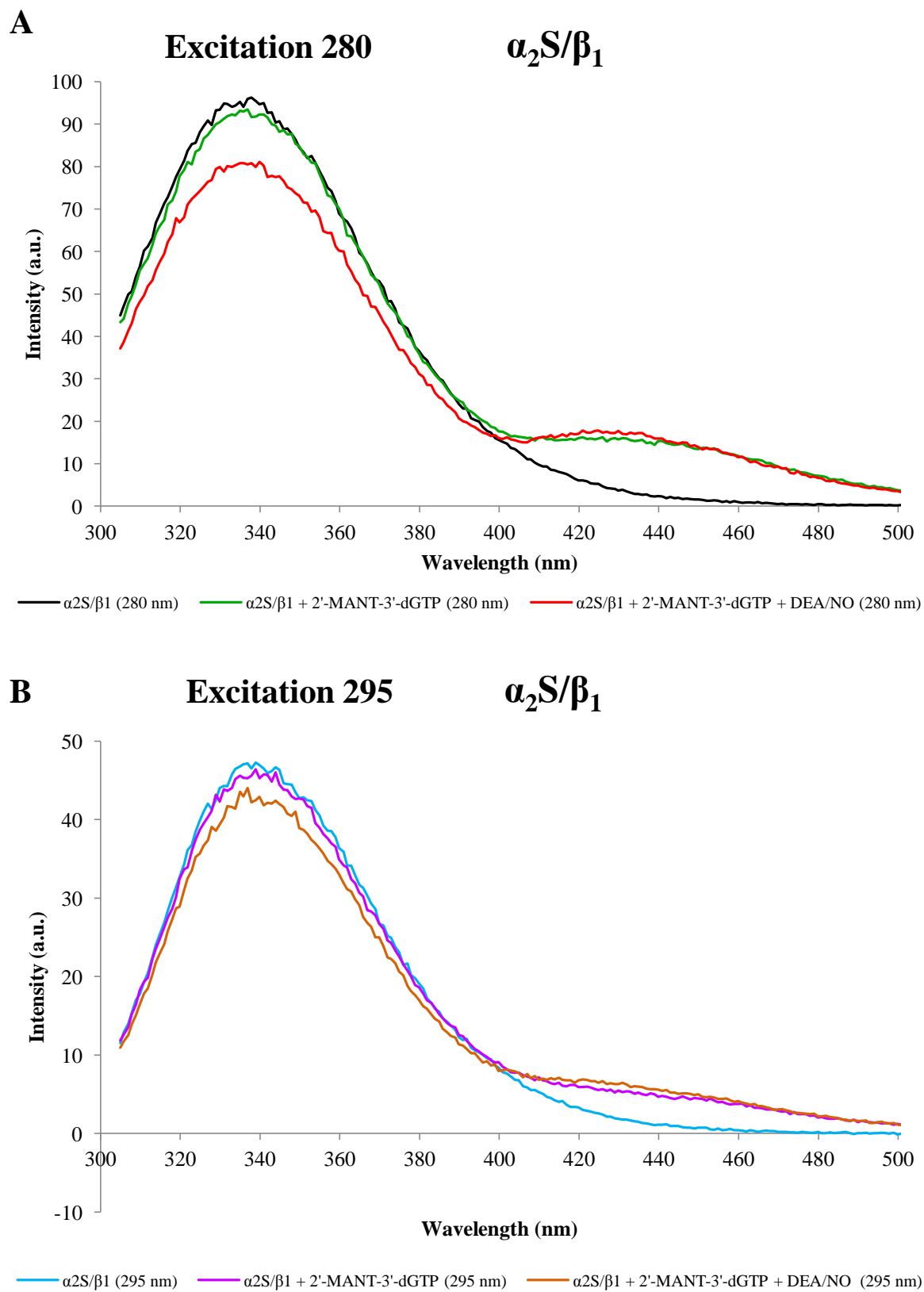


Figure 27: Fluorescence emission spectra of purified α_2S/β_1 (3 μM) in the absence and presence of 2'-MANT-3'-dGTP (3 μM) and DEA/NO (100 μM). The assay buffer consisted of 50 mM TEA/HCl, 10 mM DTT, 5 mM MnCl_2 and 1 mM EDTA (pH 7.4). The emission was scanned at excitation wavelengths of 280 (A) and 295 nm (B).

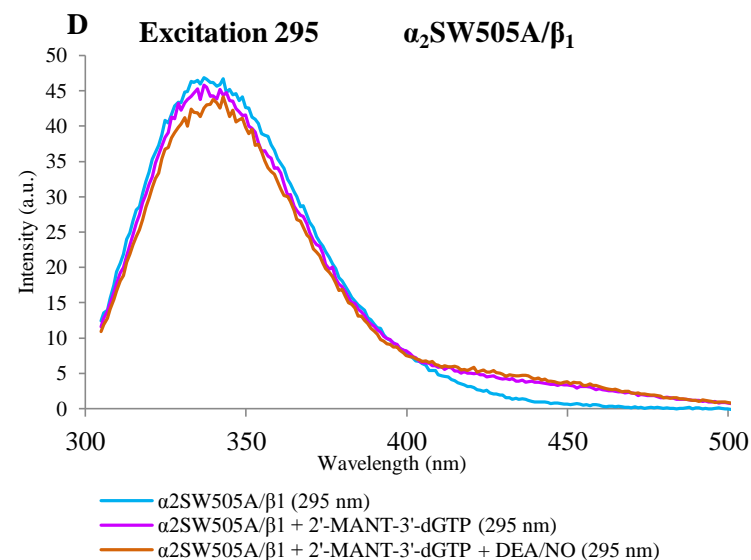
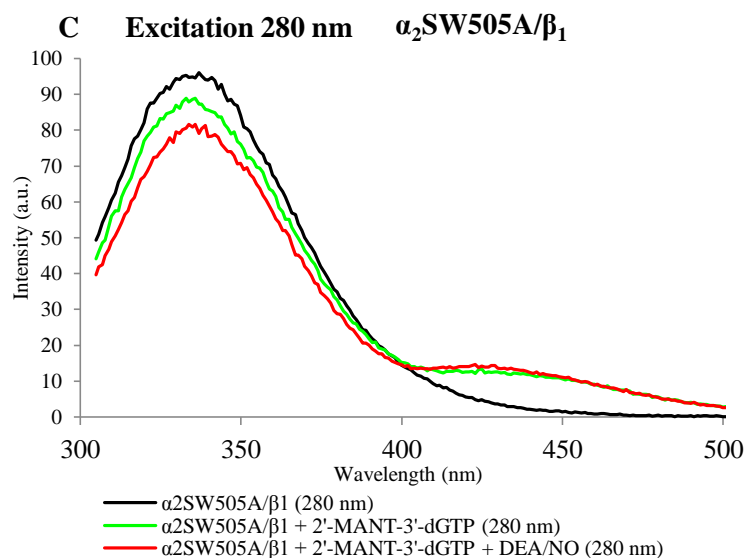
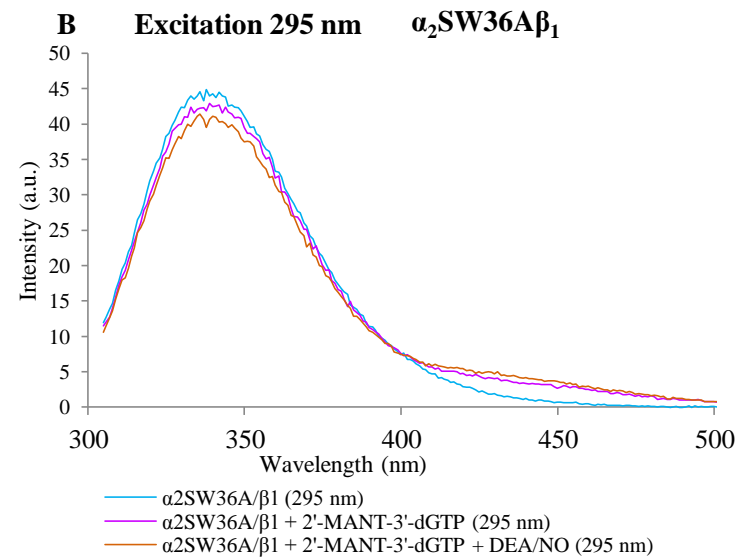
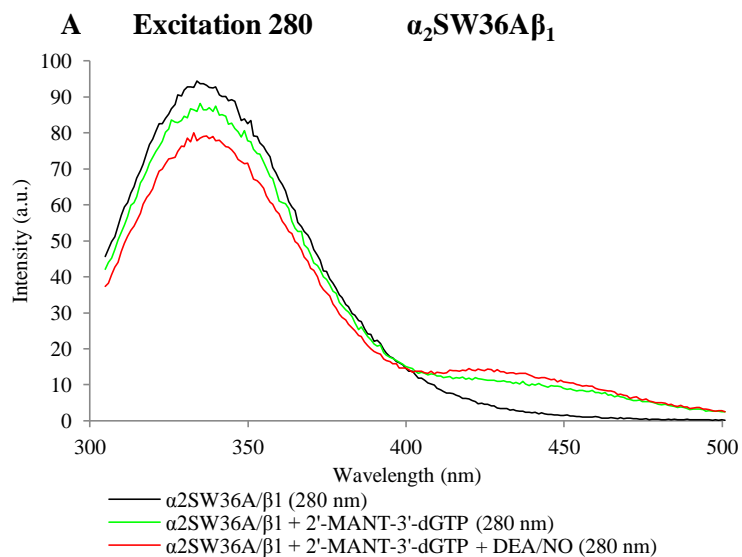


Figure 28: Fluorescence emission spectra of purified α_2 SW36A/ β_1 (A,B) and α_2 SW505A/ β_1 (C,D) (3 μ M) in the absence and presence of 2'-MANT-3'-dGTP (3 μ M) and DEA/NO (100 μ M). The assay buffer consisted of 50 mM TEA/HCl, 10 mM DTT, 5 mM MnCl₂ and 1 mM EDTA (pH 7.4). The emission was scanned at excitation wavelengths of 280 (A, C) and 295 nm (B, D).

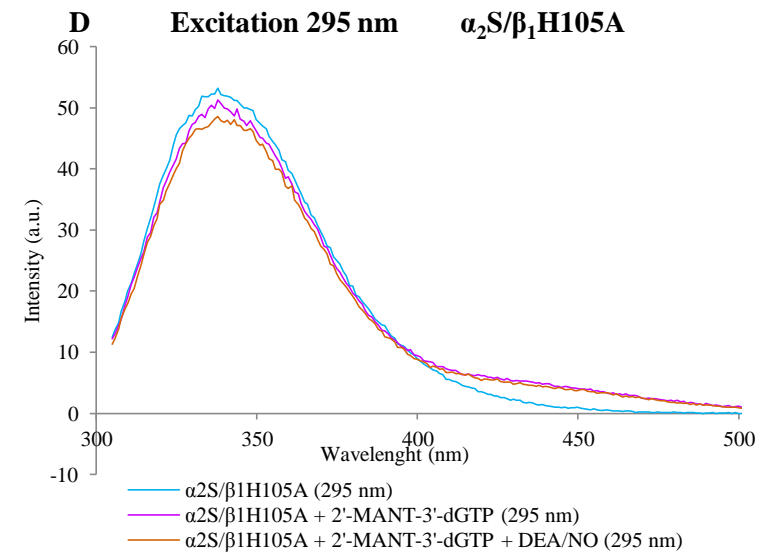
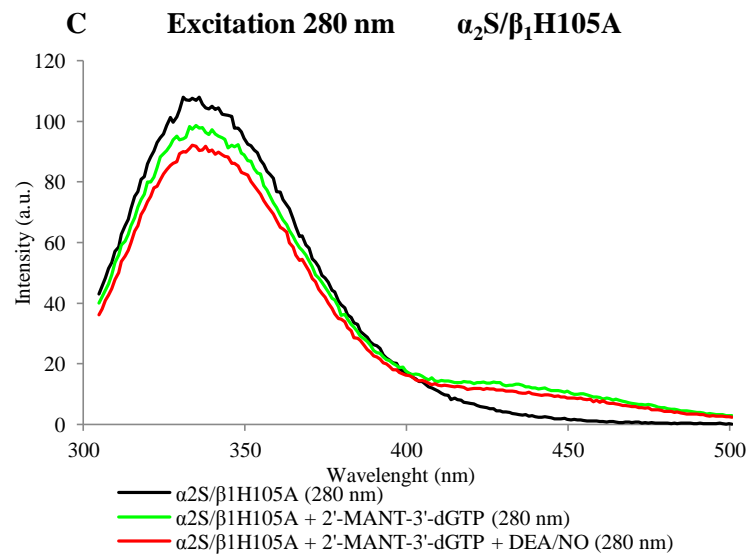
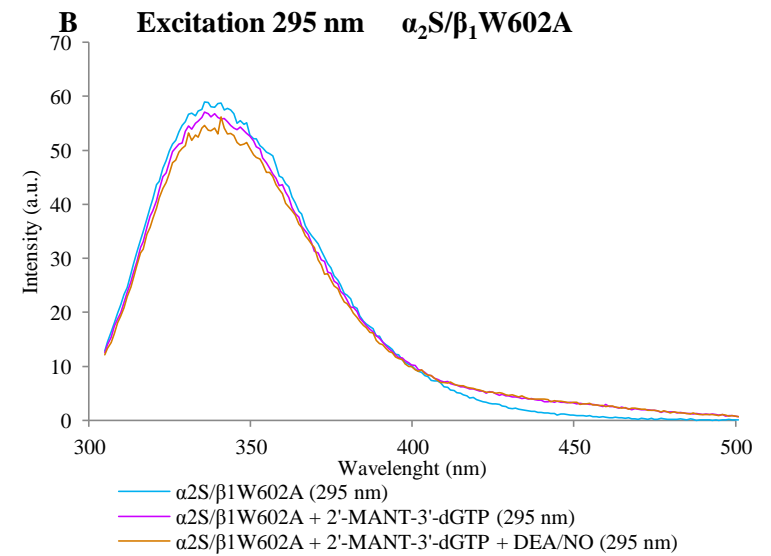
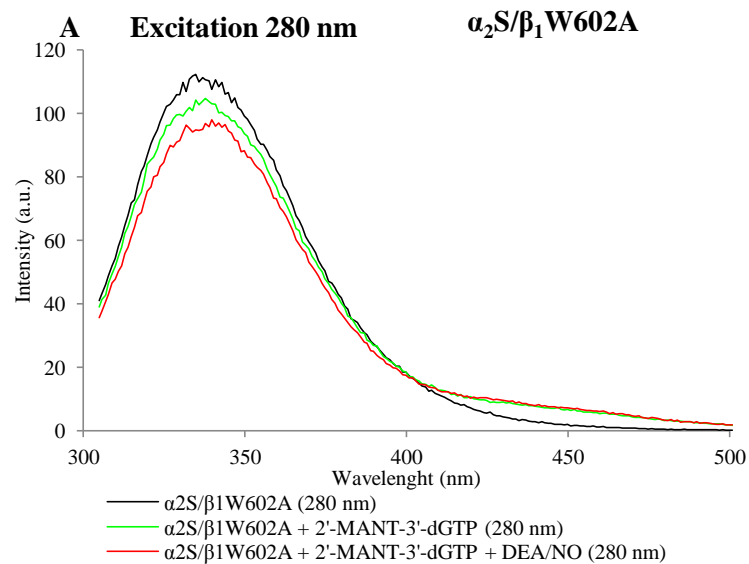


Figure 29: Fluorescence emission spectra of purified α_2S/β_1W602A and α_2S/β_1H105A (3 μ M) in the absence and presence of 2'-MANT-3'-dGTP (3 μ M) and DEA/NO (100 μ M). The assay buffer consisted of 50 mM TEA/HCl, 10 mM DTT, 5 mM MnCl₂ and 1 mM EDTA (pH 7.4). The emission was scanned at excitation wavelengths of 280 (A,C) and 295 nm (B,D).

Tryptophan and tyrosine residues of the purified α_2/β_1 were excited at 280 nm resulting in the emission maximum at 335 nm (Fig. 27A). In the presence of 2'-MANT-3'-dGTP a new fluorescence peak appeared at 430 nm and was accompanied by a decrease in fluorescence intensity at 335 nm. These new peaks reflect the FRET from tryptophan and tyrosine residues of sGC to 2'-MANT-3'-dGTP. In addition, the presence of NO-donor DEA/NO further decreased the fluorescence intensity at 335 nm and increased the one at 430 nm (Fig. 27A).

The emission spectra obtained using the tryptophan specific excitation wavelength at 295 nm (Fig. 27B) were miniature copies of those obtained using the excitation wavelength of 280 nm (Fig. 27A). For example, the fluorescence intensity at 335 nm decreased 2-fold when excitation wavelength at 295 nm was used. The presence of 2'-MANT-3'-dGTP and DEA/NO decreased the fluorescence intensity at 335 nm and increased that at 430 nm (Fig. 27B).

The emission spectra obtained for the sGC mutant α_2 SW36A/ β_1 (Fig. 28A and 28B) and α_2 SW505A/ β_1 (Fig. 28C and 28D) using the excitation wavelength at 280 and 295 nm had a similar trend in the presence of 2'-MANT-3'-dGTP and DEA/NO, as seen with the wild type enzyme.

There was no positive effect of DEA/NO for the sGC mutant α_2 S/ β_1 H105A (Fig. 29C and 29D). The analysis of the emission spectra obtained after the addition of DEA/NO revealed a decrease in fluorescence intensity at 335 nm, accompanied by a small decrease in fluorescence intensity at 430 nm, following the addition of DEA/NO.

The emission spectra of the purified α_2 S/ β_1 W602A (Fig. 29A and 29B) show that after the addition DEA/NO there was no marked increase of fluorescence intensity at 335 nm.

4.7.2. FRET efficiency

The FRET efficiency depends on the distance between the two interacting molecules. There are four tryptophane residues in the α_2 S/ β_1 and each could contribute to the FRET occurrence at basal and NO-stimulating conditions. The fluorescence emission spectra do not provide sufficient information on which tryptophan residue is responsible for the FRET. The calculation of FRET efficiency or the fraction of energy transferred might show which tryptophan residue has a major or minor influence on the FRET.

The sensitized emission method with three channels was used for spectrofluorometric measurements. Data obtained from the donor, acceptor and FRET channels were used for the calculation of FRET efficiency (E%) according to Wallrabe and Periasamy (2005). Three independent FRET experiments were performed for purified α_2S/β_1 , α_2SW36A/β_1 , $\alpha_2SW505A/\beta_1$, and α_2S/β_1H105A . A single FRET experiment was performed for α_2S/β_1W602A . Average FRET efficiencies (E%) before and after the addition of DEA/NO are presented in Fig. 30.

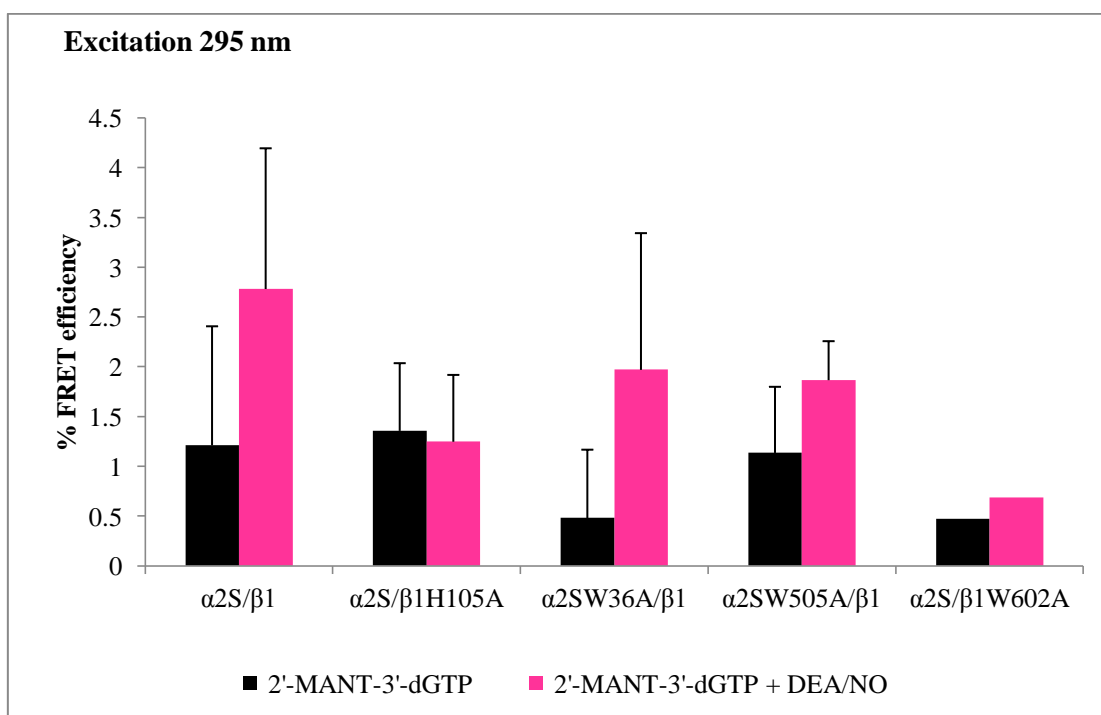


Figure 30: FRET efficiencies (%) obtained from three independent FRET experiments. The excitation wavelength of 295 nm was used. A single FRET experiment was performed for α_2S/β_1W602A .

Additionally, the difference between FRET efficiencies before and after the addition of DEA/NO was calculated to investigate which tryptophan residue is responsible for the increase of FRET efficiency under NO-stimulating conditions and to show that the amount of increase is the same for the mutant α_2SW36A/β_1 and the wild type α_2S/β_1 .

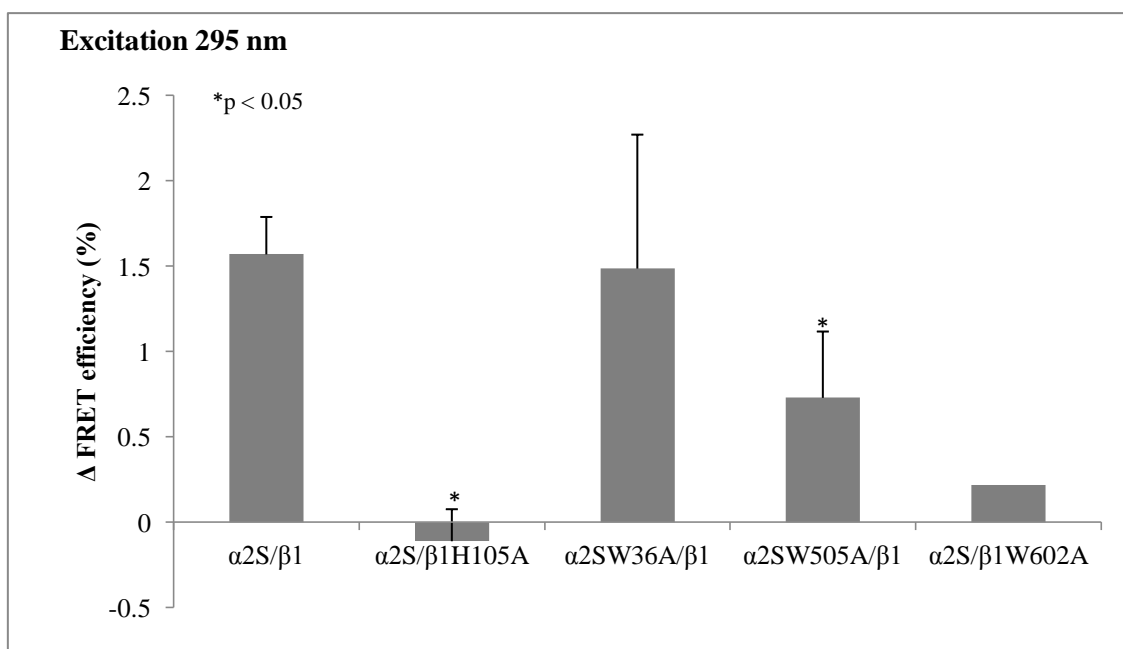


Figure 31: Increase of FRET efficiency (%) after the addition of DEA/NO. The increase was calculated from the average FRET efficiencies before and after the addition of DEA/NO.

High standard deviation indicates that FRET efficiencies strongly varied among three independent experiments (Fig. 30). The increase of FRET efficiency, which was calculated as a difference between the FRET efficiency before and after the addition of DEA/NO, does not deviate so strongly, except in the case of α_2SW36A/β_1 mutant (Fig. 31). Even though data with high standard deviations were obtained, we were able to reach some conclusions.

Under basal conditions the average FRET efficiency for α_2S/β_1 was 1.2% (Fig. 30). The addition of DEA/NO resulted in its increase for 1.6% (Fig. 31).

The basal FRET efficiency for α_2S/β_1H105A was comparable to that of the wild type enzyme (Fig. 30), but the addition of DEA/NO did not increase it; moreover it decreased a little bit (0.1%) (Fig. 31). The change of FRET efficiency after addition of DEA/NO was significantly different for α_2S/β_1H105A when compared to α_2S/β_1 .

The tryptophan 36 in the rat α_2 subunit is located at the N-terminus of sGC. Its mutation to alanine led to a decreased basal FRET efficiency from 1.2 to 0.5% (Fig. 30). Under NO-stimulated conditions the FRET efficiency increased for 1.5% (Fig. 31). Its increase was comparable to that of the wild type enzyme, as it did not differ significantly from it (Fig. 31).

The second tryptophan residue (W505) of the rat α_2 subunit is located at the end of the CC domain of sGC. The mutation of tryptophan 505 to alanine led to a small decrease in the basal FRET efficiency from 1.2 to 1.1% (Fig. 30). The addition of DEA/NO increased the FRET efficiency for 0.7%, which is less than in case of α_2S/β_1 (1.6%) and α_2SW36A/β_1 (1.5%). The FRET efficiency for $\alpha_2SW505A/\beta_1$ was significantly different from that of α_2S/β_1 (Fig. 31).

The β_1 subunit of sGC contains a tryptophan residue W602 in the substrate binding site. The mutation of W602 to alanine led to a decreased basal FRET efficiency from 1.2 to 0.5% (Fig. 33) and the addition of DEA/NO resulted in a small increase of FRET efficiency (by 0.2%) (Fig. 31).

4.8. DIRECT FLUORESCENCE EXPERIMENTS

2'-MANT-3'-dGTP is an environmentally sensitive probe because it displays an increased fluorescence upon its exposure to a hydrophobic environment. Direct fluorescence experiments were performed to analyze the microenvironment of 2'-MANT-3'-dGTP in the catalytic center before and after the addition of DEA/NO. 2'-MANT-3'-dGTP which was excited at 350 nm and its emission measured at 445 nm. The fluorescence was measured for 2'-MANT-3'-dGTP alone and in the presence of sGC and DEA/NO. The results were normalized to the fluorescence of 2'-MANT-3'-dGTP alone in each experiment. Three independent experiments were carried out for α_2S/β_1 , α_2SW36A/β_1 and $\alpha_2SW505A/\beta_1$, two for α_2S/β_1H105A , and one for α_2S/β_1W602A .

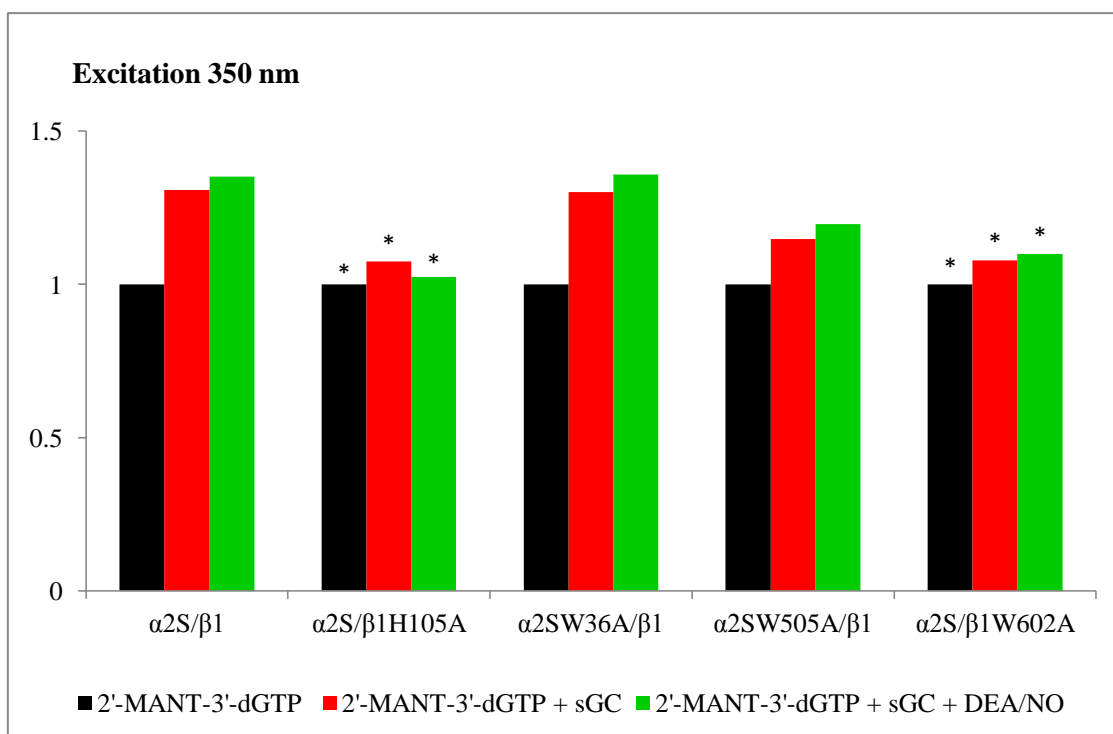


Figure 32: Normalized fluorescence intensities of 2'-MANT-3'-dGTP (black) in the presence of sGC (red) and after the addition of DEA/NO (green). Samples contained 2'-MANT-3'-dGTP (3 μ M), purified sGC (3 μ M) and DEA/NO (100 μ M). The buffer solution consisted of 25 mM HEPES/NaOH, 100 mM KCl and 3 mM $MgCl_2$ (pH 7.4). The final volume of the sample was 50 μ l. 2'-MANT-3'-dGTP was directly excited at 350 nm and the resulting fluorescence was measured at 445 nm. * Two experiments were carried out for α_2S/β_1H105A and one for α_2S/β_1W602A .

Direct fluorescence experiment (Fig. 32) showed that the fluorescence intensity of 2'-MANT-3'-dGTP increased when it was bound to the catalytic center of sGC. The increase of the fluorescence was more evident for α_2S/β_1 , α_2SW36A/β_1 , and $\alpha_2SW505A/\beta_1$ but was very small for α_2S/β_1H105A and α_2S/β_1W602A . After the addition of DEA/NO the increase in fluorescence intensity of 2'-MANT-3'-dGTP was very small and it even decreased a little bit in case of α_2S/β_1H105A .

5. DISCUSSION

The research work presented in this graduation thesis was done in the research group of Prof. Sönke Behrends at the Institute of Pharmacology, Toxicology and Clinical Pharmacy of the Technical University of Braunschweig. The research was part of the project which deals with the analysis of the activation mechanism of soluble guanylyl cyclase. The research group was already able to show conformational changes in the catalytic region of sGC isoform α_1/β_1 induced by NO (Busker et al. 2010).

5.1. GUANYLYL CYCLASE, 2'-MANT-3'-dGTP AND FRET

Soluble guanylyl cyclase is a heterodimer consisting of α and β subunits and is the key enzyme of nitric oxide/cyclic GMP-signaling pathway. Binding of nitric oxide (NO) to the prosthetic heme group in the β_1 subunit increases the synthesis rate of cyclic GMP from GTP several for 100-folds. The α_1 and β_1 subunits are expressed in most tissues while the α_2 subunit shows a more restricted expression pattern with high levels in brain, placenta, spleen and uterus (Budworth et al., 1999). The α_1 and α_2 subunits share only 27% identical amino acids in the N-terminal region but they are functionally similar (Russwurm et al., 1998). Each sGC subunit consists of four distinct domains: the N-terminal H-NOX domain, the PAS domain, CC domain and the C-terminal catalytic domain (Derbyshire and Marletta, 2012). So far the crystal structure of the heterodimeric sGC holoprotein has not been determined and the relative positions of sGC domains are lacking. It is also unknown how the NO binding to the N-terminal β_1 H-NOX may influence the conformation of the C-terminal catalytic domain (Haase et al., 2010).

There are four tryptophan residues located in different domains of the α_2 S(rat)/ β_1 (human) sGC isoform, which can serve as FRET donors when excited in sufficient proximity of the FRET acceptor. The rat α_2 subunit contains two tryptophan residues; the W36 is in the N-terminal H-NOX domain and the W505 at the end of the CC domain. The human β_1 subunit also contains two tryptophan residues; the W22 in the N-terminal H-NOX domain and the W602 in the catalytic domain within the substrate binding site.

Fluorescently labeled nucleotides 2'- MANT-NTPs are competitive inhibitors of sGC (Gille et al, 2004) which have already been used as FRET acceptors in analysis of active sites of various enzymes: mammalian membrane-bound adenylyl cyclase (Mou et al.,

2005), adenylyl cyclase toxin of *Bordetella pertussis* (Göttle et al., 2007), adenylyl cyclase toxin of *Bacillus anthracis* (Taha et al., 2008 and Suryanarayana et al., 2009), and the soluble guanylyl cyclase isoform α_1/β_1 (Busker et al., 2010).

FRET only occurs when the distance between the donor and acceptor molecules is typically between 10 to 100 Å (Periasamy and Day, 2005). This was the case for the soluble guanylyl cyclase isoform α_2S/β_1 , in which the conformation of the enzyme allowed sufficient proximity between the tryptophan residues and the 2'-MANT-3'-dGTP (preliminary experiments made by Mareike Busker, unpublished).

In our research, mutants of the $\alpha_2S(\text{rat})/\beta_1(\text{human})$ sGC isoform were used, in which individual tryptophan residues were substituted with alanine. The mutant enzymes were used to analyze which domain or which tryptophan is close to the active site of the purified enzyme in the presence or absence of NO.

5.2 MUTAGENESIS, EXPRESSION AND PURIFICATION

We performed site-directed mutagenesis in the α_2 subunit where tryptophan 36 and 505 were substituted by alanine. Mutations of the β_1 subunit were already made by the research group but we used only the β_1W602A mutant. The sGC isoform α_2S/β_1 and mutants α_2SW36A/β_1 , $\alpha_2SW505A/\beta_1$, α_2S/β_1H105A , and α_2S/β_1W602A were expressed with the baculovirus/Sf9 system and *Strep*-tag II fused C-terminally to the α_2 subunit thereby enabling purification of the whole enzyme with the affinity chromatography.

The SDS PAGE gel electrophoresis showed that affinity chromatography removed a large amount of impurities, but there were still some left (Fig. 20 and 21). The samples containing purified enzyme had two strong protein bands positioned where our proteins should appear. We assumed that the first band was the α_2S (82.7 kDa) and the second one the β_1 (70.5 kDa) (Fig. 20 and 21). Western blot analysis against α_2 and β_1 subunits (Fig. 22) confirmed the identity of both proteins observed in the SDS PAGE gel. We were also able to detect both subunits in the cytosolic fractions (Fig. 22). There were also some non-specific bands visible in cytosolic fractions but were absent in electrophoretic lanes of the purified protein. This could be due to the proteolytic breakdown of the enzyme in the cytosol or to non-specific binding of the secondary antibody to lanes overloaded with

cytosolic proteins. If the primary antibody was non-specific, additional bands would probably be much brighter.

5.3. SPECTRAL ANALYSIS

Spectral analysis showed that $\alpha_2\text{S}/\beta_1$ (Fig. 23), $\alpha_2\text{SW36A}/\beta_1$ (Fig. 24A), and $\alpha_2\text{SW505A}/\beta_1$ all contained heme (Fig. 24B). In contrast, heme was absent in $\alpha_2\text{S}/\beta_1\text{H105A}$ (Fig. 25B) which is in accordance with previous reports of Wedel et al. 1994, showing that mutation of histidin 105 to alanine in the β_1 subunit results in inability of sGC to bind heme.

Spectral analysis did not confirm the presence of heme in $\alpha_2\text{S}/\beta_1\text{W602A}$ (Fig. 25A), because the heme signal at 430 nm was very low and there was only a minor difference in spectra when absorption of $\alpha_2\text{S}/\beta_1\text{W602A}$ (Fig. 25A) was compared to that of $\alpha_2\text{S}/\beta_1\text{H105A}$ (Fig. 25B). However, it is possible that there was a remainder of heme left in the enzyme because the small peak at 430 nm completely disappeared after the addition of DEA/NO. It has been already shown that $\alpha_1\text{S}/\beta_1\text{W602A}$ contains heme (Busker M., unpublished data) and therefore it is possible that it is also present in $\alpha_2\text{S}/\beta_1\text{W602A}$. The absorption of this enzyme was measured only once and maybe a mistake was made in the purification process which resulted in a heme loss or maybe there were certain problems with the baculoviral stock $\beta_1\text{W602A}$.

5.4. GUANYLYL CYCLASE ACTIVITY ASSAY

The tryptophan at the end of the CC domain is conserved in rat (W466), dog (W467), human (W467), and mouse (W476) α_1 subunit, in rat (W505) and human (W507) α_2 subunit but not in human β_1 subunit of sGC (Supplement 1). Rothkegel et al. (2007) showed that deletion of a region at the end of the CC domain in the rat α_1 subunit ($\alpha_1\text{460-469}$) containing W466 resulted in a loss of enzymatic activity of sGC. The sequence alignments (Supplement 1) show that this region includes residues from 499 to 508 in the rat α_2 subunit and also the conserved tryptophan 505. The mutation of W505 to alanine might have impaired the activation mechanism of sGC which led to an inactive enzyme (Fig. 26, $\alpha_2\text{SW505A}/\beta_1$) although it contained heme (Fig. 24B). It is possible that tryptophan 505 of the α_2 subunit is important for activation of the $\alpha_2\text{S}/\beta_1$ sGC isoform.

Guanylyl cyclase activity assay showed that mutation of tryptophan 36 to alanine in the α_2 subunit of sGC (α_2 SW36A/ β_1) did not affect the sensitivity of the enzyme to NO (Fig. 26). The mutant α_2 S/ β_1 W602A showed loss of NO sensitivity (Fig. 26) which could be related to a low heme signal (Fig. 25A).

The mutant α_2 S/ β_1 H105A preserved a partial NO sensitivity (Fig. 26) although the enzyme did not show increased FRET efficiency following the addition of DEA/NO (Fig. 31). There was also no indication that α_2 S/ β_1 H105A contained heme (Fig. 25B). Our data could be explained by existence of a non-heme binding site for NO, which is involved in the activation process of the sGC (Cary et al., 2005; Derbyshire and Marletta, 2007). Only one assay was made and its result raised some interest, but it should be regarded with suspicion and needs further investigation.

5.5. FRET

Mutants of the α_2 S(rat)/ β_1 (human) sGC isoform were used, in which individual tryptophan residues were substituted by alanine. Three remaining tryptophan residues were used as FRET donors and the 2'-MANT-3'-dGTP as a FRET acceptor in FRET experiments. If a certain mutation resulted in a decreased FRET signal that would indicate that that tryptophan residue is responsible for the FRET signal seen in the wild type enzyme and that it is in the close proximity to the catalytic center. This was the method with which we were able to analyze the conformation of the active site of the purified α_2 / β_1 sGC isoform in the presence or absence of NO and to obtain information about the sGC conformation.

Upon excitation at 280 and 295 nm basal FRET signals between tryptophan residues of sGC and 2'-MANT-3'-dGTP were observed in fluorescence emission spectra of all enzymes (Fig. 27, 28 and 29). The addition of DEA/NO increased the FRET signal for α_2 S/ β_1 (Fig. 27), α_2 SW36A/ β_1 (Fig. 28A and B) and α_2 SW505A/ β_1 (Fig. 28C and D), but there was no positive effect of DEA/NO on α_2 S/ β_1 H105A (Fig. 29C and D). The increase was very small for α_2 S/ β_1 W602A (Fig. 29A and B) and was probably related to the low heme signal (Fig. 25A).

Fluorescence emission spectra (Fig. 27, 29C, 29D) and measurements of FRET efficiencies for α_2 S/ β_1 and α_2 S/ β_1 H105A (Fig. 30 and 31) showed that it was the binding of NO to the prosthetic heme group of α_2 S/ β_1 that led to an increase of FRET signal. The NO

binding to heme consequently changed the conformation of $\alpha_2\text{S}/\beta_1$ in a way that allowed one or more tryptophan residues to come closer to the catalytic center, where the 2'-MANT-3'-dGTP was bound. To analyze which tryptophan residues could have contributed to the basal FRET signal and to the increase of FRET signal under NO-stimulating conditions the FRET efficiency was measured for each mutant.

5.5.1. Tryptophan 36

The tryptophan residue 36 is located on the N-terminus (H-NOX domain) of the rat α_2 subunit and the 2'-MANT-3'-dGTP binds to the catalytic center of the α_2/β_1 , which is formed by dimerization of C-terminal domains in α_2 and β_1 subunits. The basal FRET efficiency was lower for $\alpha_2\text{SW36A}/\beta_1$ (0.5%) than for the wild type $\alpha_2\text{S}/\beta_1$ (1.2%) (Fig. 30), which suggested that the tryptophan residue 36 could be partly responsible for the basal FRET efficiency seen with the wild type enzyme. In other words, it is very likely that tryptophan residue 36 is close to the catalytic domain of $\alpha_2\text{S}/\beta_1$. This hypothesis could consecutively support the model proposed by Haase et al. 2010, where the PAS and H-NOX domains of sGC are folded back towards the catalytic domain (Fig. 5B). However, the tryptophan residue 36 of the α_2 subunit was not responsible for the increase of FRET efficiency after the addition of DEA/NO, as observed for the wild type enzyme, since the increase for $\alpha_2\text{SW36A}/\beta_1$ was not significantly different from it (Fig. 31).

5.5.2. Tryptophan 505

The tryptophan residue 505 is located at the end of the CC domain of rat α_2 subunit and is conserved for α subunit according to multisequence alignments presented in Supplement 1. The mutation of tryptophan 505 to alanine only slightly decreased the basal FRET efficiency (Fig. 30). After the addition of DEA/NO the FRET efficiency increased but the increase was significantly smaller for $\alpha_2\text{SW505A}/\beta_1$ than for the wild type enzyme (Fig. 31). This suggested that the binding of NO to the prosthetic heme group of $\alpha_2\text{S}/\beta_1$ triggered the movement of tryptophan 505 towards the catalytic center of the enzyme. However this suggestion cannot be considered as a proof for the increase of FRET efficiency seen in the wild type enzyme because the mutant $\alpha_2\text{SW505A}/\beta_1$ was inactive (Fig. 26).

5.5.3. Tryptophan 602

The tryptophan 602 is located in the catalytic domain of the β_1 subunit and within the substrate binding site of sGC. It was shown that W602 contributes to the basal FRET efficiency in α_1S/β_1 (Busker et al., 2010). One FRET experiment was done for α_2S/β_1W602A and the result showed that its basal FRET efficiency was much lower (0.5%) than that of α_2S/β_1 (1.2%) (Fig. 30). This result favors the possibility that tryptophan 602 could also have contributed to the basal FRET efficiency seen with the wild type enzyme (Fig. 30).

The mutant α_2S/β_1W602A had a low heme signal (Fig. 25B) and almost a complete loss of NO sensitivity (Fig. 26). These results could explain a small increase of FRET efficiency for α_2S/β_1W602A after the addition of DEA/NO (Fig. 31). Alternatively, it is also possible that the tryptophan 602 contributed to the increase of FRET efficiency in case of α_2S/β_1 because the results of the FRET experiment do not contradict. Busker et al. (2010) showed that tryptophan 602 does not contribute to the increase in FRET efficiency for the sGC isoform α_1S/β_1 .

5.5.4. Tryptophan 22

Busker et al. (2010) showed that tryptophan 22 in the β_1 subunit is not responsible for the basal FRET efficiency of α_1S/β_1 . Experiments were not carried out with α_2S/β_1W22A , therefore we cannot exclude the importance of tryptophan 22 for the basal FRET efficiency seen with the wild type enzyme (Fig. 30). The sum of decrease in basal FRET efficiency for α_2SW36A/β_1 , $\alpha_2SW505A/\beta_1$, and α_2S/β_1W602A was 1.5% and the basal FRET efficiency for α_2S/β_1 was 1.2%. The possibility that the W22 could also contribute to the basal FRET efficiency for α_2S/β_1 is therefore very small.

Winger and Marletta (2005) showed that the activity of the heterodimeric complex made only of catalytic domains of each subunit, $\alpha_{1cat}/\beta_{1cat}$, was inhibited by the presence of the β_1 H-NOX domain. Haase et al. 2010 showed close proximity of the N-terminal H-NOX domains and the catalytic region, which supported the model by Winger and Marletta. It is possible that activation mechanism of sGC moves the β_1 H-NOX domain towards the catalytic center allowing the approximation of W22 towards the 2'-MANT-3'-dGTP. Busker et. al (2010) showed that mutation of the second tryptophan residue (W22) in the β_1 subunit led to a heme free mutant α_1S/β_1W22A and that the FRET experiments did not

show increase of FRET efficiency after the addition of DEA/NO. This is the reason why our experiments were not carried out for the $\alpha_2\text{S}/\beta_1\text{W22A}$ sGC isoform; therefore we cannot exclude the importance of tryptophan 22 for the increase of FRET efficiency seen with the wild type enzyme (Fig. 31).

5.6 DIRECT FLUORESCENCE EXPERIMENT

MANT-NTPs are environmentally sensitive probes, which exhibit increased fluorescence upon their exposure to hydrophobic environment (Hiratsuka, 1983). They have been already used in analysis of conformation of catalytic sites of adenylyl cyclase toxin of *Bacillus anthracis*, the so called edema factor (Suryanarayana et al., 2009) and mammalian membrane-bound adenylyl cyclase (Mou et al., 2005).

Because we wanted to analyze the conformation of the active site of purified sGC, the fluorescence of 2'-MANT-3'-dGTP alone and in the presence of sGC and DEA/NO was measured in direct experiments. The results showed that the fluorescence of 2'-MANT-3'-dGTP increased when it was bound to the catalytic center of $\alpha_2\text{S}/\beta_1$, $\alpha_2\text{SW36A}/\beta_1$, $\alpha_2\text{SW505A}/\beta_1$, $\alpha_2\text{S}/\beta_1\text{H105A}$ and $\alpha_2\text{S}/\beta_1\text{W602A}$ (Fig. 32). This implies that the environment of 2'-MANT-3'-dGTP is more hydrophobic in the active center of the sGC than in the buffer solution. Under NO-stimulating conditions the hydrophobicity of the active center did not change substantially.

6. CONCLUSION

The tryptophan 36, located at the beginning of the H-NOX domain of the α_2 subunit and tryptophan 602 in the catalytic domain of the β_1 subunit of sGC are very likely to be the only tryptophan residues close to the substrate binding site under basal conditions. Our results also support the model proposed by Haase et al. (2010), which suggests that the PAS and H-NOX domains of sGC are folded back towards the catalytic domain.

After NO binding to the prosthetic heme group of α_2S/β_1 one or more tryptophan residues come closer to the substrate binding site. The results of the FRET experiment suggested that the sGC activation mechanism could move tryptophan 505 at the end of the CC domain of the α_2 subunit towards the substrate binding site. But this assumption is not necessarily true for the wild type enzyme since the mutation of tryptophan 505 to alanine led to an inactive enzyme.

The tryptophan 602 in the β_1 subunit could also come near the substrate binding site under NO stimulating conditions but the mutant enzyme α_2S/β_1W602A was insensitive to NO, probably because of partial loss of its heme group. Further research is needed to prove the activity, heme content and FRET signals under basal and NO-stimulating conditions.

The tryptophan residue 22 located at the beginning of the H-NOX domain of β_1 subunit could also come closer to the substrate binding site under the NO-stimulating conditions but this hypothesis was not tested for α_2S/β_1 because the mutation of tryptophan 22 led to a heme-free mutant α_1S/β_1 sGC isoform.

The environment of 2'-MANT-3'-dGTP in the catalytic center of the sGC isoform is more hydrophobic than the buffer solution and the hydrophobicity of the active center does not change substantially under NO-stimulating conditions.

We conclude that further experiments are needed to provide evidence which tryptophan residue comes close to the substrate binding site under NO-stimulating conditions. Phenylalanine mimics tryptophan in its hydrophobicity and volume and perhaps the mutation of tryptophan 22 and 505 to phenylalanine would result in an active enzyme.

7. REFERENCES

1. Behrends S: Drugs that activate specific nitric oxide sensitive guanylyl cyclase isoforms independent of nitric oxide release. *Curr Med Chem* 2003; 10: 291-301.
2. Derbyshire ER, Marletta MA: Structure and regulation of soluble guanylate cyclase. *Annu Rev Biochem* 2012; 81: 533–59.
3. Marletta MA: Nitric oxide signaling. *Encyclopedia of Biological Chemistry*; 2004; 3: 62-65.
4. Schmidt HH, Hofmann F, Stasch JP, *Handbook of experimental Pharmacology* 191, sGMP: Generators, Effectors and Therapeutic Implications, Springer, Berlin Heidelberg, 2009, 17-31, 247-275.
5. Budworth J, Meillerais S, Charles I, Powell K: Tissue distribution of the human soluble guanylate cyclases. *Biochem Biophys Res Commun* 1999; 263: 696-701.
6. Russwurm M, Behrends S, Harteneck C, Koesling D, Functional properties of a naturally occurring isoform of soluble guanylyl cyclase. *Biochem J* 1998; 335: 125–130.
7. Yuen PS, Potter LR, Garbers DL: A new form of guanylyl cyclase is preferentially expressed in rat kidney. *Biochemistry* 1990; 29:10872–78.
8. Mergia E, Friebe A, Dangel O, Russwurm M, Koesling D, Spare guanylyl cyclase NO receptors ensure high NO sensitivity in the vascular system. *The Journal of Clinical Investigation* 2006; 116: 1731–1737.
9. Russwurm M, Wittau N, Koesling D: Guanylyl cyclase/PSD-95 interaction. *J Biol Chem* 2001; 2776: 44647–44652.
10. Carry SPL, Winger JA, Marletta MA: Tonic and acute nitric oxide signaling through soluble guanylate cyclase is mediated by nonheme nitric oxide, ATP, and GTP. *PNAS*; (2005); 12: 13064-13069.
11. Derbyshire ER, Marletta MA: Butyl isocyanide as a probe of the activation mechanism of soluble guanylate cyclase. Investigating the role of non-heme nitric oxide. *J Biol Chem* 2007; 282: 35741-8.
12. Lucas KA, Pitari GM, Kazerounian S, Ruiz-Stewart I, Park J, Schulz S, Chepenik KP, Waldman SA: Guanylyl cyclases and signaling by cyclic GMP. *Pharmacol Rev* 2000; 52: 375-414.
13. Krumenacker JS, Hanafy KA, Murad F: Regulation of nitric oxide and soluble guanylyl cyclase. *Brain Res Bull* 2004; 62: 505-15.
14. Wedel B, Humbert P, Harteneck C, Foerster J, Malkewitz J, Bohme E, Schultz G, Koesling D: Mutation of His-105 in the β 1 subunit yields a nitric oxide-insensitive form of soluble guanylyl cyclase. *Proc Natl Acad Sci USA* 1994; 91: 2592–96.
15. Koglin M, Behrends S: A functional domain of the α ₁ subunit of soluble guanylyl cyclase is necessary for activation of the enzyme by nitric oxide and YC-1 but is not involved in heme binding. *The Journal of Biological Chemistry* 2003; 278: 12590-12597.
16. Kraehling JR, Busker M, Haase T, Haase N, Koglin M, Linnenbaum M, Behrends S: The amino-terminus of nitric oxide sensitive guanylyl cyclase α 1 does not affect

- dimerization but influences subcellular localization. PLoS ONE 2011; 6: e25772. doi:10.1371/journal.pone.0025772.
17. Cary SP, Winger JA, Derbyshire ER, Marletta MA: Nitric oxide signaling: no longer simply on or off. Trends Biochem Sci 2006; 31: 231-9.
 18. Ma X, Beuve A, van den Akker F: Crystal structure of the signaling helix coiled-coil domain of the β_1 subunit of the soluble guanylyl cyclase. BMC Struct Biol 2010; 10. doi:10.1186/1472-6807-10-2.
 19. Winger JA, Marletta MA. Expression and characterization of the catalytic domains of soluble guanylate cyclase: interaction with the heme domain. Biochemistry 2005; 44: 4083–90.
 20. Winger JA, Derbyshire ER, Lamers MH, Marletta MA, Kuriyan J. The crystal structure of the catalytic domain of a eukaryotic guanylate cyclase. BMC Struct Biol 2008; 8. doi: 10.1186/1472-6807-8-42.
 21. Cayman chemical: DEA NONOate.
<https://www.caymanchem.com/app/template/Product.vm/catalog/82100%3bjsessionid=E82CFBE46C8F3022588A3E751FABC75%201> (5.9.2012)
 22. Sigma-Aldrich: Diethylamine NONOate sodium salt hydrate
<http://www.sigmaaldrich.com/catalog/product/sigma/d184?lang=en®ion=SI> (5.9.2012)
 23. Haase T, Haase N, Kraehling JR, Behrends S: Fluorescent Fusion Proteins of Soluble Guanylyl Cyclase Indicate Proximity of the Heme Nitric Oxide Domain and Catalytic Domain. PLoS ONE 2010; 5(7): e11617. doi:10.1371/journal.pone.0011617.
 24. Clegg RM: Fluorescence resonance energy transfer. Curr Opin Biotechnol 1995; 6: 103-10.
 25. Chhabra, Deepak, and dos Remedios, Cristobal G: Fluorescence Resonance Energy Transfer. eLS. John Wiley & Sons Ltd, Chichester. <http://www.els.net> [doi: 10.1038/npg.els.0004170]
<http://www.els.net/WileyCDA/ElsArticle/refId-a0002979.html> (5.9.2012)
 26. Periasamy A, Day RN: Molecular imaging: FRET Microscopy and Spectroscopy, Oxford University Press, New York, 2005, 21-55, 126-145.
 27. Wallrabe H, Periasamy A: Imaging protein molecules using FRET and FLIM microscopy. Curr Opin Biotechnol 2005; 16:19-27.
 28. Hiratsuka T: New ribose-modified fluorescent analogs of adenine and guanine nucleotides available as substrates for various enzymes. Biochimica and Biophysica Acta 1983; 742: 496-508.
 29. Gille A, Lushington GH, Mou TC, Doughty MB, Johnson RA, Seifert R: Differential inhibition of adenylyl cyclase isoforms and soluble guanylyl cyclase by purine and pyrimidine nucleotides. J Biol Chem 2004; 279(19): 19955-19969.
 30. Mou TC, Gille A, Fancy DA, Seifert R, Sprang SR: Structural basis for the inhibition of mammalian membrane adenylyl cyclase by MANT-GTP. J Biol Chem 2005; 280: 7253-7261.
 31. Göttle M, Dove S, Steindel P, Shen Y, Tang WJ, Geduhn J, König B, Seifert R. Molecular analysis of the interaction of *Bordetella pertussis* adenylyl cyclase with fluorescent nucleotides. Mol Pharmacol 2007; 72: 526-35.

32. Taha HM, Schmidt J, Göttle M, Suryanarayana S, Shen Y, Tang WJ, Gille A, Geduhn J, König B, Dove S, Seifert R: Molecular analysis of the interaction of anthrax adenyl cyclase toxin, edema factor, with 2'(3')-O-(N-(methyl)anthraniloyl)-substituted purine and pyrimidine nucleotides. *Mol Pharmacol* 2008; 75: 693-703.
33. Suryanarayana S, Wang JL, Richter M, Shen Y, Tang WJ, Lushington GH, Seifert R: Distinct interactions of 2'- and 3'-O-(N-methyl)anthraniloyl-isomers of ATP and GTP with the adenyl cyclase toxin of *Bacillus anthracis*, edema factor. *Biochem Pharmacol* 2009; 78: 224-230.
34. Photochemcad (2.1). Computer program.
<http://www.photochemcad.com/> (5.9.2012)
35. Rothkegel C, Schmidt PM, Atkins DJ, Hoffmann LS, Schmidt HH, Schröder H, Stasch JP: Dimerization region of soluble guanylate cyclase characterized by bimolecular fluorescence complementation in vivo. *Mol Pharmacol* 2007; 72:1181-90.
36. ClustalW2. Multiple sequence alignment tool.
<http://www.ebi.ac.uk/Tools/msa/clustalw2/> (25.8. 2012).
37. QuikChange Primer Design Program . Agilent Technologies.
<https://www.genomics.agilent.com/CollectionSubpage.aspx?PageType=Tool&SubPageType=ToolQCPD&PageID=15> (January 2011).
38. QuikChange Lightning Site-Directed Mutagenesis Kit. Instruction manual, catalog # 210518 and #210519, Stratagen.
39. PureLink™ HiPure Plasmid DNA Purification Kits For Mini, Midi, and Maxi preparation of Plasmid DNA. Manual. Invitrogen, 2010.
40. Bac-to-Bac® TOPO® Expression System. User manual, Invitrogen, 2008.
41. Kang D, Gho YS, Suh M, Kang C: Highly sensitive and fast protein detection with coomassie brilliant blue in sodium dodecyl sulfate-polyacrylamide gel electrophoresis. *Bull Korean Chem Soc* 2002; 23 1511-1512.
42. Schultz G, Boehme E: Guanylate cyclase. GTP pyrophosphate-lyase (cyclizing), E.C 4:6 1:2. *Methods of Enzymatic Analysis* (Bergmeyer HU, Bergmeyer J, Grabl M, eds), Verlag Chemie, Weinheim, 1984, 379–389.
43. Busker M, Kraehling JR, Seeanner M, Behrends S: Analysis of nitric oxide sensitive guanylyl cyclase activation by ciguates based on MANT-GTP fluorescence. Focused conference group: P15 - endothelium in health and disease, Paper No.: 1918. *Basic & Clinical pharmacology & toxicology: Abstracts for the 16th world congress of basic and clinical pharmacology. 17-23 July 2010, Copenhagen, Denmark. 2010, 107 (suppl. 1).* <http://onlinelibrary.wiley.com/doi/10.1111/pto.2010.107.issue-s1/issuetoc>
44. 2'-MANT-3'-dGTP, Data sheet, Jena.
<http://www.jenabioscience.com/images/29c8187439/NU-231.pdf> (27.8.2012)
45. Schmidt TGM, Skerra A: The *Strep*-tag system for one-step purification and high-affinity detection or capturing of proteins. *Nature protocols* 2007; 2:1528-1535.
46. Skerra A: Das *Strep*-tag als molekulares Werkzeug zur Hochdurchsatz-Proteinreinigung in der Proteomforschung. *BIOSpektrum* 2003; 9: 189-192.


```

: . *.: *.: :* :. :. **: * :

```

| | | |
|--------------|--|-----|
| alpha2_Human | VKGQMIHVPESENILFLGSPCVKDLDELMDGRGLHLSDIPIHDATRDRVILVGEQAKAQDGL | 465 |
| alpha2_Rat | IKGQMIHVPESENAILFLGSPCVKDLDELIGRGLHLSDIPIHDATRDRVILVGEQAKAQDGL | 463 |
| alpha1_Human | LKGQMIYIVESSAILFLGSPCVDRLEDFTRGRLYLSDIPIHNALRDVVLIQEQAQDGL | 425 |
| alpha1_Dog | LKGQMIYIVESSAILFLGSPCVDRLEDFTRGRLYLSDIPIHNALRDVVLIQEQAQDGL | 425 |
| alpha1_Rat | LKGQMIYIVESSAILFLGSPCVDRLEDFTRGRLYLSDIPIHNALRDVVLIQEQAQDGL | 424 |
| alpha1_Mouse | LKGQMIYIVESSAILFLGSPCVDRLEDFTRGRLYLSDIPIHNALRDVVLIQEQAQDGL | 425 |
| beta1_Human | LKGQMIYLPEADSILFLCSPVMNLDLDRRGLYLSDIPLHDATRDLVLLGGEQFREEYKL | 365 |
| | :*****: *: :**** *.* .*: : **:*:*****:* * *: :**** : : * | |
| alpha2_Human | KKRMDKLGKATLERHQALEEEKKTVDLLYSIFPGDVAQQLVQGGQVQARKFDDVTMLFS | 525 |
| alpha2_Rat | KKRMDKLGKATLEKTHQALEEEKKTVDLLYSIFPGDVAQQLVQGGQVQARKFDDVTMLFS | 523 |
| alpha1_Human | KKRLGKLGKATLEQAHAQALEEEKKTVDLLCSIFPCEVAQQLVQGGQVQAKKFSNVTMLFS | 485 |
| alpha1_Dog | KKRLGKLGKATLEQAHAQALEEEKKTVDLLCSIFPSEVAQQLVQGGQVQAKKFSNVTMLFS | 485 |
| alpha1_Rat | KKRLGKLGKATLEHAHQALEEEKKTVDLLCSIFPSEVAQQLVQGGQVQAKKFSNVTMLFS | 484 |
| alpha1_Mouse | KKRLGKLGKATLEHAHQALEEEKKTVDLLCSIFPSEVAQQLVQGGQVQAKKFSNVTMLFS | 485 |
| beta1_Human | TQLEILTDRLQLTLRALEDEKKTDTLLYSVLPSPVANELRHKRPVPAKRYDNVTILFS | 425 |
| | ..: * . * : :****:** * ** *:* .**:* : : * * : : :****** | |
| alpha2_Human | DIVGFTAICAQCTP---MQVISMLNELYTRFDHQCG---FLDIYKVVETIGDAYCVAAGL | 578 |
| alpha2_Rat | DIVGFTAICAQCTP---MQVISMLNELYTRFDHQCG---FLDIYKVVETIGDAYCVASGL | 576 |
| alpha1_Human | DIVGFTAICSQCSP---LQVITMLNLYTRFDQCCG---ELDVYKVVETIGDAYCVAGGL | 538 |
| alpha1_Dog | DIVGFTAICSQCSP---LQVITMLNLYTRFDQCCG---ELDVYKVVETIGDAYCVAGGL | 538 |
| alpha1_Rat | DIVGFTAICSQCSP---LQVITMLNLYTRFDQCCG---ELDVYKVVETIGDAYCVAGGL | 537 |
| alpha1_Mouse | DIVGFTAICSQCSP---LQVITMLNLYTRFDQCCG---ELDVYKVVETIGDAYCVAGGL | 538 |
| beta1_Human | GIVGFNAFCSKHASGEGAMKIVNLLNDLYTRFDTLTDSRKNPFVYKVVETVGDYKMTVSGL | 485 |
| | .****.*:***: :. : : : : ** ***** . :****:* * ..** | |
| alpha2_Human | HRKSLCHAKPIALMALKMMELSEEVLTPDGRPIQMRIGIHSGSVLAGVVGVRMPRYCLFG | 638 |
| alpha2_Rat | HRKSLCHAKPIALMALKMMELSEEVLTPDGRPIQMRIGIHSGSVLAGVVGVRMPRYCLFG | 636 |
| alpha1_Human | HKESDTHAVQIALMALKMMELSDVMSPHGEPKMRIGLHSGSVFAGVVGKMPRYCLFG | 598 |
| alpha1_Dog | HKESDTHAAQIALMALKMMELSDVMSPHGEPKMRIGLHSGSVFAGVVGKMPRYCLFG | 598 |
| alpha1_Rat | HRESDTHAVQIALMALKMMELSDVMSPHGEPKMRIGLHSGSVFAGVVGKMPRYCLFG | 597 |
| alpha1_Mouse | HRESDTHAVQIALMALKMMELSDVMSPHGEPKMRIGLHSGSVFAGVVGKMPRYCLFG | 598 |
| beta1_Human | PEPCIHARSICHLALDMMEIAGQVQVD-GESVQITIGIHTGEVVTVGVIQRMMPRYCLFG | 544 |
| | . . * * . :***:**: : * * . : : : **:*:* . :***:* :***** | |
| alpha2_Human | NNVTLASKFESGSHPRINVSPTYQLLKREESFTFIPRSREELPDNFPKEIPGICYFLE | 698 |
| alpha2_Rat | NNVTLASKFESGSHPRINISPTYQLLKREDSFTFIPRSREELPDNFPKEIPGVICYFLE | 696 |
| alpha1_Human | NNVTLANKFESCSVPRKINVSPTYRLLKDCPGFVFTPRSREELPPNFPSEIPGICHFLD | 658 |
| alpha1_Dog | NNVTLANKFESCSIPRKINVSPTYRLLKDCPGFVFTPRSREELPPNFPSEIPGICHFLD | 658 |
| alpha1_Rat | NNVTLANKFESCSVPRKINVSPTYRLLKDCPGFVFTPRSREELPPNFPSPDIPGICHFLD | 657 |
| alpha1_Mouse | NNVTLANKFESCSVPRKINVSPTYRLLKDCPGFVFTPRSREELPPNFPSPDIPGICHFLD | 658 |
| beta1_Human | NTVNLTSRTETTGEKGINVSEYTYRCLMSPENS DPQFHLEHRGPVSMKKGKPEMQVIFL | 604 |
| | *.*.*.: * . :*** * * * . : . . . * . : : : : * | |
| alpha2_Human | VRTG-PKPPKPSLSSSRICKVSYNIGTMFLRETSL- | 732 |
| alpha2_Rat | LRTG-PKPPKPSLSSSRICKVSYNIGTMFLRETSL- | 730 |
| alpha1_Human | AYQQ-GTNSKPCFQK---KDVEDGNANFLGKASGID | 690 |
| alpha1_Dog | AYEP-ATNSKPFQK---KDVEDGNANFLGKASGID | 690 |
| alpha1_Rat | AYQHQPNSKPFQK---KDAEDGNANFLGKASGVD | 690 |
| alpha1_Mouse | AYHHQPNSKPFQD---KDVEDGNANFLGKASGID | 691 |
| beta1_Human | SRKNTGTEETKQDDD----- | 619 |

SUPPLEMENT 2: Strep-tag® principle and *Strep*-tag purification cycle

The basis of *Strep*-tag principle is binding of biotin to streptavidin. *Strep*-tag is an eight-amino-acid long peptide, which was selected from a random genetic library and is capable of binding to the biotin binding pocket of streptavidin (Schmidt and Skerra, 2007). When this small peptide is fused to recombinant proteins, it can serve as a purification tag. The *Strep*-tag II (Trp-Ser-His-Pro-Gln-Phe-Glu-Lys) can be placed at the C- or N-terminus. Generally, it does not interfere with folding or bioactivity, does not react with heavy metal ion buffer impurities, has no ion exchange properties and does not induce protein aggregation. Thus, there is no need for removing the tag (IBA, <http://www.iba-lifesciences.com/strep-tag.html> (27.8. 2012)). The *Strep*-tag II is largely resistant to cellular proteases, it can be used in the presence of mild detergents and it is biochemically almost inert (Schmidt and Skerra, 2007).

Streptavidin is a bacterial protein isolated from *Streptomyces avidini* and its natural ligand is d-biotin (Schmidt, 2007). *Strep*-Tactin is an engineered streptavidin with optimized binding properties for *Strep*-tag II fusion proteins (Skerra, 2003). The binding affinity of *Strep*-tag II to *Strep*-Tactin is nearly 100 times higher than to streptavidin (IBA). The *Strep*-Tactin is one of the most stable proteins known (IBA, 2012, <http://www.iba-lifesciences.com/strep-tag.html>) and is used in an immobilized form for purification of recombinant proteins together with *Strep*-tag II (Skerra, 2003).

Strep-tag II fusion proteins are generally eluted from the *Strep*-Tactin affinity column under physiological buffer conditions using a low concentration of a biotin derivate for competition. This not only allows the isolation of sensitive proteins in a native state, but also enables the purification of intact protein complexes in a preparative manner, even if only one subunit carries the tag (Schmidt and Skerra, 2007).

Strep-tag purification cycle

Step 1: The cell lysate containing the *Strep-tag II* fusion proteins is added onto a column with immobilized *Strep-Tactin*. The tagged protein binds specifically to *Strep-Tactin*.

Step 2: Host proteins are removed with small amounts of physiological wash buffer (Buffer W)

Step 3: The bound *Strep-tag II* protein is gently eluted by adding washing buffer with low concentration of desthiobiotin (Buffer E) which specifically competes for the biotin binding pocket.

Step 4: To regenerate the column the yellow azo dye HABA (2- [4'-hydroxy-benzeneazo] benzoic acid) is added (buffer R) in excess to remove desthiobiotin from the binding pocket. Once HABA binds to the binding site, the color turns to red conveniently indicating the regeneration and the regained activity status of the column.

Step 5: HABA is removed by adding wash buffer. Once the red color has disappeared the column is ready for next purification run. (IBA, 2012, <http://www.iba-lifesciences.com/strep-tag.html>)

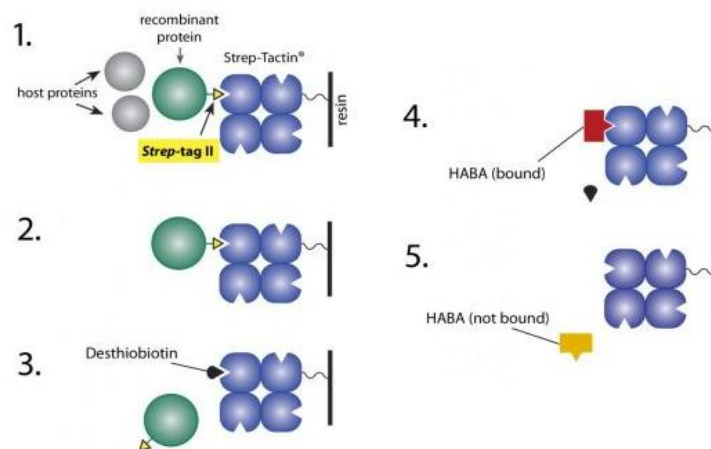


Figure 1: Schematic illustration of the *Strep-tag* purification cycle. (IBA, <http://www.iba-lifesciences.com/strep-tag.html> (27.8.2012))

Align a2SW36A

| | | | | | | | |
|-------------------|--------|--|------|------|------|------|------|
| | | Section 78 | | | | | |
| | (4159) | 4159 | 4170 | 4180 | 4190 | 4200 | 4212 |
| a2 Strep in pFB | (4151) | GCAGTAGTGTCTCCAAGCAGCATGTCTCGCAGGAAGATTTTCATCCGAGTCCCTTC | | | | | |
| 1a2_36-pBakPAC-FP | (198) | GCAGTAGTGTCTCCAAGCAGCATGTCTCGCAGGAAGATTTTCATCCGAGTCCCTTC | | | | | |
| 3a2_36-pBakPAC-FP | (206) | GCAGTAGTGTCTCCAAGCAGCATGTCTCGCAGGAAGATTTTCATCCGAGTCCCTTC | | | | | |
| | | Section 79 | | | | | |
| | (4213) | 4213 | 4220 | 4230 | 4240 | 4250 | 4266 |
| a2 Strep in pFB | (4205) | AGCTCTCTGGGCTCCGATTACCTGGAGACCAGCCCGGAAGAGGAAGGGGAATGC | | | | | |
| 1a2_36-pBakPAC-FP | (252) | AGCTCTCTGGGCTCCGATTACCTGGAGACCAGCCCGGAAGAGGAAGGGGAATGC | | | | | |
| 3a2_36-pBakPAC-FP | (260) | AGCTCTCTGGGCTCCGATTACCTGGAGACCAGCCCGGAAGAGGAAGGGGAATGC | | | | | |
| | | Section 80 | | | | | |
| | (4267) | 4267 | 4280 | 4290 | 4300 | 4310 | 4320 |
| a2 Strep in pFB | (4259) | CCCTTGTCTAAGCTCTGCTGGAAATGGCAGCCGGAGCCCGCCAGGGCCACCTGGC | | | | | |
| 1a2_36-pBakPAC-FP | (306) | CCCTTGTCTAAGCTCTGCTGGAAATGGCAGCCGGAGCCCGCCAGGGCCACCTGGC | | | | | |
| 3a2_36-pBakPAC-FP | (314) | CCCTTGTCTAAGCTCTGCTGGAAATGGCAGCCGGAGCCCGCCAGGGCCACCTGGC | | | | | |
| | | Section 81 | | | | | |
| | (4321) | 4321 | 4330 | 4340 | 4350 | 4360 | 4374 |
| a2 Strep in pFB | (4313) | TCCAGAGCAGCCGCTATGGCTGCCACCCAGTCCCCGCTGCTCTGTGCTGCTGG | | | | | |
| 1a2_36-pBakPAC-FP | (360) | TCCAGAGCAGCCGCTATGGCTGCCACCCAGTCCCCGCTGCTCTGTGCTGCTGG | | | | | |
| 3a2_36-pBakPAC-FP | (368) | TCCAGAGCAGCCGCTATGGCTGCCACCCAGTCCCCGCTGCTCTGTGCTGCTGG | | | | | |
| | | Section 82 | | | | | |
| | (4375) | 4375 | 4380 | 4390 | 4400 | 4410 | 4428 |
| a2 Strep in pFB | (4367) | GCAGCTGTGCAGTCCGCGCCGGTCCAAGAGAGCCCAACGCCCGCGGAGGGTC | | | | | |
| 1a2_36-pBakPAC-FP | (414) | GCAGCTGTGCAGTCCGCGCCGGTCCAAGAGAGCCCAACGCCCGCGGAGGGTC | | | | | |
| 3a2_36-pBakPAC-FP | (422) | GCAGCTGTGCAGTCCGCGCCGGTCCAAGAGAGCCCAACGCCCGCGGAGGGTC | | | | | |
| | | Section 83 | | | | | |
| | (4429) | 4429 | 4440 | 4450 | 4460 | 4470 | 4482 |
| a2 Strep in pFB | (4421) | AACCTGGACTCACTGGGCGAGAGTATCAGTCTCCTGACGGCGCCCTGCCTCAG | | | | | |
| 1a2_36-pBakPAC-FP | (468) | AACCTGGACTCACTGGGCGAGAGTATCAGTCTCCTGACGGCGCCCTGCCTCAG | | | | | |
| 3a2_36-pBakPAC-FP | (476) | AACCTGGACTCACTGGGCGAGAGTATCAGTCTCCTGACGGCGCCCTGCCTCAG | | | | | |
| | | Section 84 | | | | | |
| | (4483) | 4483 | 4490 | 4500 | 4510 | 4520 | 4536 |
| a2 Strep in pFB | (4475) | ACGATACACATGACTCTCAAGAGGACATTGCAGTATTATGAACATCAAGTTATT | | | | | |
| 1a2_36-pBakPAC-FP | (522) | ACGATACACATGACTCTCAAGAGGACATTGCAGTATTATGAACATCAAGTTATT | | | | | |
| 3a2_36-pBakPAC-FP | (530) | ACGATACACATGACTCTCAAGAGGACATTGCAGTATTATGAACATCAAGTTATT | | | | | |
| | | Section 85 | | | | | |
| | (4537) | 4537 | 4550 | 4560 | 4570 | 4580 | 4590 |
| a2 Strep in pFB | (4529) | GGTTATAGGGATGCAGAAAAGAATTTCCACAATATCTCTAATAGATGCTCCTCT | | | | | |
| 1a2_36-pBakPAC-FP | (576) | GGTTATAGGGATGCAGAAAAGAATTTCCACAATATCTCTAATAGATGCTCCTCT | | | | | |
| 3a2_36-pBakPAC-FP | (584) | GGTTATAGGGATGCAGAAAAGAATTTCCACAATATCTCTAATAGATGCTCCTCT | | | | | |
| | | Section 86 | | | | | |
| | (4591) | 4591 | 4600 | 4610 | 4620 | 4630 | 4644 |
| a2 Strep in pFB | (4583) | GCAGACCATTCCAACAAAGAGGAAATTTGAAGATGTCTCAGGAATTTCTCGGTGT | | | | | |
| 1a2_36-pBakPAC-FP | (630) | GCAGACCATTCCAACAAAGAGGAAATTTGAAGATGTCTCAGGAATTTCTCGGTGT | | | | | |
| 3a2_36-pBakPAC-FP | (638) | GCAGACCATTCCAACAAAGAGGAAATTTGAAGATGTCTCAGGAATTTCTCGGTGT | | | | | |
| | | Section 87 | | | | | |
| | (4645) | 4645 | 4650 | 4660 | 4670 | 4680 | 4698 |
| a2 Strep in pFB | (4637) | ACTGCAAATGTACTCGGACTGAAGTTCCAAGAAATTCAGAGAGGTTTGGTGAG | | | | | |
| 1a2_36-pBakPAC-FP | (684) | ACTGCAAATGTACTCGGACTGAAGTTCCAAGAAATTCAGAGAGGTTTGGTGAG | | | | | |
| 3a2_36-pBakPAC-FP | (692) | ACTGCAAATGTACTCGGACTGAAGTTCCAAGAAATTCAGAGAGGTTTGGTGAG | | | | | |
| | | Section 88 | | | | | |
| | (4699) | 4699 | 4710 | 4720 | 4730 | 4740 | 4752 |
| a2 Strep in pFB | (4691) | GAATTCCTTTAAGATATGCTTTGATGAGAATGAGCGAGTCCTTCGAGCTGTAGGC | | | | | |
| 1a2_36-pBakPAC-FP | (738) | GAATTCCTTTAAGATATGCTTTGATGAGAATGAGCGAGTCCTTCGAGCTGTAGGC | | | | | |
| 3a2_36-pBakPAC-FP | (746) | GAATTCCTTTAAGATATGCTTTGATGAGAATGAGCGAGTCCTTCGAGCTGTAGGC | | | | | |
| | | Section 89 | | | | | |
| | (4753) | 4753 | 4760 | 4770 | 4780 | 4790 | 4806 |
| a2 Strep in pFB | (4745) | AGCACATTGCAGGATTTCTTCAATGGCTTCGATGCATTGTTGGAACACATTAGG | | | | | |
| 1a2_36-pBakPAC-FP | (792) | AGCACATTGCAGGATTTCTTCAATGGCTTCGATGCATTGTTGGAACACATTAGG | | | | | |
| 3a2_36-pBakPAC-FP | (800) | AGCACATTGCAGGATTTCTTCAATGGCTTCGATGCATTGTTGGAACACATTAGG | | | | | |
| | | Section 90 | | | | | |
| | (4807) | 4807 | 4820 | 4830 | 4840 | 4850 | 4860 |
| a2 Strep in pFB | (4799) | ACTTCATTTGGGAAACAGGCCACTCTAGAGTACCATCTTTCCCTATGCAAAGAG | | | | | |
| 1a2_36-pBakPAC-FP | (846) | ACTTCATTTGGGAAACAGGCCACTCTAGAGTACCATCTTTCCCTATGCAAAGAG | | | | | |
| 3a2_36-pBakPAC-FP | (854) | ACTTCATTTGGGAAACAGGCCACTCTAGAGTACCATCTTTCCCTATGCAAAGAG | | | | | |
| | | Section 91 | | | | | |
| | (4861) | 4861 | 4870 | 4880 | 4890 | 4900 | 4914 |
| a2 Strep in pFB | (4853) | CTTCCT - GAAGGTACTCTC - AAACCTCCACTACTT - CCACCCCC - ACCATA - CA | | | | | |
| 1a2_36-pBakPAC-FP | (900) | CTTCCT - GAAGGTACTCTC - AAACCTCCACTACTT - CCACCCCC - ACCATA - CA | | | | | |
| 3a2_36-pBakPAC-FP | (908) | CTTCCT - GAAGGTACTCTC - AAACCTCCACTACTT - CCACCCCC - ACCATA - CA | | | | | |

Mutation: TGG to GCG.

| | | | | | | |
|-------------------------------|-----------------|--|--|------|------|------|
| Section 127 | | | | | | |
| | (5545) | 5545 | 5550 | 5560 | 5570 | 5588 |
| | a2 Strep in pFB | (5545) | GGCCCAGGATGGCTTGAAAAAGAGGATGGATAAAATTTAAAAGCCA | | | |
| Aa2_505-GATC-MBa2W505A-448500 | (127) | GGCCCAGGATGGCTTGAAAAAGAGGATGGATAAAATTTAAAAGCCA | | | | |
| Ba2_505-GATC-MBa2W505A-448500 | (134) | GGCCCAGGATGGCTTGAAAAAGAGGATGGATAAAATTTAAAAGCCA | | | | |
| Ca2_505-GATC-MBa2W505A-448500 | (126) | GGCCCAGGATGGCTTGAAAAAGAGGATGGATAAAATTTAAAAGCCA | | | | |
| Section 128 | | | | | | |
| | (5589) | 5589 | 5600 | 5610 | 5620 | 5632 |
| | a2 Strep in pFB | (5589) | CCTTAGAAAAAACTCACCAGGCCCTGGAAGAAGAGAAAAAGAAAG | | | |
| Aa2_505-GATC-MBa2W505A-448500 | (171) | CCTTAGAAAAAACTCACCAGGCCCTGGAAGAAGAGAAAAAGAAAG | | | | |
| Ba2_505-GATC-MBa2W505A-448500 | (178) | CCTTAGAAAAAACTCACCAGGCCCTGGAAGAAGAGAAAAAGAAAG | | | | |
| Ca2_505-GATC-MBa2W505A-448500 | (170) | CCTTAGAAAAAACTCACCAGGCCCTGGAAGAAGAGAAAAAGAAAG | | | | |
| Section 129 | | | | | | |
| | (5633) | 5633 | 5640 | 5650 | 5660 | 5676 |
| | a2 Strep in pFB | (5633) | ACAGTGGATCTGCTGTATTCCATTTCCCTGGTGTAGTAGCCCA | | | |
| Aa2_505-GATC-MBa2W505A-448500 | (215) | ACAGTGGATCTGCTGTATTCCATTTCCCTGGTGTAGTAGCCCA | | | | |
| Ba2_505-GATC-MBa2W505A-448500 | (222) | ACAGTGGATCTGCTGTATTCCATTTCCCTGGTGTAGTAGCCCA | | | | |
| Ca2_505-GATC-MBa2W505A-448500 | (214) | ACAGTGGATCTGCTGTATTCCATTTCCCTGGTGTAGTAGCCCA | | | | |
| Section 130 | | | | | | |
| | (5677) | 5677 | 5690 | 5700 | 5710 | 5720 |
| | a2 Strep in pFB | (5677) | GCAGTTGTCGCAACGACAGCAAGTACAGGCCAGAAAGTTTGATG | | | |
| Aa2_505-GATC-MBa2W505A-448500 | (259) | GCAGTTGTCGCAACGACAGCAAGTACAGGCCAGAAAGTTTGATG | | | | |
| Ba2_505-GATC-MBa2W505A-448500 | (266) | GCAGTTGTCGCAACGACAGCAAGTACAGGCCAGAAAGTTTGATG | | | | |
| Ca2_505-GATC-MBa2W505A-448500 | (258) | GCAGTTGTCGCAACGACAGCAAGTACAGGCCAGAAAGTTTGATG | | | | |
| Section 131 | | | | | | |
| | (5721) | 5721 | 5730 | | | 5764 |
| | a2 Strep in pFB | (5721) | ATGTCACTATGCTCTTCTCTGACATTGTGGGCTTCACAGCTATA | | | |
| Aa2_505-GATC-MBa2W505A-448500 | (303) | ATGTCACTATGCTCTTCTCTGACATTGTGGGCTTCACAGCTATA | | | | |
| Ba2_505-GATC-MBa2W505A-448500 | (310) | ATGTCACTATGCTCTTCTCTGACATTGTGGGCTTCACAGCTATA | | | | |
| Ca2_505-GATC-MBa2W505A-448500 | (302) | ATGTCACTATGCTCTTCTCTGACATTGTGGGCTTCACAGCTATA | | | | |
| Section 132 | | | | | | |
| | (5765) | 5765 | 5770 | 5780 | 5790 | 5808 |
| | a2 Strep in pFB | (5765) | TGTGCCAGTGTACTCCCATGTCAGGTGATCAGCATGCTCAATGA | | | |
| Aa2_505-GATC-MBa2W505A-448500 | (347) | TGTGCCAGTGTACTCCCATGTCAGGTGATCAGCATGCTCAATGA | | | | |
| Ba2_505-GATC-MBa2W505A-448500 | (354) | TGTGCCAGTGTACTCCCATGTCAGGTGATCAGCATGCTCAATGA | | | | |
| Ca2_505-GATC-MBa2W505A-448500 | (346) | TGTGCCAGTGTACTCCCATGTCAGGTGATCAGCATGCTCAATGA | | | | |
| Section 133 | | | | | | |
| | (5809) | 5809 | 5820 | 5830 | 5840 | 5852 |
| | a2 Strep in pFB | (5809) | ACTTTACACGAGATTTGATCACCAGTGTGGCTTTTTGGATATTT | | | |
| Aa2_505-GATC-MBa2W505A-448500 | (391) | ACTTTACACGAGATTTGATCACCAGTGTGGCTTTTTGGATATTT | | | | |
| Ba2_505-GATC-MBa2W505A-448500 | (398) | ACTTTACACGAGATTTGATCACCAGTGTGGCTTTTTGGATATTT | | | | |
| Ca2_505-GATC-MBa2W505A-448500 | (390) | ACTTTACACGAGATTTGATCACCAGTGTGGCTTTTTGGATATTT | | | | |
| Section 134 | | | | | | |
| | (5853) | 5853 | 5860 | 5870 | 5880 | 5896 |
| | a2 Strep in pFB | (5853) | ACAAGGTAGAAACAATAGGGGACGCATACTGTGTTGCATCAGGG | | | |
| Aa2_505-GATC-MBa2W505A-448500 | (435) | ACAAGGTAGAAACAATAGGGGACGCATACTGTGTTGCATCAGGG | | | | |
| Ba2_505-GATC-MBa2W505A-448500 | (442) | ACAAGGTAGAAACAATAGGGGACGCATACTGTGTTGCATCAGGG | | | | |
| Ca2_505-GATC-MBa2W505A-448500 | (434) | ACAAGGTAGAAACAATAGGGGACGCATACTGTGTTGCATCAGGG | | | | |
| Section 135 | | | | | | |
| | (5897) | 5897 | 5910 | 5920 | 5930 | 5940 |
| | a2 Strep in pFB | (5897) | CTTCACAGGAAAAGCCTATGCCATGCGAAGCCATTGCTCTGAT | | | |
| Aa2_505-GATC-MBa2W505A-448500 | (479) | CTTCACAGGAAAAGCCTATGCCATGCGAAGCCATTGCTCTGAT | | | | |
| Ba2_505-GATC-MBa2W505A-448500 | (486) | CTTCACAGGAAAAGCCTATGCCATGCGAAGCCATTGCTCTGAT | | | | |
| Ca2_505-GATC-MBa2W505A-448500 | (478) | CTTCACAGGAAAAGCCTATGCCATGCGAAGCCATTGCTCTGAT | | | | |
| Section 136 | | | | | | |
| | (5941) | 5941 | 5950 | 5960 | 5970 | 5984 |
| | a2 Strep in pFB | (5941) | GGCCTTAAAGATGATGGAGCTTTCAGAAGAGGTTCTGACTCCTG | | | |
| Aa2_505-GATC-MBa2W505A-448500 | (523) | GGCCTTAAAGATGATGGAGCTTTCAGAAGAGGTTCTGACTCCTG | | | | |
| Ba2_505-GATC-MBa2W505A-448500 | (530) | GGCCTTAAAGATGATGGAGCTTTCAGAAGAGGTTCTGACTCCTG | | | | |
| Ca2_505-GATC-MBa2W505A-448500 | (522) | GGCCTTAAAGATGATGGAGCTTTCAGAAGAGGTTCTGACTCCTG | | | | |
| Section 137 | | | | | | |
| | (5985) | 5985 | 5990 | 6000 | 6010 | 6028 |
| | a2 Strep in pFB | (5985) | ATGGAAGACCCATTTCAGATGCGGATAGGCATTTCATTGAGGCTCT | | | |
| Aa2_505-GATC-MBa2W505A-448500 | (567) | ATGGAAGACCCATTTCAGATGCGGATAGGCATTTCATTGAGGCTCT | | | | |
| Ba2_505-GATC-MBa2W505A-448500 | (574) | ATGGAAGACCCATTTCAGATGCGGATAGGCATTTCATTGAGGCTCT | | | | |
| Ca2_505-GATC-MBa2W505A-448500 | (566) | ATGGAAGACCCATTTCAGATGCGGATAGGCATTTCATTGAGGCTCT | | | | |
| Section 138 | | | | | | |
| | (6029) | 6029 | 6040 | 6050 | 6060 | 6072 |
| | a2 Strep in pFB | (6029) | GTGCTAGCTGGTGTGGTTCGGAGTGAGAATGCCCGCATATTGCT | | | |
| Aa2_505-GATC-MBa2W505A-448500 | (611) | GTGCTAGCTGGTGTGGTTCGGAGTGAGAATGCCCGCATATTGCT | | | | |
| Ba2_505-GATC-MBa2W505A-448500 | (618) | GTGCTAGCTGGTGTGGTTCGGAGTGAGAATGCCCGCATATTGCT | | | | |
| Ca2_505-GATC-MBa2W505A-448500 | (610) | GTGCTAGCTGGTGTGGTTCGGAGTGAGAATGCCCGCATATTGCT | | | | |

| | | | | | | |
|-------------------------------|------------------------|--|------|------|------|------|
| | | Section 139 | | | | |
| | (6073) | 6073 | 6080 | 6090 | 6100 | 6116 |
| | a2 Strep in pFB (6073) | TTTGGAAATAATGTCACTCTGGCAAGCAAATTTGAATCTGGAA | | | | |
| Aa2_505-GATC-MBa2W505A-448500 | (655) | TTTGGAAATAATGTCACTCTGGCAAGCAAATTTGAATCTGGAA | | | | |
| Ba2_505-GATC-MBa2W505A-448500 | (662) | TTTGGAAATAATGTCACTCTGGCAAGCAAATTTGAATCTGGAA | | | | |
| Ca2_505-GATC-MBa2W505A-448500 | (654) | TTTGGAAATAATGTCACTCTGGCAAGCAAATTTGAATCTGGAA | | | | |
| | | Section 140 | | | | |
| | (6117) | 6117 | 6130 | 6140 | 6150 | 6160 |
| | a2 Strep in pFB (6117) | GTCATCCTCGGCGCATCAACATCAGCCCACTACTTACCAATTA | | | | |
| Aa2_505-GATC-MBa2W505A-448500 | (699) | GTCATCCTCGGCGCATCAACATCAGCCCACTACTTACCAATTA | | | | |
| Ba2_505-GATC-MBa2W505A-448500 | (706) | GTCATCCTCGGCGCATCAACATCAGCCCACTACTTACCAATTA | | | | |
| Ca2_505-GATC-MBa2W505A-448500 | (698) | GTCATCCTCGGCGCATCAACATCAGCCCACTACTTACCAATTA | | | | |
| | | Section 141 | | | | |
| | (6161) | 6161 | 6170 | 6180 | 6190 | 6204 |
| | a2 Strep in pFB (6161) | CTAAAACGAGAAGACAGTTTACATTTATTCCCTCGTTCTCGTGA | | | | |
| Aa2_505-GATC-MBa2W505A-448500 | (743) | CTAAAACGAGAAGACAGTTTACATTTATTCCCTCGTTCTCGTGA | | | | |
| Ba2_505-GATC-MBa2W505A-448500 | (750) | CTAAAACGAGAAGACAGTTTACATTTATTCCCTCGTTCTCGTGA | | | | |
| Ca2_505-GATC-MBa2W505A-448500 | (742) | CTAAAACGAGAAGACAGTTTACATTTATTCCCTCGTTCTCGTGA | | | | |
| | | Section 142 | | | | |
| | (6205) | 6205 | 6210 | 6220 | 6230 | 6248 |
| | a2 Strep in pFB (6205) | AGAACTTCCAGACAACCTT - CCAAAGGAAATCCCTGGGGTCTGC | | | | |
| Aa2_505-GATC-MBa2W505A-448500 | (787) | AGAACTTCCAGACAACCTT TCCAAAGGAAATCCCTGGGGTCTGC | | | | |
| Ba2_505-GATC-MBa2W505A-448500 | (794) | AGAACTTCCAGACAACCTT - CCAAAGGAAATCCCTGGGGTCTGC | | | | |
| Ca2_505-GATC-MBa2W505A-448500 | (786) | AGAACTTCCAGACAACCTT - CCAAAGGAAATCCCTGGGGTCTGC | | | | |
| | | Section 143 | | | | |
| | (6249) | 6249 | 6260 | 6270 | 6280 | 6292 |
| | a2 Strep in pFB (6248) | TATTTCTGGAGT TAAGGACTGG - CCCAAAGCCACCAA - GCCA | | | | |
| Aa2_505-GATC-MBa2W505A-448500 | (831) | TATTTCTGGAGT TAAGGACTGG - CCCAAAGCCACCAAAGGCCA | | | | |
| Ba2_505-GATC-MBa2W505A-448500 | (837) | TATTTCTGGAGT TAAGGACTGG - CCCAAAGCCACCAA - GCCA | | | | |
| Ca2_505-GATC-MBa2W505A-448500 | (829) | TATTTCTGGAGT TAAGGACTGG - CCCAAAGCCACCAA - GCCA | | | | |
| | | Section 144 | | | | |
| | (6293) | 6293 | 6300 | 6310 | 6320 | 6336 |
| | a2 Strep in pFB (6290) | TCCCT - GTCTTCATCGA - GAATAAAAAA - GGTTCCTACAA - TA | | | | |
| Aa2_505-GATC-MBa2W505A-448500 | (874) | TCCCTTGTCTTCATCGA GAATAAAAAA AGGTTCCTACAA TA | | | | |
| Ba2_505-GATC-MBa2W505A-448500 | (880) | TCCCT - GTCTTCATCGA - GAATAAAAAA - GGTTCCTACAA - TA | | | | |
| Ca2_505-GATC-MBa2W505A-448500 | (871) | TCCCT - GTCTTCATCGA - GAATAAAAAA AGGTTCCTACAA - TA | | | | |
| | | Section 145 | | | | |
| | (6337) | 6337 | 6350 | 6360 | 6370 | 6380 |
| | a2 Strep in pFB (6330) | TTGG - CAC - GATGTTCC - TCCGA - GAACTAGCC - TCTGGA - C | | | | |
| Aa2_505-GATC-MBa2W505A-448500 | (918) | TTGGG CAC C GATGTTCC C TCCGA A GAACTAGCC C TCTGGGAGC | | | | |
| Ba2_505-GATC-MBa2W505A-448500 | (920) | TTGG - CAC - GATGTTCC - TCCGA - CAACTAGCC - TCTGGA - C | | | | |
| Ca2_505-GATC-MBa2W505A-448500 | (912) | TTGG - CAC - GATGTTCC - TCCGA - GAACTAGCC - TCTGGA - C | | | | |
| | | Section 146 | | | | |
| | (6381) | 6381 | 6390 | 6400 | 6410 | 6424 |
| | a2 Strep in pFB (6368) | CACCC - GCA - GTTCGA AAAAATAAAAGGGCGAATCTGCAGATAT | | | | |
| Aa2_505-GATC-MBa2W505A-448500 | (962) | CACCCCGCAAGTCCGA - - - - - | | | | |
| Ba2_505-GATC-MBa2W505A-448500 | (958) | CACCC - GCA - GTTCGA AAAAATAAAAGGGCGAATCTGCAGATAT | | | | |
| Ca2_505-GATC-MBa2W505A-448500 | (950) | CACCC - GCA - GTTCGA AAAAATAAAAGGGCGAATCTGCAGATAT | | | | |
| | | Section 147 | | | | |
| | (6425) | 6425 | 6430 | 6440 | 6450 | 6468 |
| | a2 Strep in pFB (6410) | CCATCACACTGGCGGCG - CTTTCGAATCTAGA - GCCTG - CAGT | | | | |
| Aa2_505-GATC-MBa2W505A-448500 | (978) | ----- | | | | |
| Ba2_505-GATC-MBa2W505A-448500 | (999) | CCATCACACTGGCGGCGTTTTCGAATCTAGA - GCCTG - CAGT | | | | |
| Ca2_505-GATC-MBa2W505A-448500 | (992) | CCATCACACTGGCGGCGCGTTTCGAATCTAGAAGCCTGGCAGC | | | | |
| | | Section 148 | | | | |
| | (6469) | 6469 | 6480 | 6490 | 6500 | 6512 |
| | a2 Strep in pFB (6451) | CTCGAGGCATGCGGTACCAAGCTT - GTCGA - GAAGTACTAGA - G | | | | |
| Aa2_505-GATC-MBa2W505A-448500 | (978) | ----- | | | | |
| Ba2_505-GATC-MBa2W505A-448500 | (1041) | CTCCAGGTATGCAGTACCAAGCTT - GTCGA - GAAGTACTAGA - G | | | | |
| Ca2_505-GATC-MBa2W505A-448500 | (1036) | CTCGAGGCATGCGGTACCAAGCTTGTTCGA GAAGTACTAGAAG | | | | |
| | | Section 149 | | | | |
| | (6513) | 6513 | 6520 | 6530 | 6540 | 6556 |
| | a2 Strep in pFB (6492) | GATCATAATC - AGCCATACCACATTTGT - - - - - AGAGGTTTTACTTTG | | | | |
| Aa2_505-GATC-MBa2W505A-448500 | (978) | ----- | | | | |
| Ba2_505-GATC-MBa2W505A-448500 | (1082) | GATC - - - - - | | | | |
| Ca2_505-GATC-MBa2W505A-448500 | (1080) | GATCATAATCAGCCATACCACATTTGTATAAGGTTTTACTTT | | | | |
| | | Section 150 | | | | |
| | (6557) | 6557 | 6570 | 6580 | 6590 | 6600 |
| | a2 Strep in pFB (6533) | CTTTAAAACCTCCACACCTCCCTGAACTCTGAAACATAAA | | | | |
| Aa2_505-GATC-MBa2W505A-448500 | (978) | ----- | | | | |
| Ba2_505-GATC-MBa2W505A-448500 | (1086) | ----- | | | | |
| Ca2_505-GATC-MBa2W505A-448500 | (1124) | GCTTTAAGAAACCTCCACACCTCCCTGAAACCTTGA | | | | |

| | | | | | | |
|-------------------------------|--------|--|-------------------------------------|-----------|-------------|-------------------------|
| | | | | | Section 151 | |
| | (6601) | 6601 | 6610 | 6620 | 6630 | 6644 |
| a2 Strep in pFB | (6577) | ATGAATGC | AAT | TGTTGTTGT | TAACTTGT | TATGTCAGCTTATAA |
| Aa2_505-GATC-MBa2W505A-448500 | (978) | ----- | ----- | ----- | ----- | ----- |
| Ba2_505-GATC-MBa2W505A-448500 | (1086) | ----- | ----- | ----- | ----- | ----- |
| Ca2_505-GATC-MBa2W505A-448500 | (1166) | AAC | TATAA | AAT | GAAATGCAA | TGGTTGTATGGAACTTGGGTTA |
| | | | | | | Section 152 |
| | (6645) | 6645 | 6650 | 6660 | 6670 | 6688 |
| a2 Strep in pFB | (6621) | TGGTTA | CAAA | TAA | GCAATA | CATCACAAATTTCACAAATAAAG |
| Aa2_505-GATC-MBa2W505A-448500 | (978) | ----- | ----- | ----- | ----- | ----- |
| Ba2_505-GATC-MBa2W505A-448500 | (1086) | ----- | ----- | ----- | ----- | ----- |
| Ca2_505-GATC-MBa2W505A-448500 | (1210) | TGTGCC | C | --- | TCTACAA | CGGTACACAAATTAG |
| | | | | | | Section 153 |
| | (6689) | 6689 | 6700 | 6710 | 6720 | 6732 |
| a2 Strep in pFB | (6665) | CATTTTTT | CACTGCATTCTAGTTGTGGTTTGTCCAAACTCATC | | | |
| Aa2_505-GATC-MBa2W505A-448500 | (978) | ----- | ----- | ----- | ----- | ----- |
| Ba2_505-GATC-MBa2W505A-448500 | (1086) | ----- | ----- | ----- | ----- | ----- |
| Ca2_505-GATC-MBa2W505A-448500 | (1241) | ----- | ----- | ----- | ----- | ----- |
| | | | | | | Section 154 |
| | (6733) | 6733 | 6740 | 6750 | 6760 | 6776 |
| a2 Strep in pFB | (6709) | AATGTATCTTATCATGTCTGGATCTGATCACTGCTTGAGCCTAG | | | | |
| Aa2_505-GATC-MBa2W505A-448500 | (978) | ----- | ----- | ----- | ----- | ----- |
| Ba2_505-GATC-MBa2W505A-448500 | (1086) | ----- | ----- | ----- | ----- | ----- |
| Ca2_505-GATC-MBa2W505A-448500 | (1241) | ----- | ----- | ----- | ----- | ----- |
| | | | | | | Section 155 |
| | (6777) | 6777 | 6790 | 6800 | 6810 | 6820 |
| a2 Strep in pFB | (6753) | GAGATCCGAACCAGATAAGTGAAATCTAGTTCAAACTATTTTG | | | | |
| Aa2_505-GATC-MBa2W505A-448500 | (978) | ----- | ----- | ----- | ----- | ----- |
| Ba2_505-GATC-MBa2W505A-448500 | (1086) | ----- | ----- | ----- | ----- | ----- |
| Ca2_505-GATC-MBa2W505A-448500 | (1241) | ----- | ----- | ----- | ----- | ----- |
| | | | | | | Section 156 |
| | (6821) | 6821 | 6830 | 6840 | 6850 | 6864 |
| a2 Strep in pFB | (6797) | TCATTTTTAATTTTCGTATTAGCTTACGACGCTACACCCAGTTC | | | | |
| Aa2_505-GATC-MBa2W505A-448500 | (978) | ----- | ----- | ----- | ----- | ----- |
| Ba2_505-GATC-MBa2W505A-448500 | (1086) | ----- | ----- | ----- | ----- | ----- |
| Ca2_505-GATC-MBa2W505A-448500 | (1241) | ----- | ----- | ----- | ----- | ----- |